TRANSIENT CONJUGATE HEAT TRANSFER IN A CIRCULAR DUCT FOR POWER-LAW FLUID WITH VISCOUS DISSIPATION

by

Alan L. Briggs

BS, Istanbul Technical University, 1989

MS, University of Pittsburgh, 1995

Submitted to the Graduate Faculty of

School of Engineering in partial fulfillment

of the requirements for the degree of

Doctor of Philosophy

University of Pittsburgh

2003

UNIVERSITY OF PITTSBURGH

SCHOOL OF ENGINEERING

This dissertation was presented

by

Alan L. Briggs

It was defended on

August 27, 2003

and approved by

James. L. Chen, Emeritus Professor , Department of Mechanical Engineering

Laura. Schaefer, Assistant Professor, Department of Mechanical Engineering

Scott. Mao, Professor, Department of Mechanical Engineering

Dissertation Director: Minking K. Chyu, Leighton Orr Professor and Chairman, Department of Mechanical Engineering

TRANSIENT CONJUGATE HEAT TRANSFER IN A CIRCULAR DUCT FOR POWER-LAW FLUID WITH VISCOUS DISSIPATION

Alan L Briggs, PhD

University of Pittsburgh, 2003

The study of unsteady forced convection heat transfer in tubes imposed to cyclic variations has been motivated by heat exchanger applications. This study investigates the heat transfer behavior associated with a thermal transient in a forced convection.

In this analysis, the effects of the duct wall heat capacity and convection from the ambient are considered, while axial conduction is neglected. The fluid inlet temperature is varied periodically with time. Incompressible, hydrodynamically developed laminar flow of non-Newtonian fluid flow is assumed. The transient conjugate heat transfer problem for fully-developed laminar flow of non-Newtonian fluids in circular duct is studied by numerical analysis. Control volume based finite difference method is adopted in the numerical procedure for the integration of the governing equations. For the non-Newtonian fluid part, power-law model is used. Heat generation from viscous dissipation is also taken into account and is represented by Brinkman number. The study investigates the effects of non-dimensional parameters on wall, fluid and bulk temperatures. In this dissertation, special focus is placed on the effects of the flow index, Brinkman, and Nusselt numbers.

TABLE OF CONTENTS

LIST OF TABLES

LIST OF FIGURES

NOMENCLATURE

A	Duct radius
a^*	Dimensionless wall heat capacity = $\frac{\rho c_p a}{\rho_w c_w l}$
b	Body force
Br	Brinkman number = $\frac{m U^{n+1}}{a^{n-1} \Delta T_0 k}$
c_p	Fluid specific heat
h	Heat transfer coefficient
k	Thermal conductivity of fluid
l	Wall thickness
m	Consistency index
n	Power-law index
Nu_0	Outside Nusselt number = $\frac{h a}{k}$, external thermal resistance
P^*	Dimensionless pressure quantity = $\frac{P_{m,e} - P}{\rho U^2}$
Pe	Peclet number = $\frac{U a}{\alpha}$, dimensionless independent heat transfer parameter
Pr	Prandtl number = $\frac{m c_p U^{n-1}}{k a^{n-1}}$, ratio of momentum and thermal diffusivities
Re	Reynolds number = $\frac{\rho U^{2-n} a^n}{m}$, ratio of inertia and viscous forces
r	Radial coordinate

R	Dimensionless radial coordinate = $\frac{r}{a}$
T	Dimensionless time = $\frac{\alpha t}{a^2}$
T	Temperature
T_0	Cycle mean temperature
U	Mean velocity
V_z^*	Dimensionless velocity = $\frac{V_z}{U}$
w	Frequency of oscillations
z	Axial coordinate
Z^*	Dimensionless axial coordinate = $\frac{z}{a}$

Greek Symbols

Θ	Dimensionless temperature = $\frac{T - T_0}{\Delta T_0}$
Θ_∞	Dimensionless ambient temperature = $\frac{T_\infty - T_0}{\Delta T_0}$
Ω	Dimensionless frequency oscillations $= \frac{w a^2}{\alpha}$
Φ	Dissipation function
ρ	Density
μ	Fluid dynamic viscosity
α	Thermal diffusivity of fluid
ΔT_0	Amplitude of inlet oscillations

Subscript

M	Mean value
N	North control volume face

N	Grid point in north direction
S	South control volume face
S	Grid point in south direction
W	Wall
$_\infty$	Free stream value

ACKNOWLEDGEMENT

This work could not be completed without encouragement, support, and assistance of many individuals. First and foremost, my deepest gratitude goes to my family who has stood behind me in this work and shared the burden of my prolonged PhD program.

I would like to express my special thanks to committee chairperson and my academic advisor Professor Minking Chyu for his encouragement, guidance, support and understanding.

A special note of gratitude must be extended to Professor James Chen for his support and valuable critical comments throughout this work.

It was my good fortune to have Professor Laura Schaefer serve as my committee member. I extend my gratitude for her helpful suggestions and constructive criticism.

A special thanks is extended to Professor Scott Mao for his valuable suggestions and comments.

1.0 INTRODUCTION

The study of unsteady forced convection heat transfer in tubes imposed to cyclic variations has been motivated by heat exchanger applications. This study investigates the heat transfer behavior associated with a thermal transient in a forced convection in a circular duct. The motivation behind the thermal response of internal flow subject to variations is provided by devices of the regenerative type of heat exchanger through which hot and cold fluid pass in succession. Usually, the conditions at the inner surface of the solid are assumed to be given, but in fact the thermal conditions at the wall are generally unknown, and the heat transfer problem for the solid wall must be analyzed simultaneously with the heat transfer for the fluid.

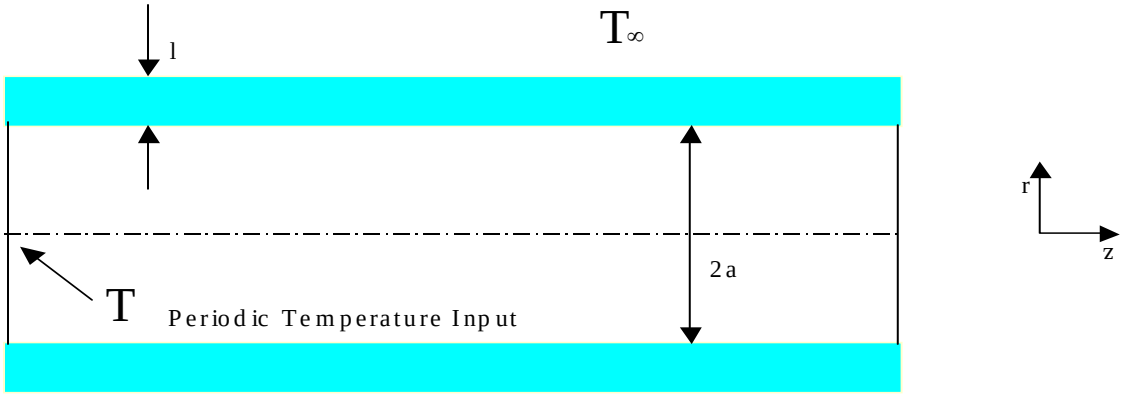

Figure 1 Physical Description of the Problem

In this analysis, the effects of the duct wall heat capacity and convection from the ambient are considered, while axial conduction is neglected. The fluid inlet temperature is varied periodically with time. Incompressible,

hydrodynamically developed laminar flow of non-newtonian fluid flow is assumed. The last assumption implies that a hydrodynamic entrance length is present which allows establishing a fully developed flow. Except for liquidmetals and gases, the hydrodynamic entrance region is much shorter than the thermal entrance region. It is also assumed that physical properties of the wall and fluid are constant.

In this present work, viscous dissipation effects will also be taken into account. Viscous dissipation can result in large local temperature increases, especially in the wall region. Undesired reactions may occur if those temperatures are not controlled properly. Lin et al. [27] points out the importance of viscous dissipation in the design of the control systems of heat transfer devices in organic-cooled nuclear reactors. We believe it is important to investigate any physical effects, such as viscous dissipation, which may lead to pronounced heat transfer.

1.1 LITERATURE SURVEY

Unsteady forced convection in tubes with periodic variation of the inlet condition is of interest in heat exchangers. The available work in this area is still limited.

Sparrow and DeFarios [33] studied the transient conjugate problem of a slug flow inside a parallel plate duct with a periodically varying inlet temperature (1968). The series solution results in a complex eigenvalue problem.

Cotta, Mikhailov and Ozisik [18]extended their work to a circular duct (1987). They solved the complex eigenvalue problem by applying the Count method. The results are presented in the graphical form as a function of axial position for different values of the parameters. In both studies, the viscous dissipation is considered to be negligible.

Travelho and Santos [35] solved the Sparrow and DeFarios' problem by using the Laplace transform (1991). The amplitudes and phase lags with respect to the inlet conditions are determined for the complex wall temperature, fluid bulk temperature, and wall heat flux from the solution. However, their solution becomes inaccurate as Z becomes equal to or larger than one.

Santos and Travelho [36] solved the transient laminar forced convection in the thermal entrance region of a circular duct with a periodically varying inlet temperature by applying a Laplace transformation (1998). They also included convection interaction with an ambient medium outside the duct. In their study, viscous dissipation effects are neglected, and slug flow idealization of the velocity field is utilized. However, in the design of heat transfer devices

in organic-cooled nuclear reactors, where Non-Newtonian fluids are used, viscous dissipation becomes significant [27]. In the analysis of laminar forced convection of Newtonian fluids flowing in circular ducts, Barletta (1997) showed that the effect of viscous dissipation is very relevant in the fully developed region, both if the wall temperature is uniform and if convection with an external isothermal fluid occurs [5].

2.0 ANALYSIS

2.1 STATEMENT OF THE PROBLEM

The objective of this work presented in the following text is to study the heat transfer problem presented by Santos and Travelho [36] (1998). We will extend their work by considering Non-Newtonian fluid flow and by taking the effect of the viscous dissipation into account. The assumptions we make for the particular problem are as follows:

•Fluid flow is hydrodynamically developed and laminar

•Power-law fluids are to be studied

•Convective heat transfer from the ambient outside and the duct thermal capacity effects are considered

•Axial conduction is neglected

•Physical properties of the wall and fluid are constant

2.2 GOVERNING EQUATIONS

The linear momentum equation is given in Eulerian form by:

$$\rho \frac{D\mathbf{V}}{Dt} = div\mathbf{T} + \rho\mathbf{b} \qquad (2\text{-}1)$$

where $\frac{D}{Dt}$ is the material time derivative, which denotes differentiation with respect to t, holding x fixed where b is the body force vector and T is the Cauchy stress tensor. The

balance of angular momentum yields that the Cauchy stress is symmetric: $T=T^T$.

The energy equation for forced convection heat transfer with viscous dissipation is as follows:

$$\rho\, c_p \frac{DT}{Dt} = div(k\ grad\ T) + \Phi \qquad (2\text{-}2)$$

where Φ is dissipation function.

For the problem under consideration, the reduced momentum equation for a circular duct in the axial direction is

$$\frac{1}{r}\frac{\partial}{\partial r}(r\tau_{rz)}) = -\frac{\partial p}{\partial z} \tag{2-3}$$

where, $\tau_{rz} = m\left|\frac{dV_z}{dr}\right|^{n-1}\frac{dV_z}{dr}$, m consistency index and n is power-law index.

Under the conditions we stated in section 2.1, the temperature field is described by the energy equation in the following form:

$$\rho c_p(\frac{\partial T}{\partial t} + V_z\frac{\partial T}{\partial z}) = k(\frac{\partial^2 T}{\partial r^2} + \frac{1}{r}\frac{\partial T}{\partial r}) + \tau_{rz}(\frac{dV_z}{d\,r}) \tag{2-4}$$

With the initial, inlet and boundary conditions given respectively by:

$$T(r,z,0) = T_0 \tag{2-5}$$

$$T(r,0,t) = T_0 + \Delta T_0\ Sin\,\omega t \tag{2-6}$$

$$\left.\frac{\partial T(r,z,t)}{\partial r}\right|_{r=0} = 0\,, \tag{2-7}$$

$$-k\left.\frac{\partial T(r,z,t)}{\partial r}\right|_{r=a} = l\,(\rho\,c)_w\frac{\partial T(a,z,t)}{\partial t} + h(T\,(a,z,t) - T_\infty) \tag{2-8}$$

The last boundary condition was obtained from the energy balance on the wall where T_∞ is the ambient temperature.

We introduce the following dimensionless quantities:

$R = \frac{r}{a}$ dimensionless radial coordinate (2-9)

$Z^* = \frac{z}{a}$ dimensionless axial coordinate (2-10)

$\mathrm{T} = \frac{\alpha t}{a^2}$ dimensionless time (2-11)

$$P^* = \frac{P_{m,e} - P}{\rho U^2}$$ dimensionless pressure quantity (2-12)

$$V_z^* = \frac{V_z}{U}$$ dimensionless velocity (2-13)

$$\Theta = \frac{T - T_0}{\Delta T_0},$$ dimensionless temperature (2-14)

$$\Theta_\infty = \frac{T_\infty - T_0}{\Delta T_0}$$ dimensionless temperature (2-15)

$$a^* = \frac{\rho\, c_p\, a}{\rho_w\, c_w\, l},$$ dimensionless wall heat capacity (2-16)

$$\Omega = \frac{w\, a^2}{\alpha}$$ dimensionless frequency oscillations (2-17)

Applying the dimensionless quantities to the momentum and energy equations, .the problem under consideration is given in dimensionless form as:

$$\frac{1}{R}\ \frac{\partial}{\partial R}(R(\frac{dV_z^*}{dR})^n) = \mathrm{Re}\,(\frac{dP^*}{dZ^*})$$ (2-18)

Where $\mathrm{Re} = \frac{\rho U^{2-n} a^n}{m}$ (2-19)

$$\frac{\partial \Theta}{\partial \mathrm{T}} + Pe\,(V_z^* \frac{\partial \Theta}{\partial Z^*}) = (\frac{\partial^2 \Theta}{\partial R^2} + \frac{1}{R}\frac{\partial \Theta}{\partial R}) + Br \left|\frac{dV_z^*}{dR}\right|^{n-1} \left(\frac{dV_z^*}{dR}\right)^2$$ (2-20)

with boundary conditions,

$$\Theta(R, Z^*, 0) = 0$$ (2-21)

$$\Theta(R, 0, \mathrm{T}) = Sin\ \Omega \mathrm{T}$$ (2-22)

$$\left.\frac{\partial \Theta(R, Z^*, \mathrm{T})}{\partial R}\right|_{R=0} = 0$$ (2-23)

$$-\left.\frac{\partial \Theta(R, Z^*, \mathrm{T})}{\partial R}\right|_{R=1} = \frac{1}{a^*}\frac{\partial \Theta(1, Z^*, \mathrm{T})}{\partial \mathrm{T}} + Nu_0(\Theta(1, Z^*, \mathrm{T}) - \Theta_\infty)$$ (2-24)

where

$$Pe = \mathrm{Re}\ \mathrm{Pr} = \frac{\rho U^{2-n} a^{n}}{m} \frac{m c_p U^{n-1}}{k\ a^{n-1}} = \frac{\rho c_p U a}{k} = \frac{U a}{\alpha}$$ is the Peclet number, (2-25)

$$Br = \frac{m\ U^{n+1}}{a^{n-1}\ \Delta T_0 k}$$ is the Brinkman number,and (2-26)

$$Nu_0 = \frac{h a}{k}$$, is the outside Nusselt number, (2-27)

2.3 DISCRETIZATION

The algebraic equations involving the unknown values of the dependent variable Φ at the chosen grid points are derived from the differential equation governing Φ. The calculation domain is divided into a number of nonoverlapping control volumes shown in Figures 2 and 4, such that one control volume surrounds each grid point. Then the differential equation is integrated over each control volume. Piecewise profiles between the grid points are used to evaluate the integrals. Integrating the energy equation over the control volume and using a fully-implicit scheme we have as follows,

$$\frac{\Theta_p - \Theta_p^o}{\Delta \mathrm{T}} \quad \frac{R_n^2 - R_s^2}{2} \Delta Z^* + Pe\ V_{zp}^* (\Theta_p - \Theta_w) \frac{R_n^2 - R_s^2}{2}$$
$$= \left[R_n \left(\frac{\Theta_N - \Theta_p}{\Delta R_n}\right) - R_S \left(\frac{\Theta_P - \Theta_S}{\Delta R_S}\right) \right] \Delta Z^* + \Delta Z^* Br\ R_P\ \Delta R \left| \frac{V_n^* - V_s^*}{\Delta R} \right|^{n-1} \left(\frac{V_n^* - V_s^*}{\Delta R} \right)^2$$

(2-28)

Rearranging the equation in the form as:

$$a_p\ \Theta_p = a_w\ \Theta_w + a_N\ \Theta_N + a_S\ \Theta_S + a_p^o\ \Theta_p^o + d$$ (2-29)

$$a_W = (Pe\ V_{zp}^* \frac{R_n^2 - R_s^2}{2})$$ (2-30)

$$a_N = \frac{R_n \Delta Z^*}{\Delta R_n} \tag{2-31}$$

$$a_S = \frac{R_S \Delta Z^*}{\Delta R_S} \tag{2-32}$$

$$a_p^o = \frac{R_n^2 - R_s^2}{2} \frac{\Delta Z^*}{\Delta \mathrm{T}} \tag{2-33}$$

$$d = \Delta Z^* Br\, R_p\ \Delta R \left| \frac{V_n^* - V_s^*}{\Delta R} \right|^{n-1} \left(\frac{V_n^* - V_s^*}{\Delta R} \right)^2 \tag{2-34}$$

$$a_p = a_w + a_N + a_S + a_p^o \tag{2-35}$$

We need to construct an additional equation for Θ at the boundary since the boundary temperature is not given. The equation for the wall boundary condition is integrated over half the control volume adjacent to the wall as shown in Figure 3, which leads to,

$$-\left(\frac{\Theta_P - \Theta_S}{\Delta R_S}\right) = \frac{1}{a^*}\left(\frac{\Theta_P - \Theta_P^0}{\Delta \mathrm{T}}\right) + Nu_0\left(\Theta_P - \Theta_\infty\right) \tag{2-36}$$

Rearranging the equation gives the following;

$$a_S = \frac{1}{\Delta R_S} \tag{2-37}$$

$$a_P^0 = \frac{1}{a^* \Delta \mathrm{T}} \tag{2-38}$$

$$d = Nu_0\, \Theta_\infty \tag{2-39}$$

$$a_P = a_S + a_P^0 + Nu_0 \tag{2-40}$$

Equation 2-29 is solved using LU decomposition method. Once the coefficient matrix is converted to LU equivalent, the solution can be found. The L matrix is a record of operations required to make the coefficient matrix into the upper-triangular matrix U. The same transformations are applied to the right hand side. Then after we augment the right hand side to U and back-substitute, the solution appears. [39]

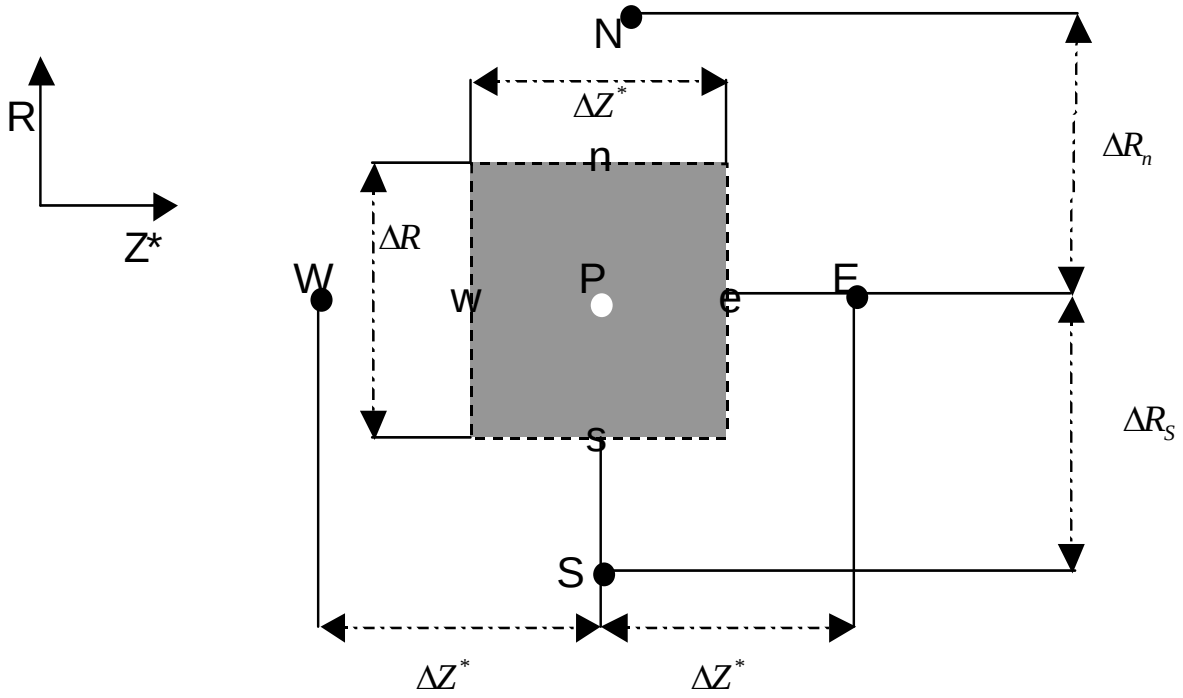

Figure 2 Control Volume for Discretization

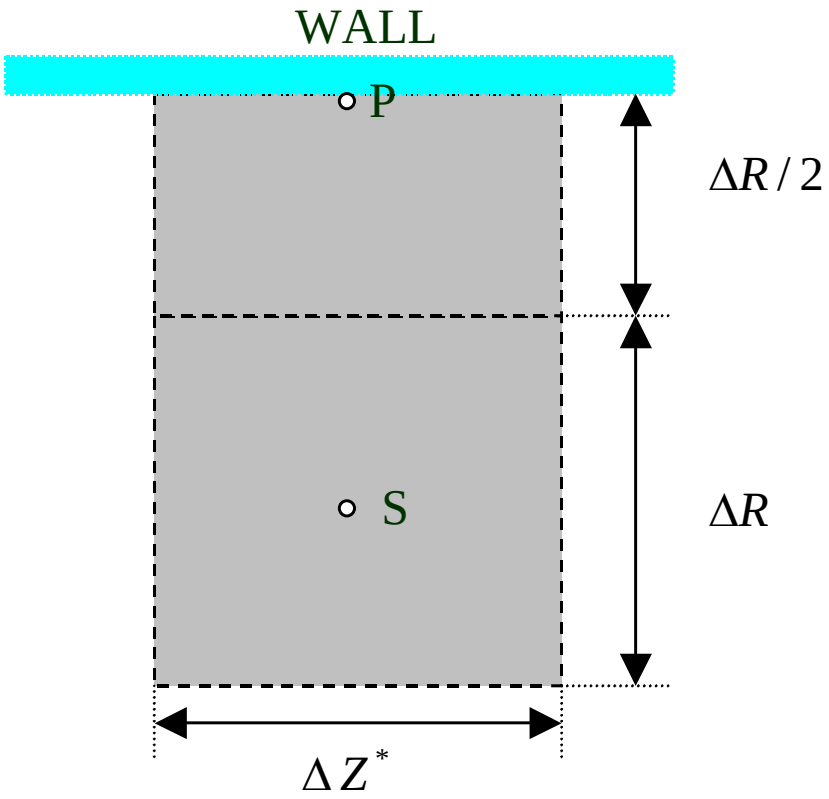

Figure 3 Half Control Volume near the Boundary

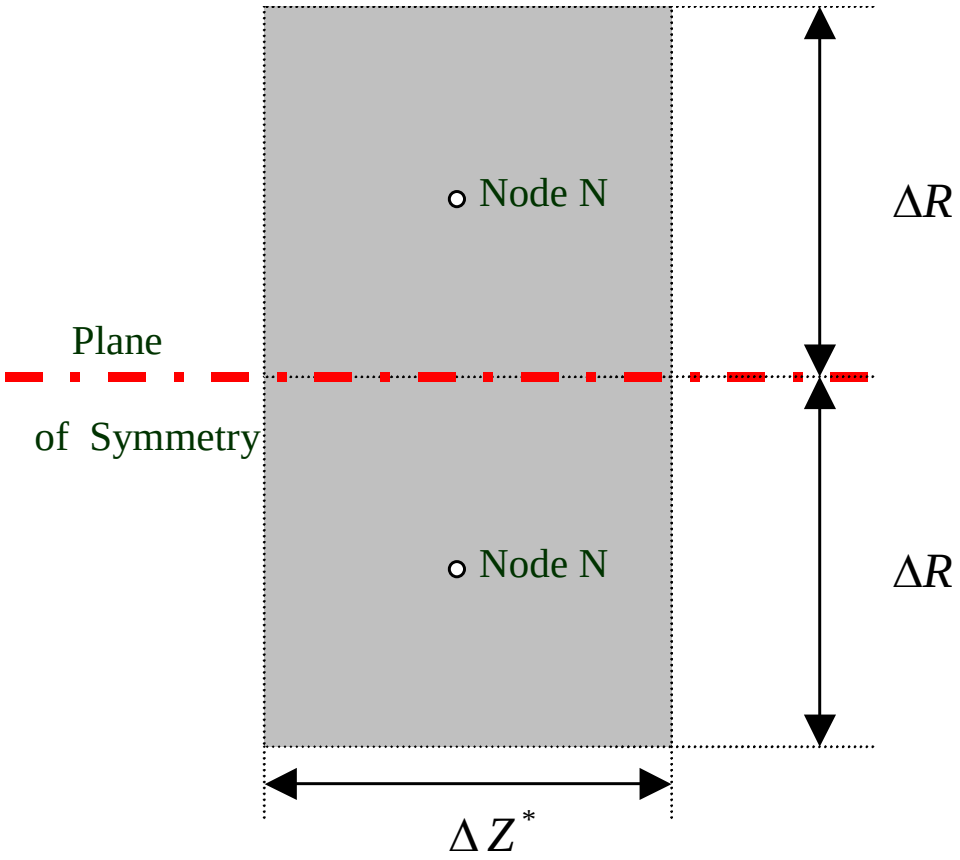

Figure 4 Control Volume Adjacent to Plane of Symmetry

3.0 VERIFICATION

3.1 ANSYS RESULTS

In order to verify our results obtained using control volume based finite difference, computations have been performed on ANSYS, a commercial FEM code. The model in Figure 5 is run on an Intel NT with four processors by ANSYS 5.7. The results and comparisons are summarized in the following. In order to be consistent with what we have for a control volume based finite difference model, half size of the quad elements in radial direction is used adjacent to the symmetry line. The half model shown in Figure 5 is generated using total of 1020 nodes and 950 quad elements to save CPU time. The pipe wall is designed to be sufficiently thin so that the temperature variations across the thickness of the wall are negligible.

For the given problem, the momentum equation can be solved independently. Once a solution for the flow field is obtained, the energy equation is activated and transient solution is switched on. It takes 3941 cumulative iterations to reach the desired convergence,1.0E-17. The specified convergence criterion is met using the MSU advection formulation. The global iteration is set to be 350, and total CPU time in seconds is 164.70, where 136.06 seconds are spent for calculations. The results are reflected about the symmetry line to have a full model for post-processing purpose. Computations have been performed for the following conditions:

Fluid Properties:

Air at 300 K

ρ = 1.1614 kg/m**3

μ = 184.6e-07 kg/m-s

k = 0.0263 W/m-K

c_p = 1007 J/kg-K

Solid Properties:

Stainless Steel (AISI 304) at 300 K ρ = 8055 kg/m**3

k = 15 W/m-K

c_P = 480 J/kg-K

Geometric Properties:

a = 0.0025 m

z = 0.0125 m

l = 0.0002 m

Loading:

ΔP = 0.0375 Pa

$T(r,z,0)$ = 320 K

T_0 = 320 K

ΔT_0 = 40 K

$T(r,0,t) = T_0 + \Delta T_0 \, Sin\, \omega t$

$\omega = 2\pi/32$ 1/s

h = 250 W/m**2-K

T_∞ =300 K

3.1.1 Analytical Solution for Velocity

The axial component of the velocity field is given by, $V_z(r) = \frac{3n+1}{n+1} U \left[1 - \left(\frac{r}{a} \right)^{(n+1)/n} \right]$ where the case n=1 corresponds to a Newtonian fluid [8]. In dimensionless form, the velocity profile for non-Newtonian flows becomes $V_z^*(R) = \frac{3n+1}{n+1} \left[1 - R^{(n+1)/n} \right]$.

Figure 9 displays the dimensionless velocity profiles of Newtonian and non-Newtonian flows. The curve labeled as n=1 corresponds to Newtonian fluid profile. The curves labeled n<1 represent shear-thinning non-Newtonian flow. Those fluids deliver the highest localized viscous heating due to high near-wall shear rates. These high shear rates contribute to elevated local viscous heating effects. The curves labeled n>1 represent shear-thickening non-Newtonian flows. Note in Figure 9, the increase in the wall shear rate and the increasingly plug-like nature of the profile as power-law index decreases.

The velocity field for this problem is fully-developed throughout the pipe. The velocity profile for Newtonian-fluid follows the "Hagen-Poiseuille" paraboloid, given by,

$$V_z(r) = \frac{r^2}{4\mu}\left(-\Delta P / L\right)\left[1-\left(\frac{r}{a}\right)^2\right]$$

From the above, the centerline velocity is:

$$V_z\big|_{r=0} = 0.2539 \quad m/s$$

The mean velocity is half of the centerline velocity,

$$U = 0.1269 \quad m/s$$

$$\mathrm{Re} = \frac{\rho U a}{\mu} = 40 \text{ (laminar flow)}$$

The mass flow rate is,

$\dot{m} = \rho U A_f$ = 2.894*E-06 kg/s where A_f is the flow area

The flow is considered to be Newtonian where n is equal to one.

The inspection of the results depicted in Table 1 reveals that centerline velocity, mean velocity, and mass flow rate are appeared to be in good agreement with the analytical solution. As depicted in Figures 6, 7 and 8, the velocity profile is found to be consistent with the Hagen-Poiseuille paraboloid. Figure 8 shows that the maximum velocity is at the center of the pipe, whereas we have zero velocity at the walls as a result of the no-slip boundary condition.

Table 1 Comparison of centerline velocity, mean velocity and mass flow rate.

		Target	ANSYS
$V_z\|_{r=0}$	m/s	0.2539	0.2539
U	m/s	0.1269	0.1263
$\overset{\circ}{m}$	kg/s	2.894e-06	2.880e-06

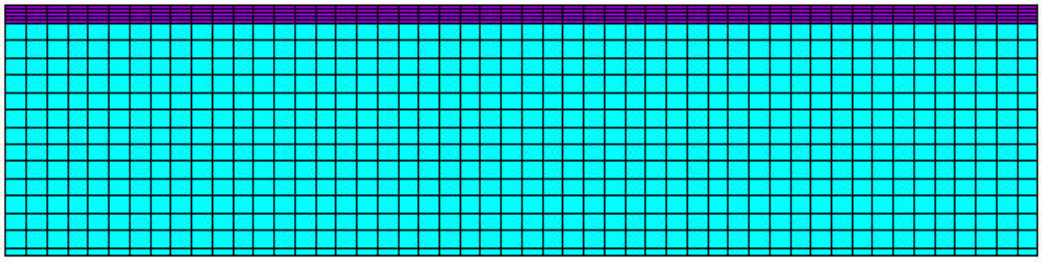

Figure 5 Finite Element Subdivision of the half pipe

Figure 6 Contours of Axial Velocity for Ansys Solution

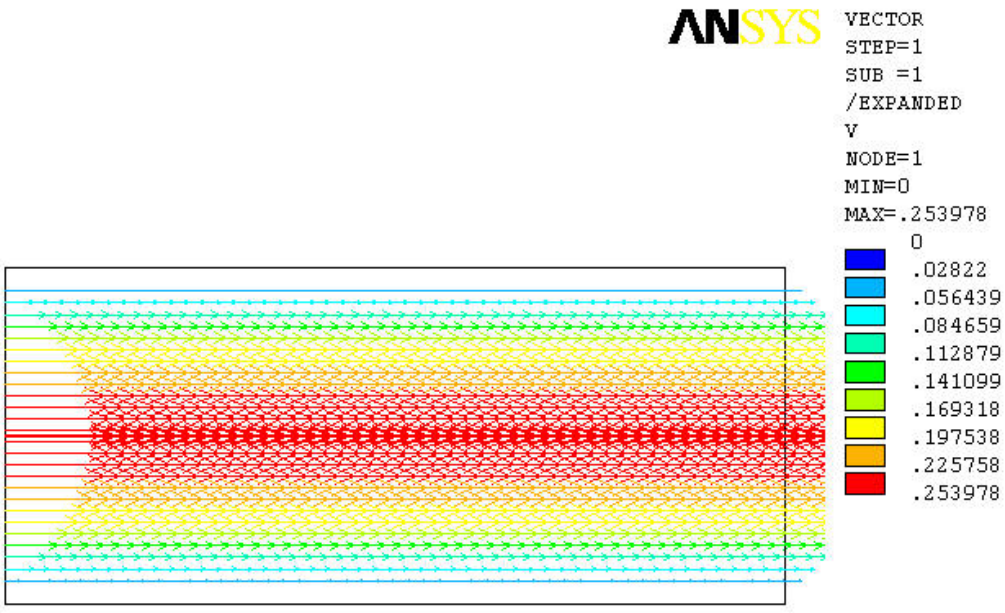

Figure 7 Vectors of Axial Velocity for Ansys Solution

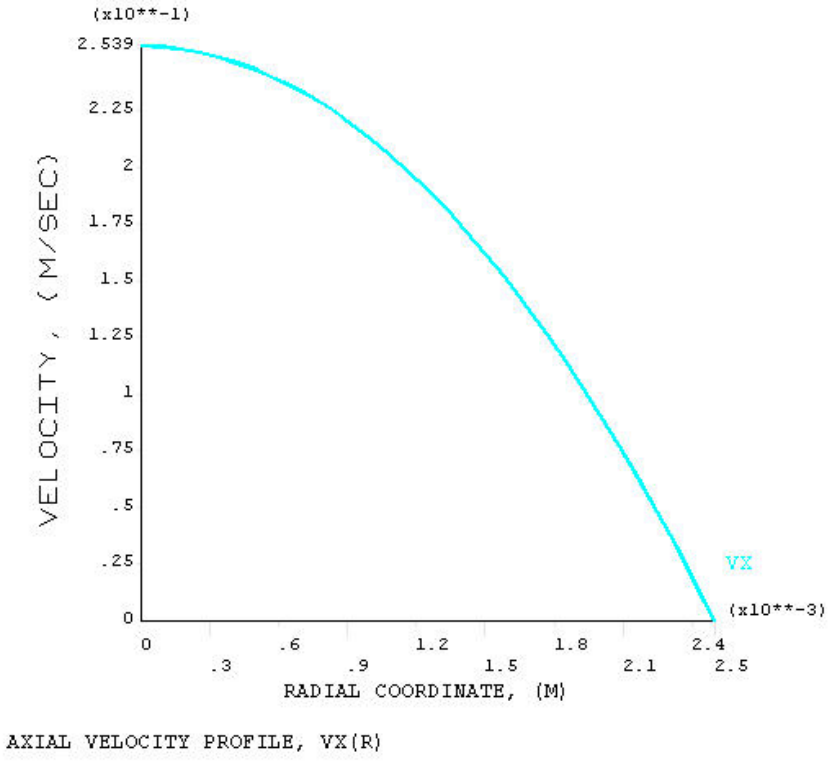

Figure 8 Axial Velocity Profile for Ansys Solution

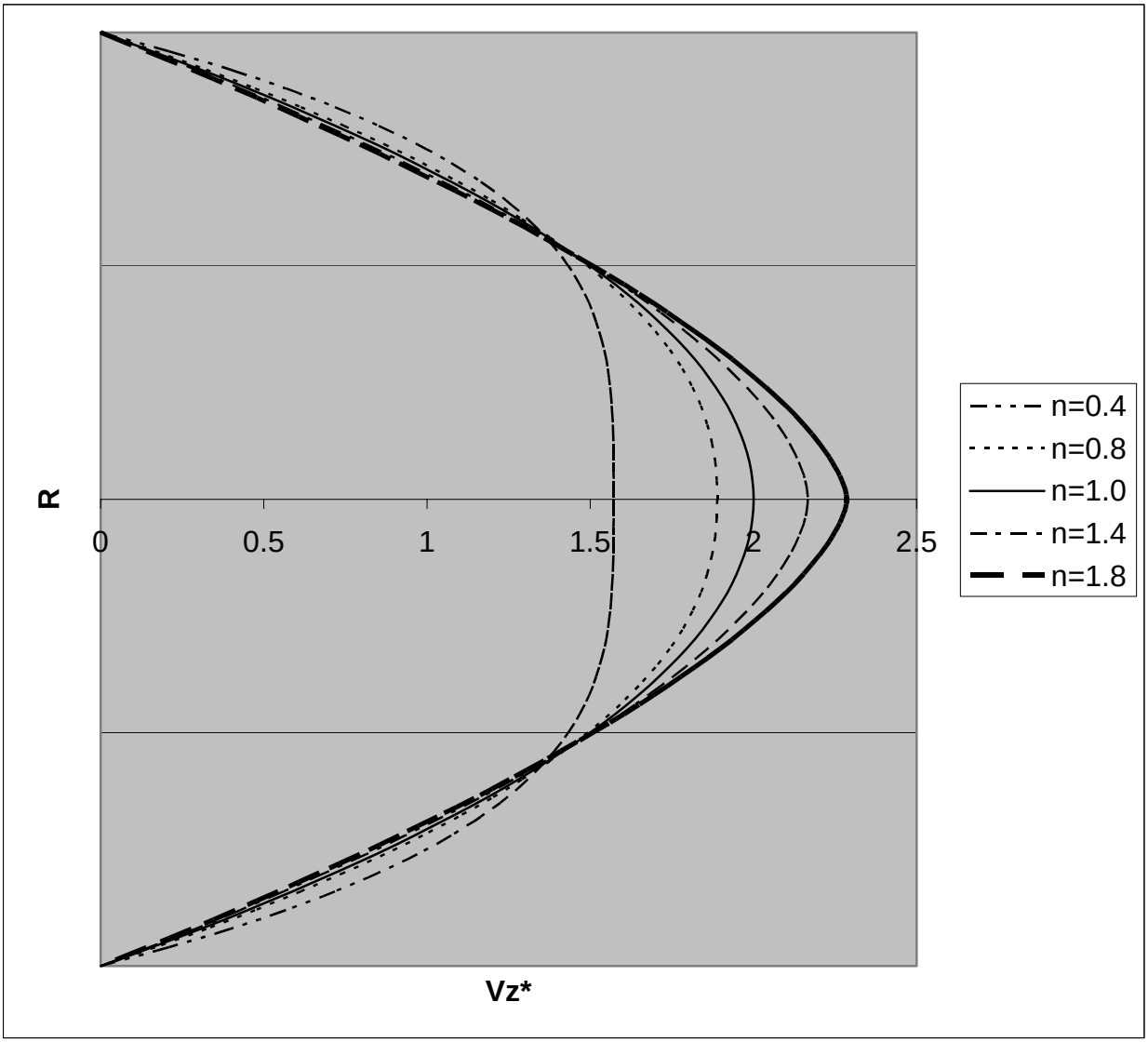

Figure 9 Dimensionless Velocity Profiles for the steady-state laminar flow of power-law liquids in a straight pipe.

3.1.2 Temperature Solution

Using the conditions stated earlier leads to the following dimensionless values,

$Nu_o = \frac{h\,a}{k}$ =23.76425

Br = 279 E-09

a^* = 0.00378

Ω = 0.05459

Pe = 14.01245

T_{final} =115.13856

ΔT = 3.59808

Θ_∞ = -0.5

During the energy equation solution, a bug was discovered within Ansys version 5.7. An initial attempt was made to solve the energy equation using the Initial Condition command (I.C.) of ANSYS. It is found that this command tends to set the initial conditions to zero all the time, not to the specified one. Discovering this error forces us to set the desired initial condition as a boundary condition for steady-state case. After running for the steady-state case, boundary conditions are deleted for all nodes, and a new set of boundary conditions are applied for the transient solution. Since all the results are stored in memory for the steady-state case, ANSYS recognizes those nodal results as if they were initial conditions for the transient solution. This method appears to work fine, as can be seen in Figure 10. At zero time, we have the specified initial condition for temperature.

The same figure shows the specified inlet temperature in time. For our problem, the inlet temperature field is subject to a sine function in time. Figures 11, 12, 13, and 14 show temperature contours at different times. The inlet temperature takes the value of its initial one at t=32 s. As seen from these figures, forced convection dominates the temperature profile in this case. The fluid temperature is damped within a distance from the inlet. Figure 15 shows the temperature profiles at different axial locations of the inner wall. The temperature profile in time tends to

flatten as the distance from the inlet increases. The effect from ambient is more noticeable downstream, where the inlet temperature has less effect on those regions. Figures 16, 17, 18, and 19 exhibit this effect more clearly.

The influence of forced convection can be seen in Figure 20. Dimensionless temperature increases as we move towards the center of the pipe. Comparing Figures 21 and 22, we can see this result more clearly. The thermal wave has more penetration near the center than the wall, where the dimensionless wall temperature decays with time.

The results we obtained from the control volume based finite difference output are put in dimensional form in order to compare with the Ansys solution. As seen in Figure 23, the two solutions are in good agreement. In fact, the maximum error is found to be 0.6 percent at z=0.0075 m. We also compared two results at the wall as a function of time (Figure 24). The maximum error is found to be 1.9 percent, but keep in mind that those results are obtained from two different algorithms with different solution techniques. Also, using the finite difference solution, we have made some approximations and used additional equations for the wall temperature. Ansys results appear to be higher values in magnitude than the finite difference solution for each case. The difference between the two solutions in time is less pronounced as we move away from the wall. This difference may be reduced by decreasing the time step, ΔT. This fact will be clear later as we do a stability analysis. Since it is very expensive in terms of CPU time and storage to work with small time steps ΔT, we adopt the current one.

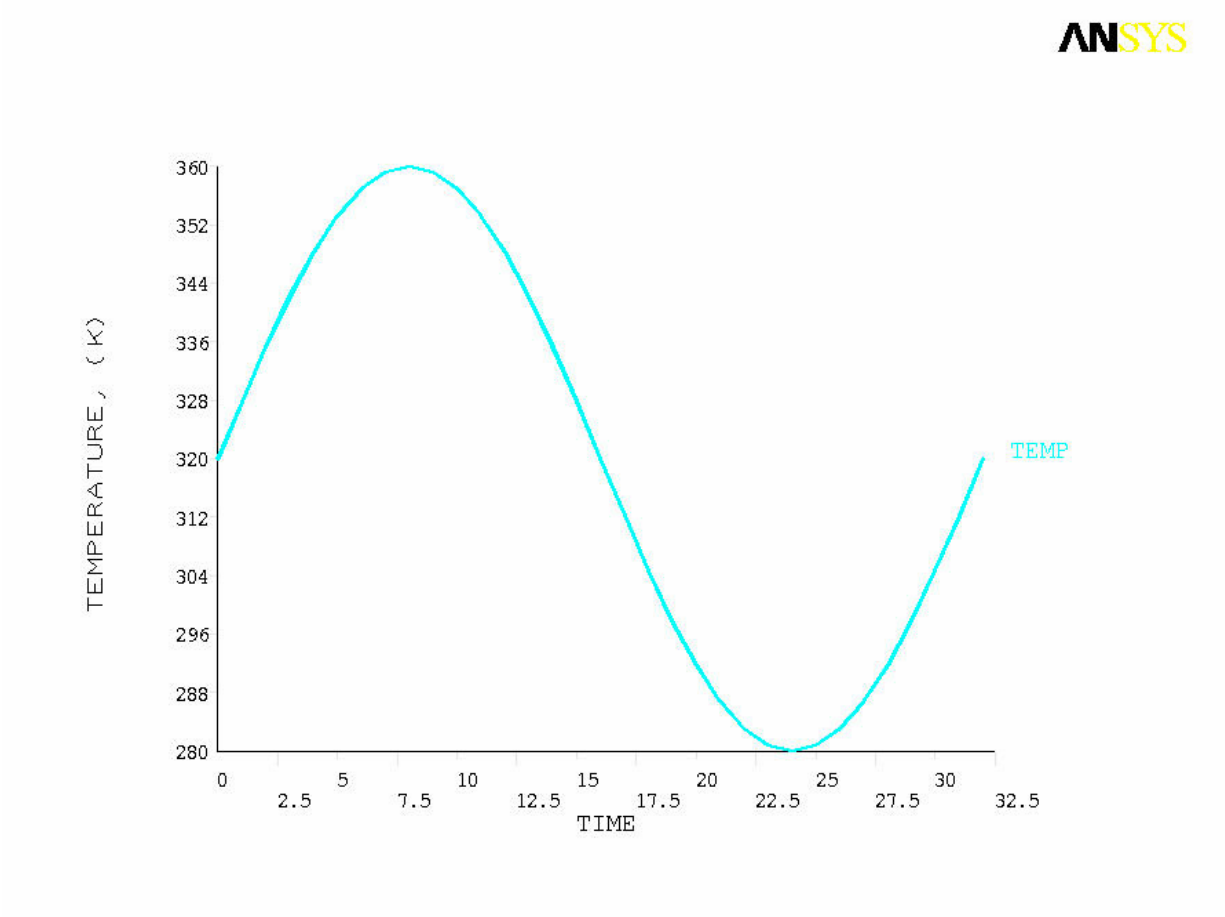

Figure 10 Inlet Temperature Profile

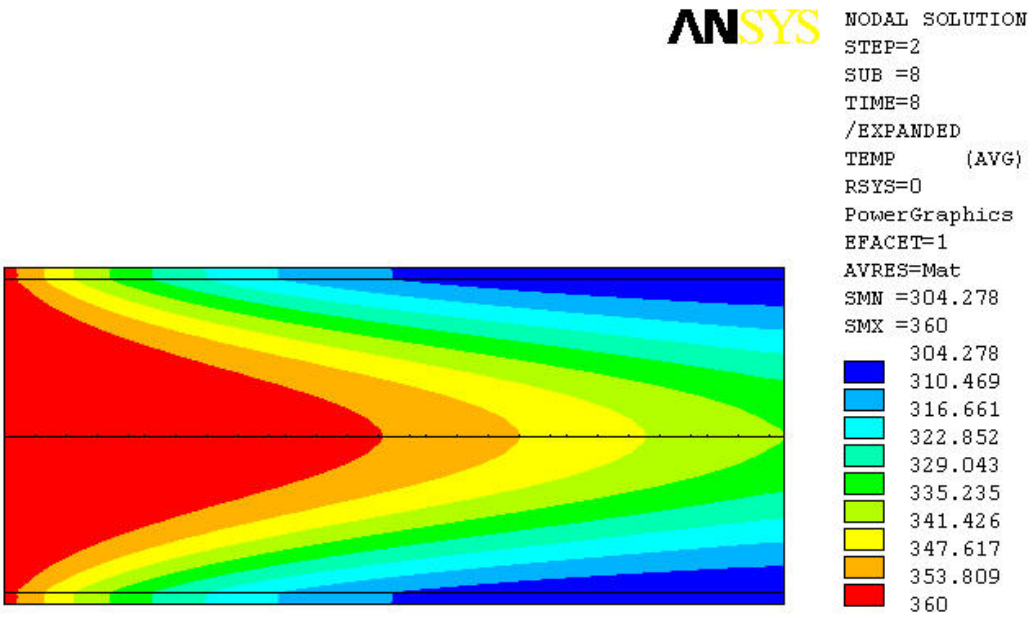

Figure 11 Contours of Temperature at t=8sec

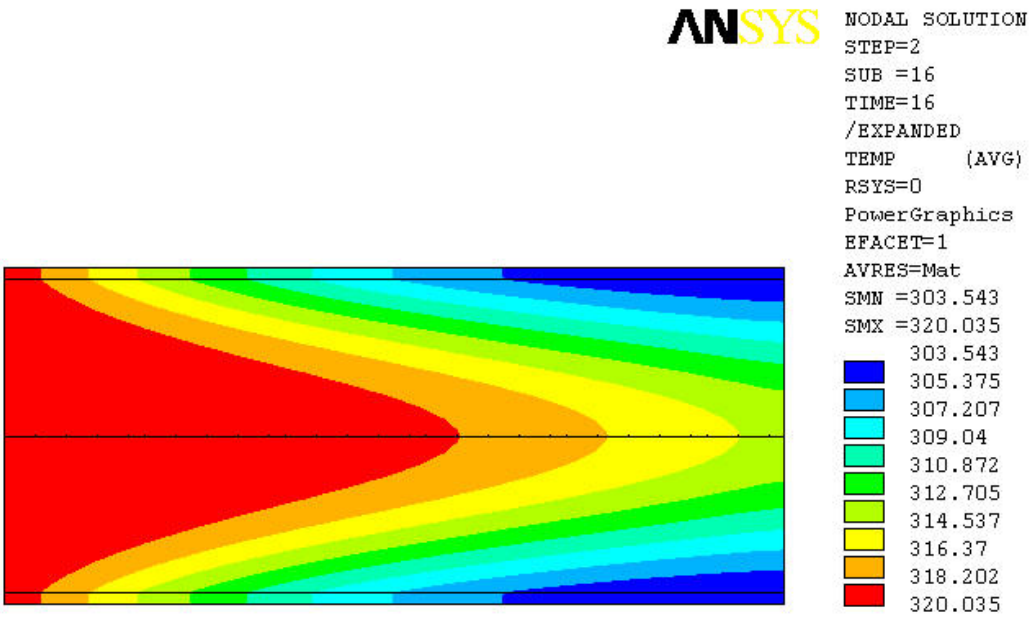

Figure 12 Contours of Temperature at t=16 sec

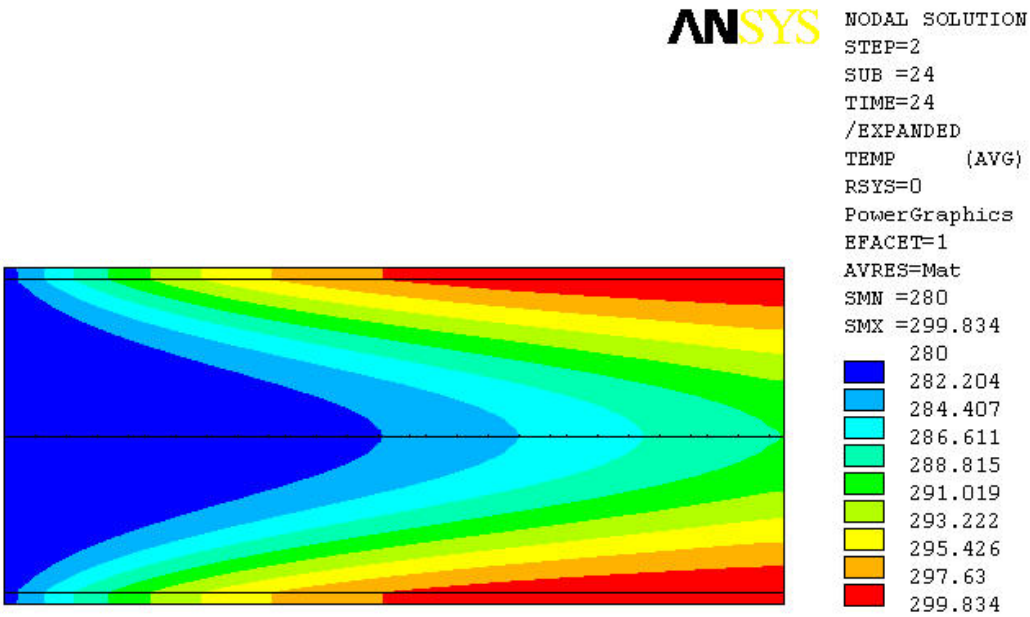

Figure 13 Contours of Temperature at t=24 sec

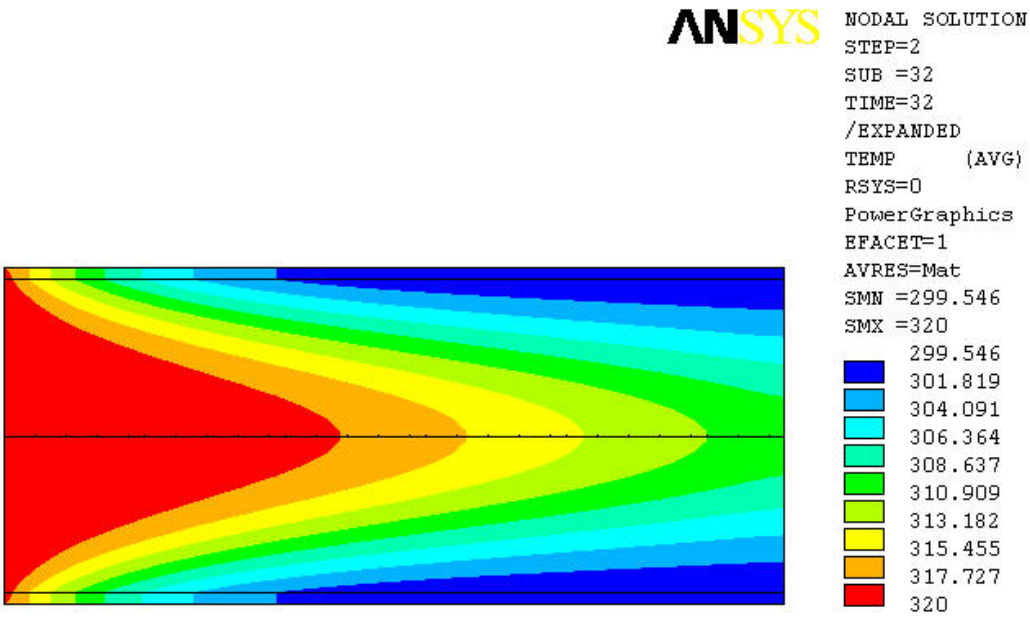

Figure 14 Contours of Temperature at t=32 sec

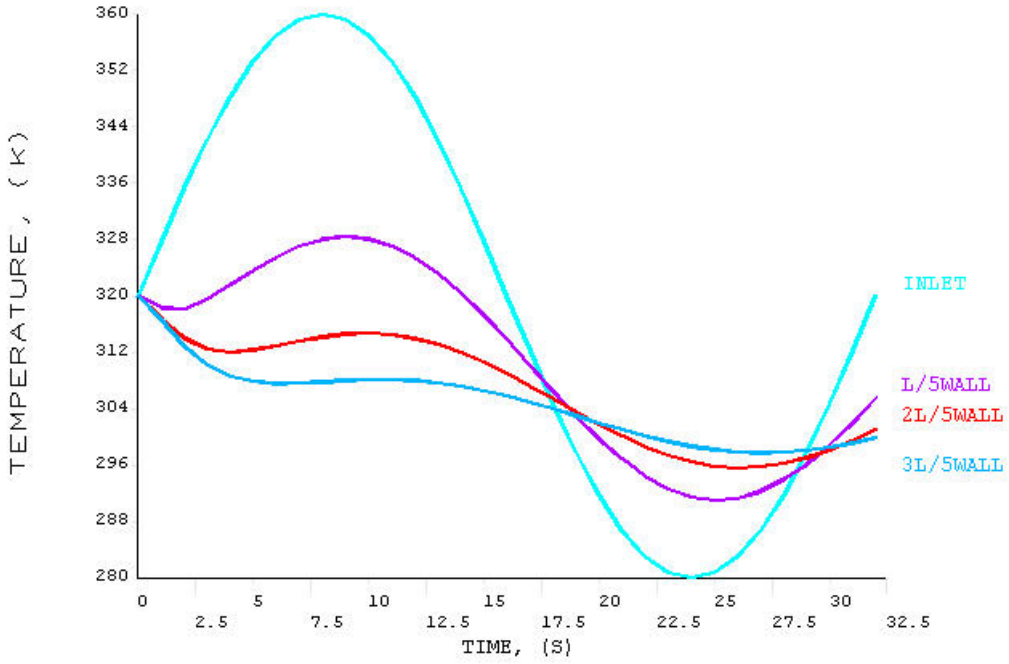

Figure 15 Temperature vs. time for various nodal locations

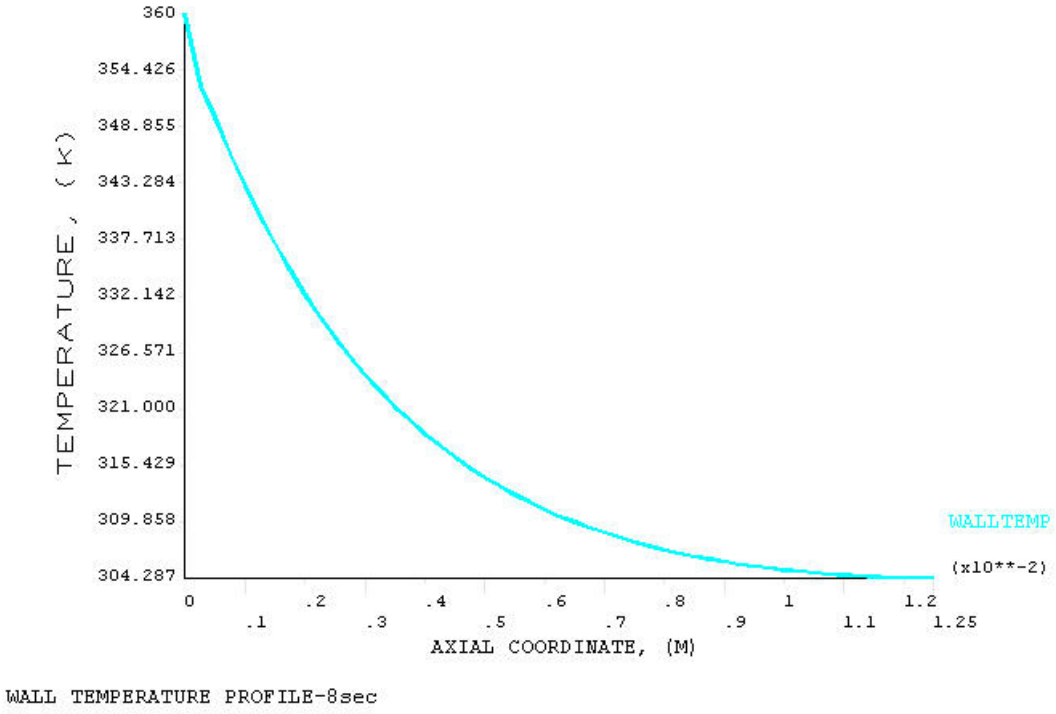

Figure 16 Wall temperature profile at t=8 sec

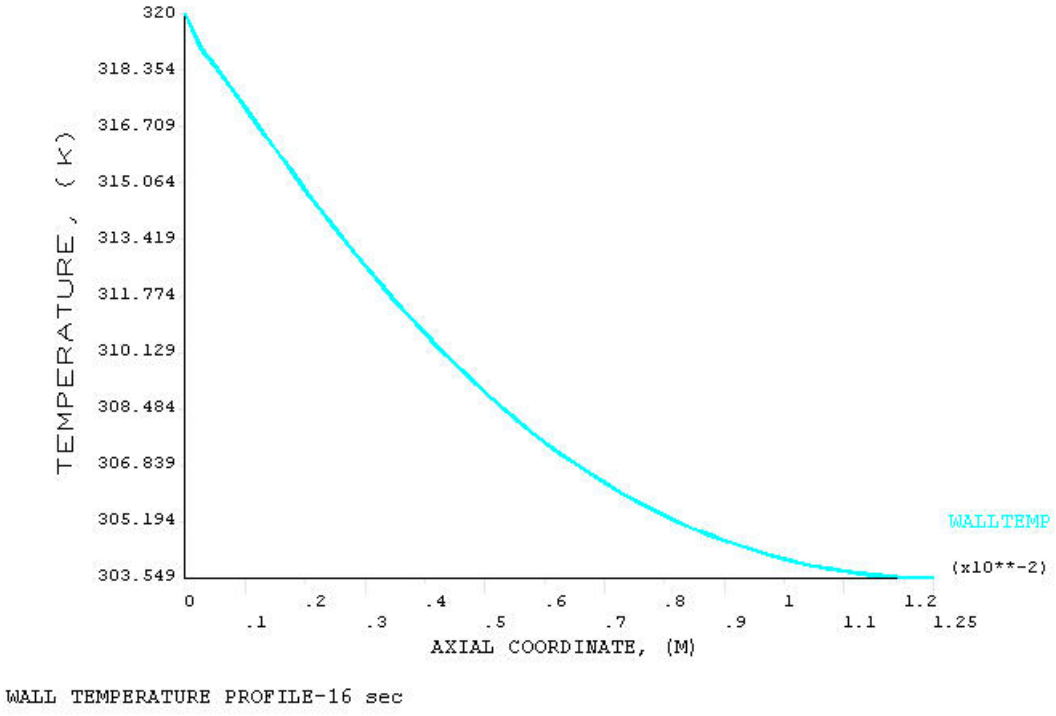

Figure 17 Wall temperature profile at t=16sec

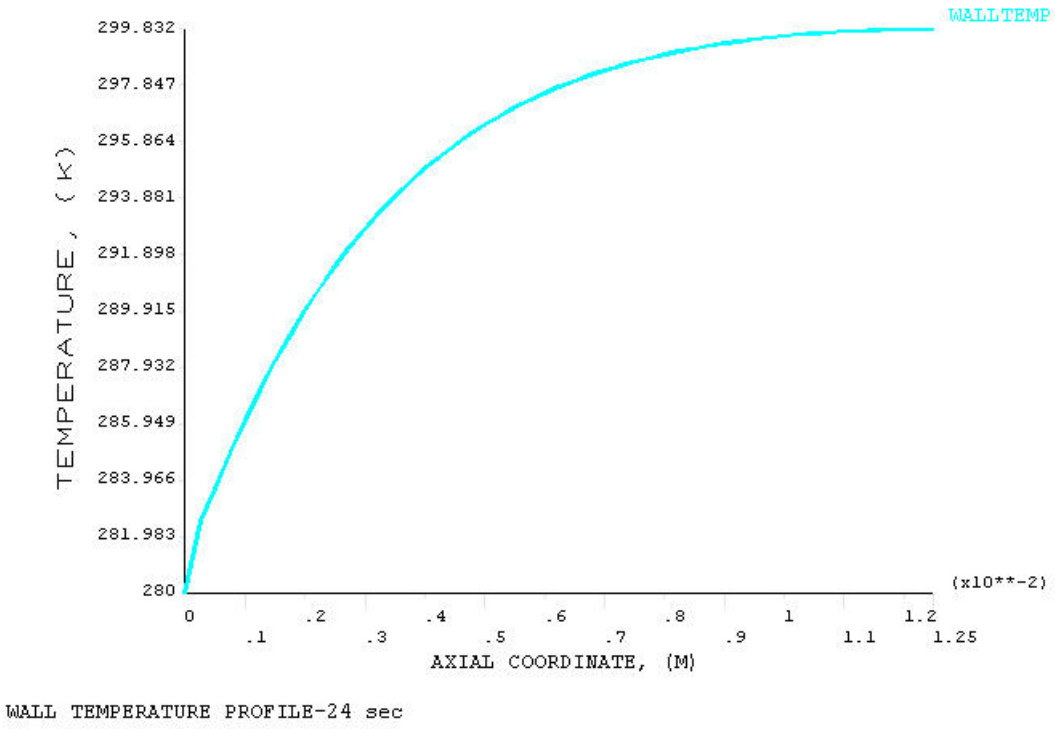

Figure 18 Wall temperature profile at t=24sec

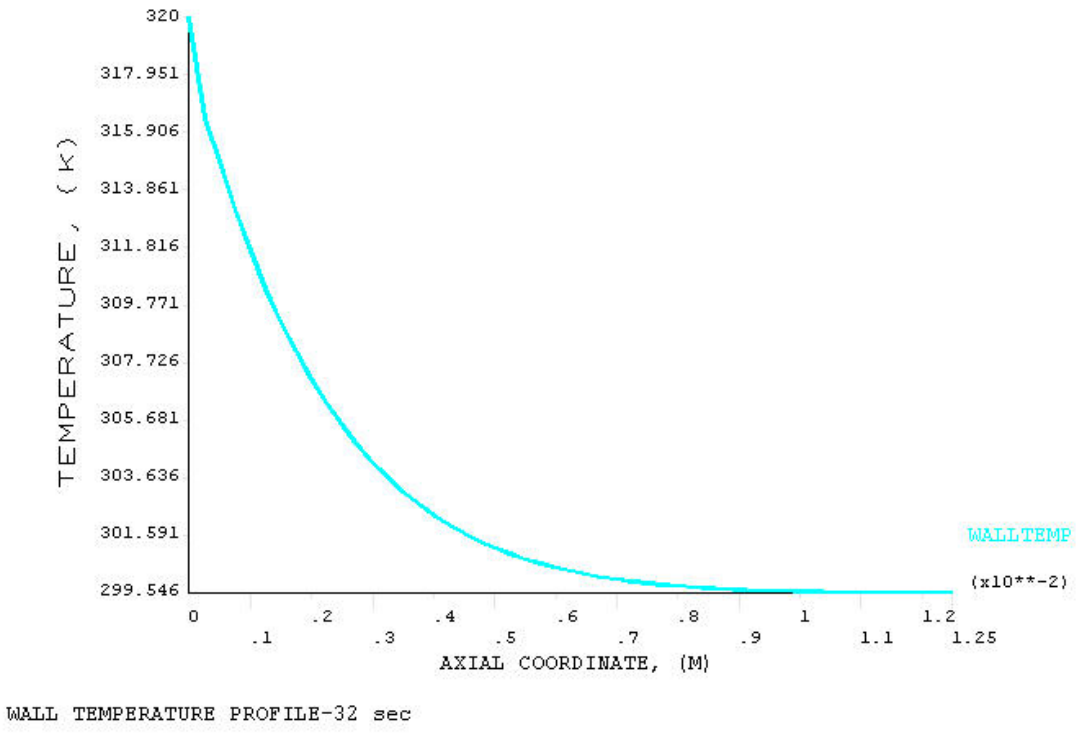

Figure 19 Wall temperature profile at t=32sec

Table 2 Ansys output parameters

PARAMETER STATUS- (46 PARAMETERS DEFINED)
(INCLUDING 25 INTERNAL PARAMETERS)

NAME	VALUE	TYPE	DIMENSIONS		
CP	1007.00000	SCALAR			
H	250.000000	SCALAR			
K	2.630000000E-02	SCALAR			
L	1.250000000E-02	SCALAR			
MDOT	2.883928751E-06	SCALAR			
MU	1.846000000E-05	SCALAR			
PI	3.14159265	SCALAR			
PIN	3.750000000E-02	SCALAR			
R	2.500000000E-03	SCALAR			
RF	9.260000000E-05	SCALAR			
RHO	1.16140000	SCALAR			
RSO	2.000000000E-04	SCALAR			
TAMB	300.000000	SCALAR			
TAU	3.605977865E-03	SCALAR			
TC_O	309.784274	SCALAR			
TIME		TABLE	6	12	1
TIN	300.000000	SCALAR			
TM_O	305.290971	SCALAR			
TW_O	320.000000	SCALAR			
VXC	0.253957389	SCALAR			
VXM	0.126465718	SCALAR			

Table 3 Ansys time history of wall temperatures at various locations

TIME	173 TEMP	156 TEMP	146 TEMP	136 TEMP
INLET	L/5 WALL	2L/5 WALL	3L/5 WALL	
0.0000	320.000	320.000	320.000	320.000
0.0000	320.000	320.000	320.000	320.000
1.0000	327.804	318.314	316.782	316.487
2.0000	335.307	318.200	313.962	312.889
3.0000	342.223	319.506	312.435	310.238
4.0000	348.284	321.498	312.027	308.626
5.0000	353.259	323.631	312.315	307.834
6.0000	356.955	325.567	312.933	307.583
7.0000	359.231	327.090	313.621	307.637
8.0000	360.000	328.066	314.211	307.823
9.0000	359.231	328.408	314.594	308.020
10.000	356.955	328.077	314.701	308.146
11.000	353.259	327.068	314.495	308.151
12.000	348.284	325.408	313.964	308.005
13.000	342.223	323.153	313.114	307.693
14.000	335.307	320.387	311.969	307.217
15.000	327.804	317.213	310.568	306.585
16.000	320.000	313.750	308.961	305.819
17.000	312.196	310.130	307.208	304.943
18.000	304.693	306.492	305.373	303.990
19.000	297.777	302.975	303.528	302.995
20.000	291.716	299.714	301.742	301.995
21.000	286.741	296.834	300.083	301.029
22.000	283.045	294.445	298.616	300.133
23.000	280.769	292.640	297.395	299.341
24.000	280.000	291.487	296.469	298.683
25.000	280.769	291.032	295.872	298.186
26.000	283.045	291.290	295.628	297.867
27.000	286.741	292.253	295.746	297.740
28.000	291.716	293.883	296.221	297.808
29.000	297.777	296.118	297.035	298.070
30.000	304.693	298.872	298.157	298.515
31.000	312.196	302.039	299.543	299.126
32.000	320.000	305.497	301.141	299.880

Table 4 Control volume based Finite difference output

Program to solve unsteady conjugate heat transfer problem SOLUTION at Z= 3.00000

**********RESULTS**********

NEAR-CENTER TEMP= 0.08952493263542 AT TIME= 3.5980800000000
NEAR-CENTER TEMP= 0.18814268660827 AT TIME= 7.1961600000000
NEAR-CENTER TEMP= 0.28525034552911 AT TIME= 10.794240000000
NEAR-CENTER TEMP= 0.37408152311415 AT TIME= 14.392320000000
NEAR-CENTER TEMP= 0.44900897659823 AT TIME= 17.990400000000
NEAR-CENTER TEMP= 0.50551081052496 AT TIME= 21.588480000000
NEAR-CENTER TEMP= 0.54019686355965 AT TIME= 25.186560000000
NEAR-CENTER TEMP= 0.55083008931134 AT TIME= 28.784640000000
NEAR-CENTER TEMP= 0.53633168303619 AT TIME= 32.382720000000
NEAR-CENTER TEMP= 0.49676251153875 AT TIME= 35.980800000000
NEAR-CENTER TEMP= 0.43327618586320 AT TIME= 39.578880000000
NEAR-CENTER TEMP= 0.34804159145023 AT TIME= 43.176960000000
NEAR-CENTER TEMP= 0.24413489326620 AT TIME= 46.775040000000
NEAR-CENTER TEMP= 0.12540297096191 AT TIME= 50.373120000000
NEAR-CENTER TEMP= -0.003.6980950629 AT TIME= 53.971200000000
NEAR-CENTER TEMP= -0.13828448523566 AT TIME= 57.569280000000
NEAR-CENTER TEMP= -0.27323996877993 AT TIME= 61.167360000000
NEAR-CENTER TEMP= -0.40341825146715 AT TIME= 64.765440000000
NEAR-CENTER TEMP= -0.52384505431667 AT TIME= 68.363520000000
NEAR-CENTER TEMP= -0.62991251696682 AT TIME= 71.961600000000
NEAR-CENTER TEMP= -0.71755871985305 AT TIME= 75.559680000000
NEAR-CENTER TEMP= -0.78342562141196 AT TIME= 79.157760000000
NEAR-CENTER TEMP= -0.82498948466387 AT TIME= 82.755840000000
NEAR-CENTER TEMP= -0.84065888709783 AT TIME= 86.353920000000
NEAR-CENTER TEMP= -0.82983662609632 AT TIME= 89.952000000000
NEAR-CENTER TEMP= -0.79294319974349 AT TIME= 93.550080000000
NEAR-CENTER TEMP= -0.73140100523563 AT TIME= 97.148160000000
NEAR-CENTER TEMP= -0.64757989657428 AT TIME= 100.74624000000
NEAR-CENTER TEMP= -0.54470622103384 AT TIME= 104.34432000000
NEAR-CENTER TEMP= -0.42673885241873 AT TIME= 107.94240000000
NEAR-CENTER TEMP= -0.29821700398014 AT TIME= 111.54048000000
NEAR-CENTER TEMP= -0.16408568595541 AT TIME= 115.13856000000

NODE= 1 TEMPERATURE= -0.497200566213283 AT R= 1.00000
NODE= 2 TEMPERATURE= -0.470287883059376 AT R= 0.92593
NODE= 3 TEMPERATURE= -0.441305854226295 AT R= 0.85185
NODE= 4 TEMPERATURE= -0.410393541707785 AT R= 0.77778
NODE= 5 TEMPERATURE= -0.377967528071125 AT R= 0.70370
NODE= 6 TEMPERATURE= -0.344700939566505 AT R= 0.62963
NODE= 7 TEMPERATURE= -0.311478540982138 AT R= 0.55556
NODE= 8 TEMPERATURE= -0.279328470579036 AT R= 0.48148
NODE= 9 TEMPERATURE= -0.249337901944855 AT R= 0.40741
NODE= 10 TEMPERATURE= -0.222565105345318 AT R= 0.33333
NODE= 11 TEMPERATURE= -0.199961914507722 AT R= 0.25926
NODE= 12 TEMPERATURE= -0.182317513586017 AT R= 0.18519
NODE= 13 TEMPERATURE= -0.170227669407784 AT R= 0.11111
NODE= 14 TEMPERATURE= -0.164085685955409 AT R= 0.03704

WALL TEMP= -0.11972192219324 AT TIME= 3.5980800000000
WALL TEMP= -0.20809788001526 AT TIME= 7.1961600000000
WALL TEMP= -0.27305373700169 AT TIME= 10.794240000000
WALL TEMP= -0.32059197856653 AT TIME= 14.392320000000
WALL TEMP= -0.35526429046777 AT TIME= 17.990400000000
WALL TEMP= -0.38052510568670 AT TIME= 21.588480000000
WALL TEMP= -0.39899570905171 AT TIME= 25.186560000000
WALL TEMP= -0.41266149024978 AT TIME= 28.784640000000
WALL TEMP= -0.42301937498003 AT TIME= 32.382720000000
WALL TEMP= -0.43118825844394 AT TIME= 35.980800000000
WALL TEMP= -0.43799208748776 AT TIME= 39.578880000000
WALL TEMP= -0.44402283233687 AT TIME= 43.176960000000
WALL TEMP= -0.44968876455213 AT TIME= 46.775040000000
WALL TEMP= -0.45525207125117 AT TIME= 50.373120000000
WALL TEMP= -0.46085877957736 AT TIME= 53.971200000000
WALL TEMP= -0.46656315980858 AT TIME= 57.569280000000
WALL TEMP= -0.47234816065036 AT TIME= 61.167360000000
WALL TEMP= -0.47814296162384 AT TIME= 64.765440000000
WALL TEMP= -0.48383837182467 AT TIME= 68.363520000000
WALL TEMP= -0.48930053687106 AT TIME= 71.961600000000
WALL TEMP= -0.49438321793345 AT TIME= 75.559680000000
WALL TEMP= -0.49893876422317 AT TIME= 79.157760000000
WALL TEMP= -0.50282780236596 AT TIME= 82.755840000000
WALL TEMP= -0.50592760420080 AT TIME= 86.353920000000
WALL TEMP= -0.50813906189337 AT TIME= 89.952000000000
WALL TEMP= -0.50939219017420 AT TIME= 93.550080000000
WALL TEMP= -0.50965008515788 AT TIME= 97.148160000000
WALL TEMP= -0.50891129329936 AT TIME= 100.74624000000
WALL TEMP= -0.50721057874040 AT TIME= 104.34432000000
WALL TEMP= -0.50461811906041 AT TIME= 107.94240000000
WALL TEMP= -0.50123720501307 AT TIME= 111.54048000000
WALL TEMP= -0.49720056621328 AT TIME= 115.13856000000

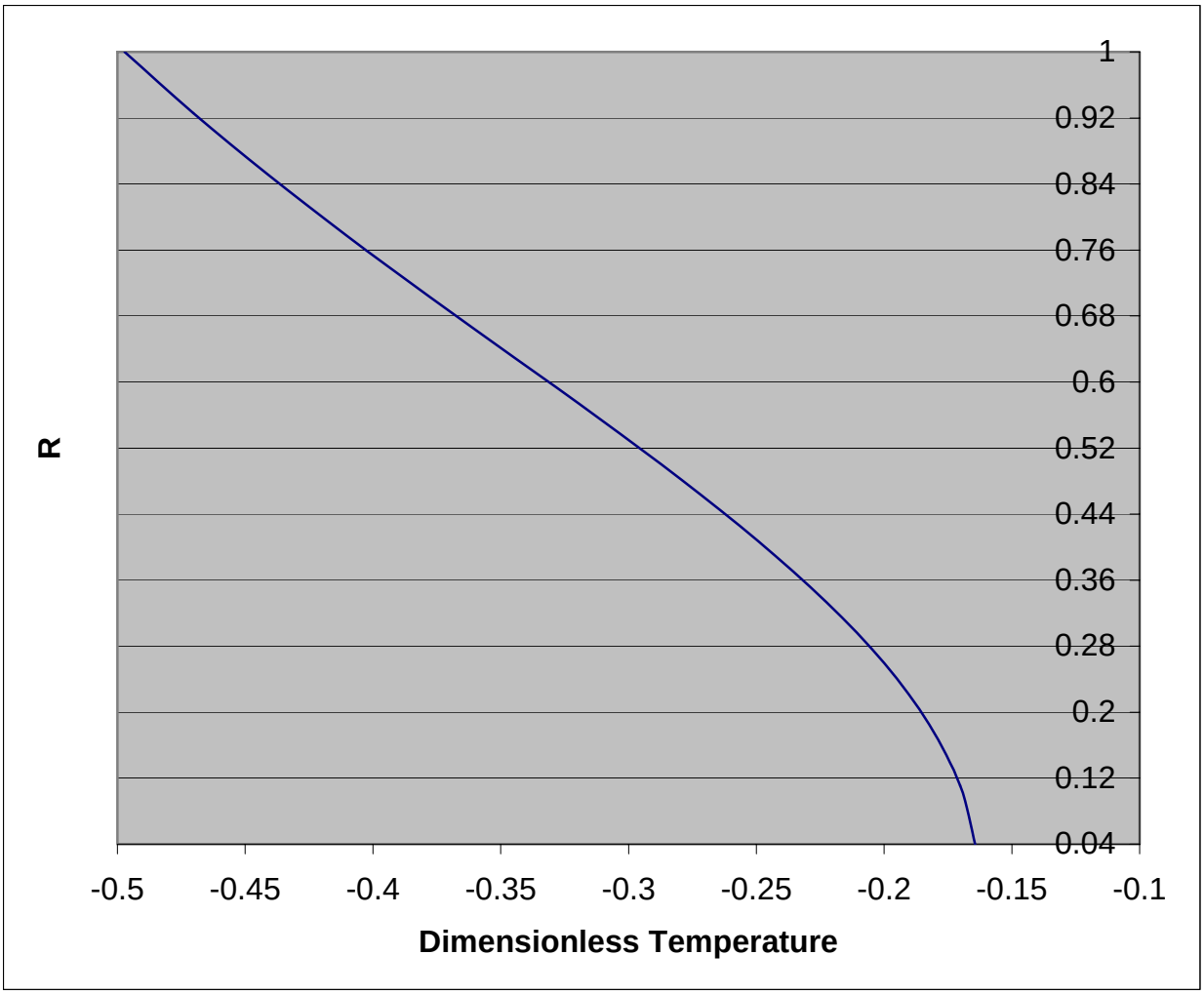

Figure 20 Dimensionless Temperature Profile at Z^* = 3, with Nu_o = 23.76425, Br =279E-09, a^* = 0.00378, Ω = 0.05459, Pe = 14.01245, T_{final} =115.13856, ΔT = 3.59808, Θ_∞ = -0.5, n=1.

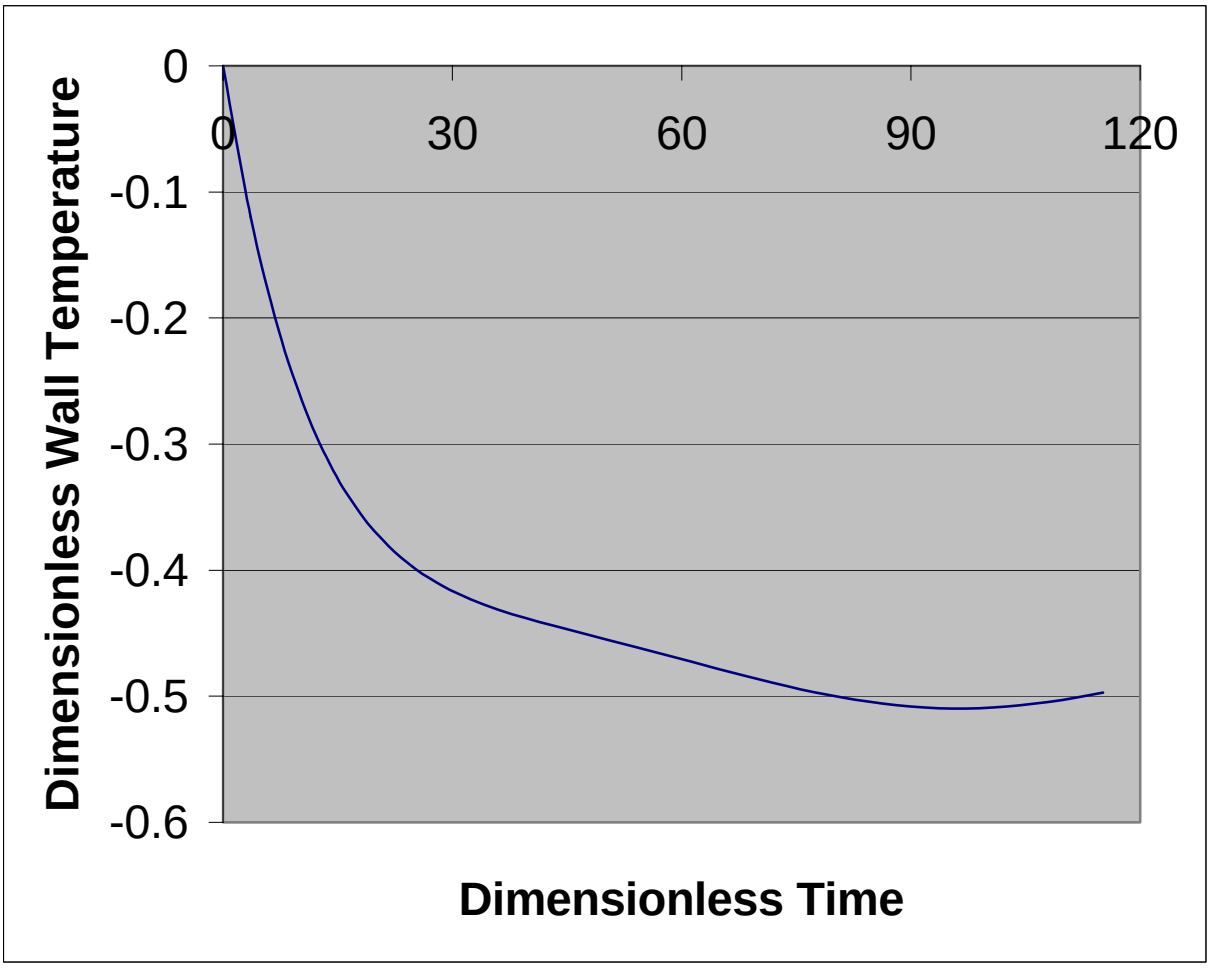

Figure 21Dimensionless Wall Temperature vs.Dimensionless Time at Z^* =3,R=1with Nu_o = 23.76425, Br =279E09, a^* =0.00378, Ω =0.05459, Pe =14.01245, T_{final} =115.13856, ΔT =3.59808, Θ_∞ =-0.5, n=1.

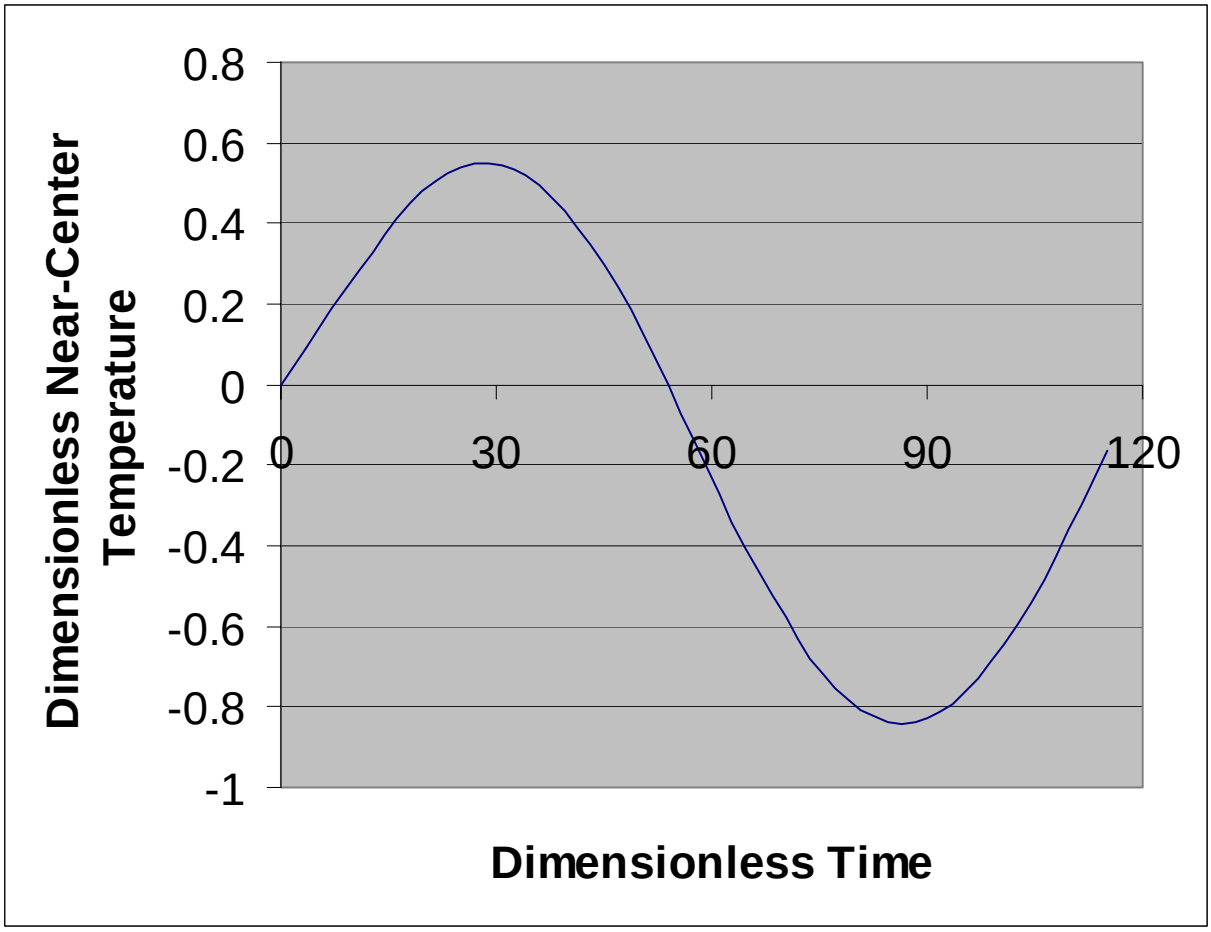

Figure 22 Dimensionless Temperature vs. Dimensionless Time at Z^* = 3,
R=0.03704,with Nu_o = 23.76425, Br =279E09, a^* =0.00378, Ω =0.05459, Pe =14.01245, T_{final} =115.13856, ΔT =3.59808, Θ_∞ =-0.5, n=1.

Table 5 Temperature values at z=0.0075 m , t=32 s.

Node	R	C.V	ANSYS
1	0.25000E-02	300.11	299.88
2	0.23148E-02	301.18	301.31
3	0.21296E-02	302.34	302.84
4	0.19444E-02	303.58	304.43
5	0.17593E-02	304.88	306.06
6	0.15741E-02	306.21	307.67
7	0.13889E-02	307.54	309.22
8	0.12037E-02	308.82	310.66
9	0.10185E-02	310.02	311.95
10	0.83334E-03	311.09	313.05
11	0.64815E-03	312.00	313.96
12	0.46297E-03	312.70	314.64
13	0.27778E-03	313.19	315.11
14	0.92600E-04	313.43	315.35

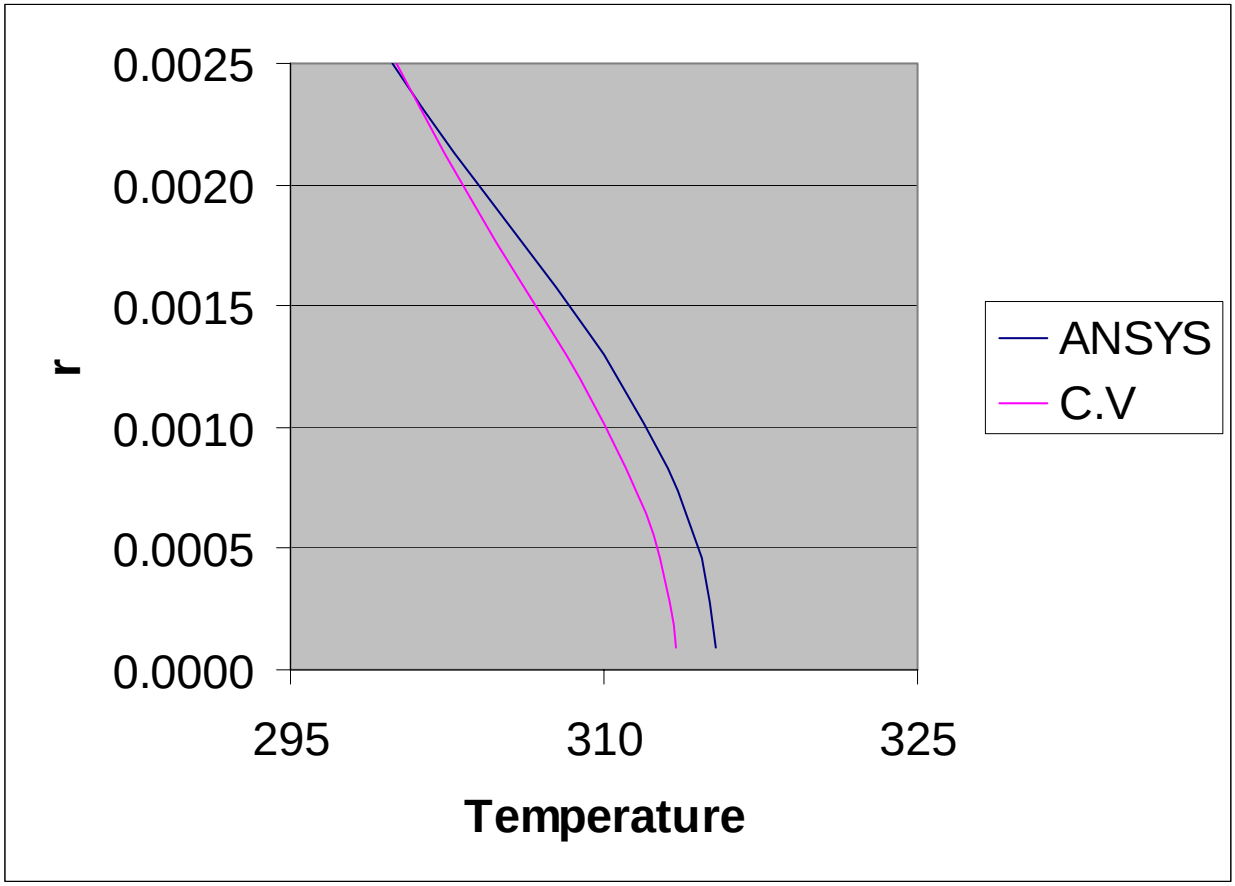

Figure 23 Comparison of Temperature profile at z=0.0075 m, t=32 s.

Table 6 Comparison of time history of wall temperatures at z=0.0075 m

TIME	ANSYS	C.V
0.0000	320.000	320.000
1.0000	316.487	315.211
2.0000	312.889	311.676
3.0000	310.238	309.077
4.0000	308.626	307.176
5.0000	307.834	305.789
6.0000	307.583	304.778
7.0000	307.637	304.040
8.0000	307.823	303.493
9.0000	308.020	303.079
10.000	308.146	302.752
11.000	308.151	302.239
12.000	308.005	302.239
13.000	307.693	302.012
14.000	307.217	301.789
15.000	306.585	301.565
16.000	305.819	301.337
17.000	304.943	301.106
18.000	303.990	300.874
19.000	302.995	300.646
20.000	301.995	300.427
21.000	301.029	300.224
22.000	300.133	300.042
23.000	299.341	299.886
24.000	298.683	299.762
25.000	298.186	299.674
26.000	297.867	299.624
27.000	297.740	299.613
28.000	297.808	299.643
29.000	298.070	299.711
30.000	298.515	299.815
31.000	299.126	299.950
32.000	299.880	300.111

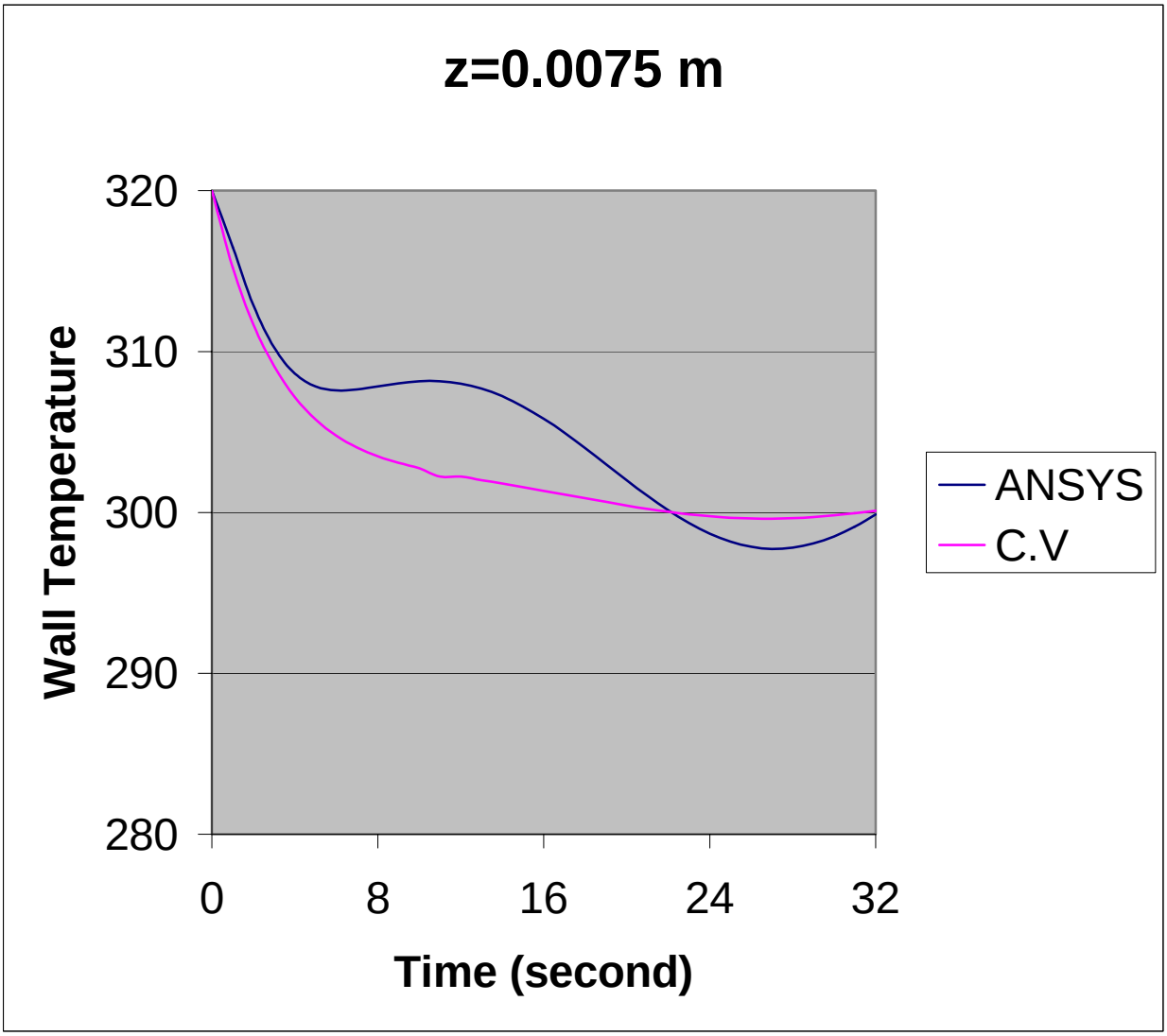

Figure 24 Comparison of Wall Temperatures in time at z=0.0075 m

Table 7 Comparison of Temperature in time at z=0.0075 m, r= 0.92600E-04 m

Node 14-Near Center Temperature

TIME	ANSYS	C.V
0.0000	320.000	320.000
1.0000	324.736	323.580
2.0000	329.969	327.525
3.0000	335.097	331.410
4.0000	339.837	334.963
5.0000	343.888	337.960
6.0000	347.014	340.220
7.0000	349.047	341.607
8.0000	349.882	342.033
9.0000	349.470	341.453
10.000	347.816	339.870
11.000	344.978	337.331
12.000	341.060	333.921
13.000	336.211	329.765
14.000	330.616	325.016
15.000	324.488	319.852
16.000	318.062	314.468
17.000	311.584	309.070
18.000	305.304	303.863
19.000	299.463	299.046
20.000	294.284	294.803
21.000	289.967	291.297
22.000	286.677	288.662
23.000	284.542	287.000
24.000	283.642	286.373
25.000	284.013	286.806
26.000	285.641	288.282
27.000	288.462	290.743
28.000	292.369	294.096
29.000	297.211	298.211
30.000	302.802	302.930
31.000	308.927	308.071
32.000	315.351	313.436

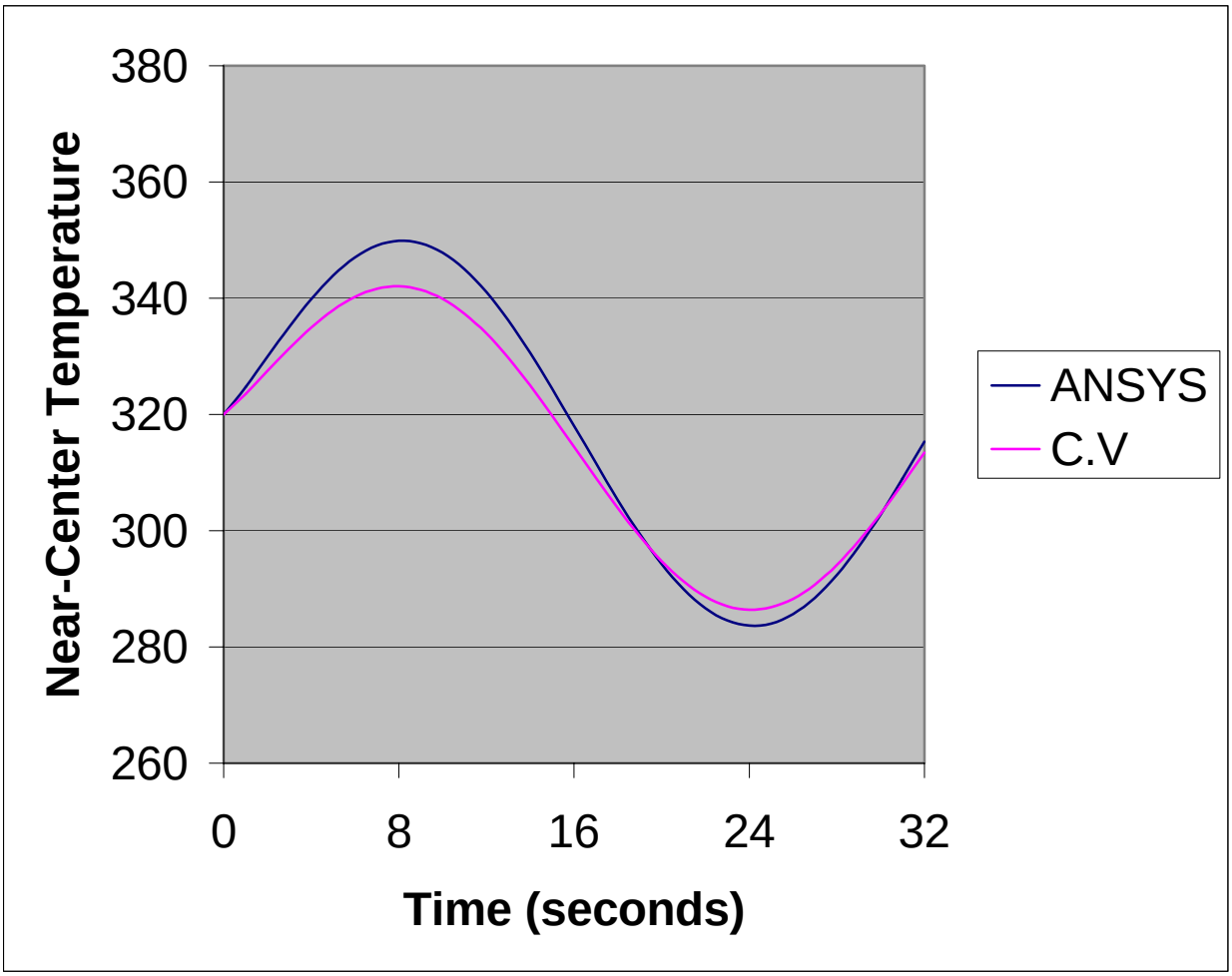

Figure 25 Comparison of Temperature in time at z=0.0075 m, r=0.92600E-04 m

3.2 BENCHMARK SOLUTION: GRAETZ PROBLEM

The problems of steady state conduction of heat and diffusion in a fluid flowing in a circular duct have been studied by many investigators. Let's take the case when the duct wall is maintained at a constant temperature different from the uniform temperature of the fluid at the entrance, and the fluid axial conduction, viscous dissipation, flow work, and thermal energy sources are negligible. This problem is known as the Graetz problem named after Graetz who presented the first published solution [26]. The assumptions and boundary conditions made by Graetz are constant thermal diffusivity, constant tube wall temperature, temperature symmetrical about the axis, uniform temperature at the tube inlet, fully developed parabolic velocity profile at the tube inlet, and negligible conduction in the direction of flow. With those assumptions, for one directional flow in a circular tube, the energy equation becomes,

$$\rho c_p V_z \frac{\partial T}{\partial z} = k \frac{1}{r} \frac{\partial}{\partial r}\left(r \frac{\partial T}{\partial r}\right) \tag{3-1}$$

Equation (3.1) can be written in dimensionless form as

$$\frac{(1-R^2)}{2} \frac{\partial \Theta}{\partial Z^*} = \frac{1}{R} \frac{\partial}{\partial R}\left(R \frac{\partial \Theta}{\partial R}\right) \tag{3–2}$$

, where $Z^* = \dfrac{\alpha\ z}{D^2 V_{AVE}}$ (3-3)

$$R = \frac{r}{a} \tag{3-4}$$

$$\Theta = \frac{T - T_S}{T_e - T_S} \tag{3-5}$$

The assumptions stated before correspond to the following boundary conditions:

$$\Theta = 1 \qquad at \quad Z^* = 0 \tag{3.6}$$

$$\Theta = 0 \qquad at \quad R = 1 \tag{3.7}$$

$$\frac{\partial \Theta}{\partial R} = 0 \qquad at \quad R = 0 \tag{3.8}$$

The solution to Equation (3-2) may be written as [26]

$$\Theta = \sum_{n=0}^{\infty} C_n R_n \exp(-2\lambda_n^2 Z^*) \tag{3.9}$$

where λ_n, R_n, C_n are the eigenvalues, eigenfunctions, and constants, respectively.

Integrating equation (3.2) over the control volume, we have:

$$\frac{1}{2}(\Theta_p - \Theta_w)\left[\left(\frac{R_n^2 - R_s^2}{2}\right) - \left(\frac{R_n^4 - R_s^4}{4}\right)\right] = \left[R_n\left(\frac{\Theta_N - \Theta_p}{\Delta R_n}\right) - R_S\left(\frac{\Theta_P - \Theta_S}{\Delta R_S}\right)\right]\Delta Z^* \tag{3.10}$$

Rearranging the equation in the form as:

$$a_p\,\Theta_p = a_w\,\Theta_w + a_N\,\Theta_N + a_S\,\Theta_S \tag{3.11}$$

$$a_W = \left(\frac{R_n^2 - R_s^2}{2}\right) - \left(\frac{R_n^4 - R_s^4}{4}\right) \tag{3.12}$$

$$a_N = \frac{R_n\,\Delta Z^*}{\Delta R_n} \tag{3.13}$$

$$a_S = \frac{R_S\,\Delta Z^*}{\Delta R_S} \tag{3.14}$$

$$a_P = a_W + a_N + a_S \tag{3.15}$$

The dimensionless temperature distribution for the Graetz problem is displayed in Figures 26, 27 and, 28. As seen from these figures, the control volume based finite difference solution and the Graetz solutions are in excellent agreement.

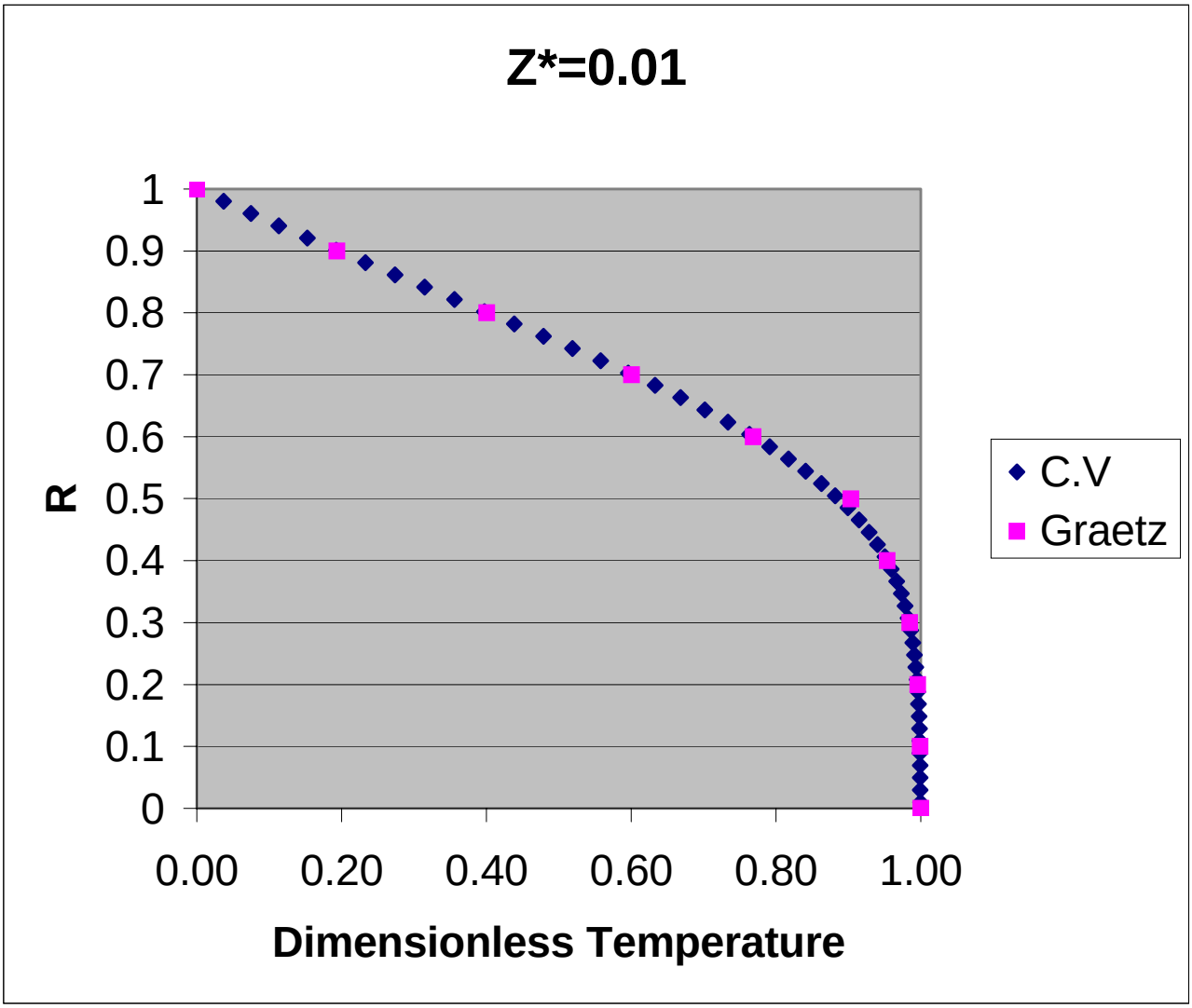

Figure 26 Comparison of Control Volume based Finite Difference Solution and Graetz Solution at Z^* = 0.01 with, Θ_{WALL} = 0, Θ_{INLET} = 1

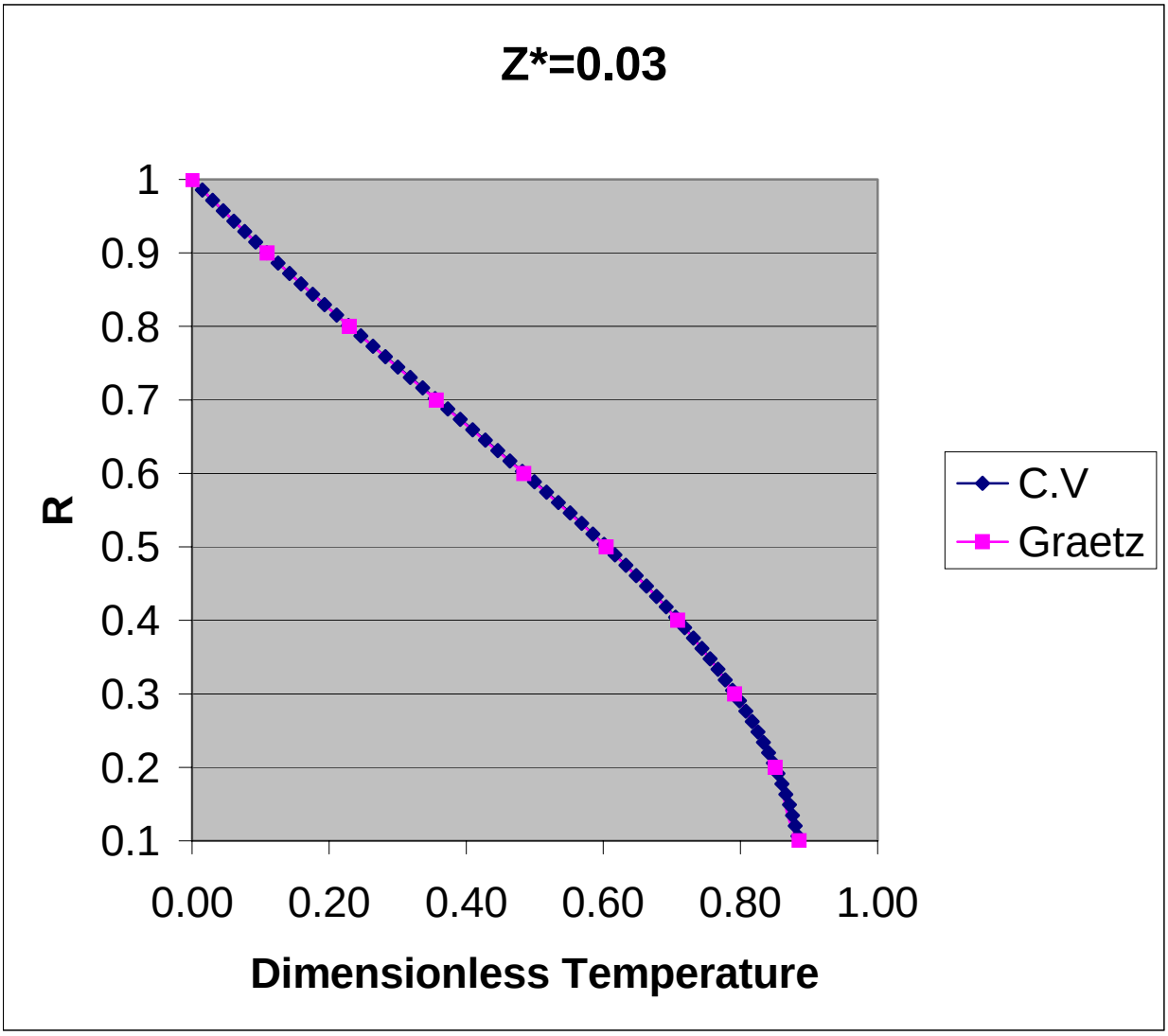

Figure 27 Comparison of Control Volume based Finite Difference Solution and Graetz Solution at Z^* = 0.03, Θ_{WALL} = 0, Θ_{INLET} = 1

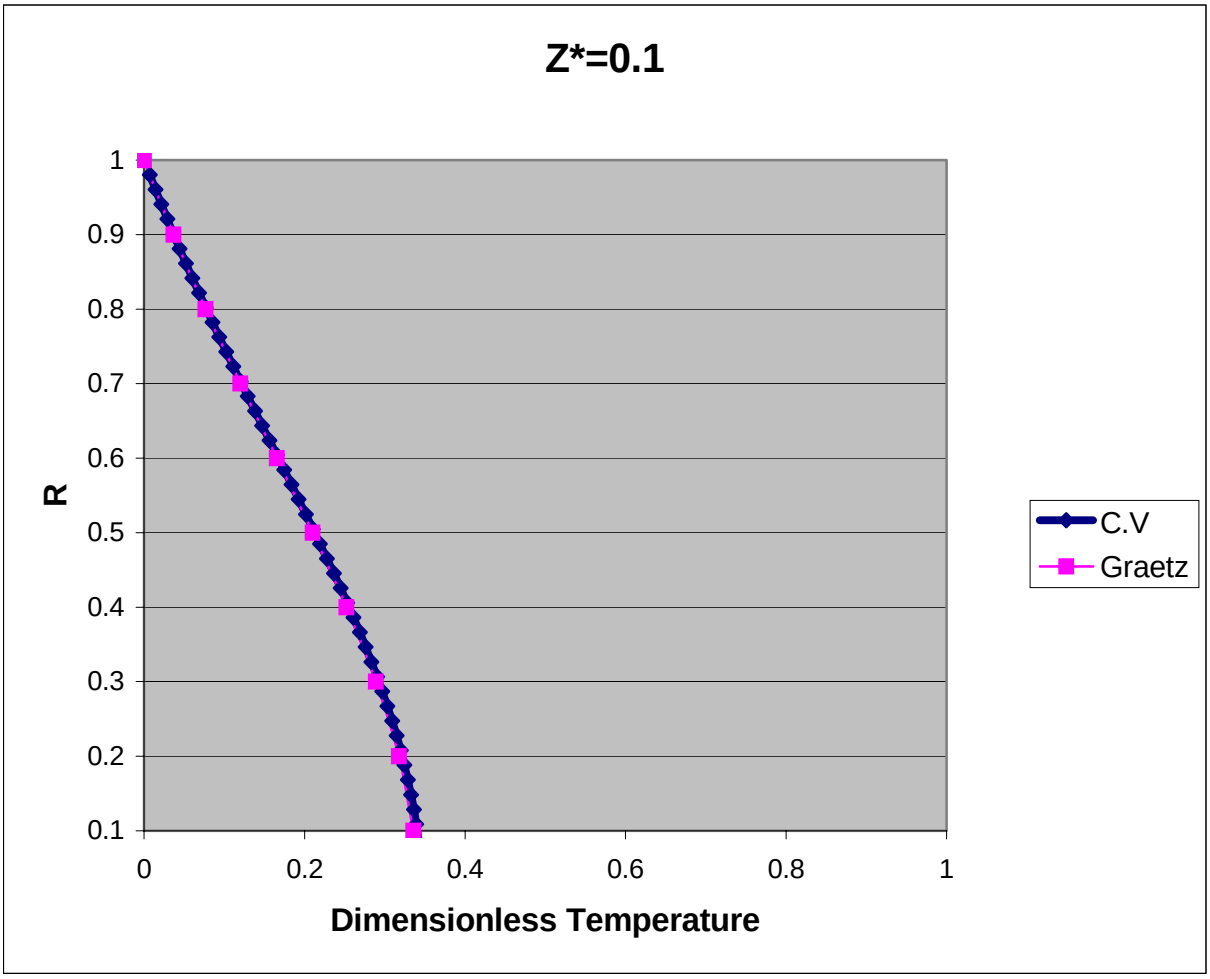

Figure 28 Comparison of Control Volume based Finite Difference Solution and Graetz Solution at Z^* = 0.1, Θ_{WALL} = 0, Θ_{INLET} = 1

4.0 RESULTS

4.1 STABILITY ANALYSIS

We adopted the fully implicit scheme in our work up to this point. It would be interesting to see how our solution would look like if another time scheme is used. For this purpose, we seek a solution for the same energy equation using an explicit scheme. The explicit scheme essentially assumes that the old value Θ_p^o prevails throughout the entire time step except at time $\mathrm{T}+\Delta\mathrm{T}$. Also, on the other hand, the fully implicit scheme assumes that, at time T, Θ_p suddenly drops from Θ_p^o to Θ_p and then stays at Θ_p over the whole time step.

Integrating the energy equation (2.20) over the control volume and using the explicit scheme we have as follows,

$$\frac{\Theta_p-\Theta_p^o}{\Delta\mathrm{T}}\quad\frac{R_n^2-R_s^2}{2}\Delta Z^*+Pe\,V_{zp}^*(\Theta_p^o-\Theta_w^o)\frac{R_n^2-R_s^2}{2}$$
$$=\left[R_n\left(\frac{\Theta_N^o-\Theta_p^o}{\Delta R_n}\right)-R_S\left(\frac{\Theta_P^o-\Theta_S^o}{\Delta R_S}\right)\right]\Delta Z^*+\Delta Z^*Br\;R_P\;\Delta R\;\left|\frac{V_n^*-V_s^*}{\Delta R}\right|^{n-1}\left(\frac{V_n^*-V_s^*}{\Delta R}\right)^2 \tag{4.1}$$

Rearranging the equation in the form as:

$$a_p\,\Theta_p=a_W^o\,\Theta_W^o+a_N^o\,\Theta_N^o+a_S^o\,\Theta_S^o+a_p^o\,\Theta_p^o+d \tag{4.2}$$

$$a_W^o=\left(Pe\;V_{zp}^*\frac{R_n^2-R_s^2}{2}\right) \tag{4.3}$$

$$a_N^o=\frac{R_n\,\Delta Z^*}{\Delta R_n} \tag{4.4}$$

$$a_S^o = \frac{R_S \, \Delta Z^*}{\Delta R_S} \tag{4.5}$$

$$a_p^o = \frac{R_n^2 - R_s^2}{2} \frac{\Delta Z^*}{\Delta \mathrm{T}} - a_W^o \; - a_N^o \; - a_S^o \tag{4.6}$$

$$d = \Delta Z^* Br \, R_p \; \Delta R \; \left| \frac{V_n^* - V_s^*}{\Delta R} \right|^{n-1} \left(\frac{V_n^* - V_s^*}{\Delta R} \right)^2 \tag{4.7}$$

$$a_p = a_W^o + a_N^o + a_S^o + a_p^o \tag{4.8}$$

The equation for the wall boundary condition is integrated over the half control volume adjacent to the wall, which leads to,

$$-\left(\frac{\Theta_P^o - \Theta_S^o}{\Delta R_S} \right) = \frac{1}{a^*} \left(\frac{\Theta_P - \Theta_P^o}{\Delta T} \right) + Nu_0 (\Theta_P^o - \Theta_\infty) \tag{4.9}$$

Rearranging the equation gives the following;

$$a_S^o = \frac{1}{\Delta R_S} \tag{4.10}$$

$$a_P^o = \frac{1}{a^* \Delta T} - \frac{1}{\Delta R_S} - Nu_0 \tag{4.11}$$

$$d \; = \; Nu_0 \; \Theta_\infty \tag{4.12}$$

$$a_P = a_S^o + a_P^0 + Nu_0 \tag{4.13}$$

For the explicit scheme, Θ_p is explicitly obtainable in terms of the known temperatures $\Theta_W^o \; , \Theta_N^o \; , \Theta_S^o \; , \Theta_p^o$ Examining equations 4.6 and 4.11, we note that the coefficient of Θ_p^o can become negative, which violates the rule of positive coefficients. If this rule is violated, physically unrealistic results could emerge, because the negative coefficient implies that a higher Θ_p^o results in a lower Θ_p [28]. This condition is the stability criterion for the explicit scheme. The time step $\Delta \mathrm{T}$ would have to be small enough so that a_P^o is positive. With the current input values, an unrealistic solution can be obtained for $\Delta \mathrm{T} \geq 0.0018$ as displayed in Figure 29. For this

time step and larger, the coefficient of Θ_p^o is negative. As we use a smaller time step, the result of the explicit scheme shows in very good agreement with the fully implicit scheme as shown in Table 8. Since we are restricted to use small time steps to avoid instability for the explicit scheme, it becomes very costly in terms of CPU time and storage. On the other hand, the fully implicit scheme ensures that the coefficient of Θ_p^o is never negative. It can be used with a large time step and it satisfies the requirement of physically satisfactory behavior. For this reason, we will continue to use the fully implicit scheme in this work.

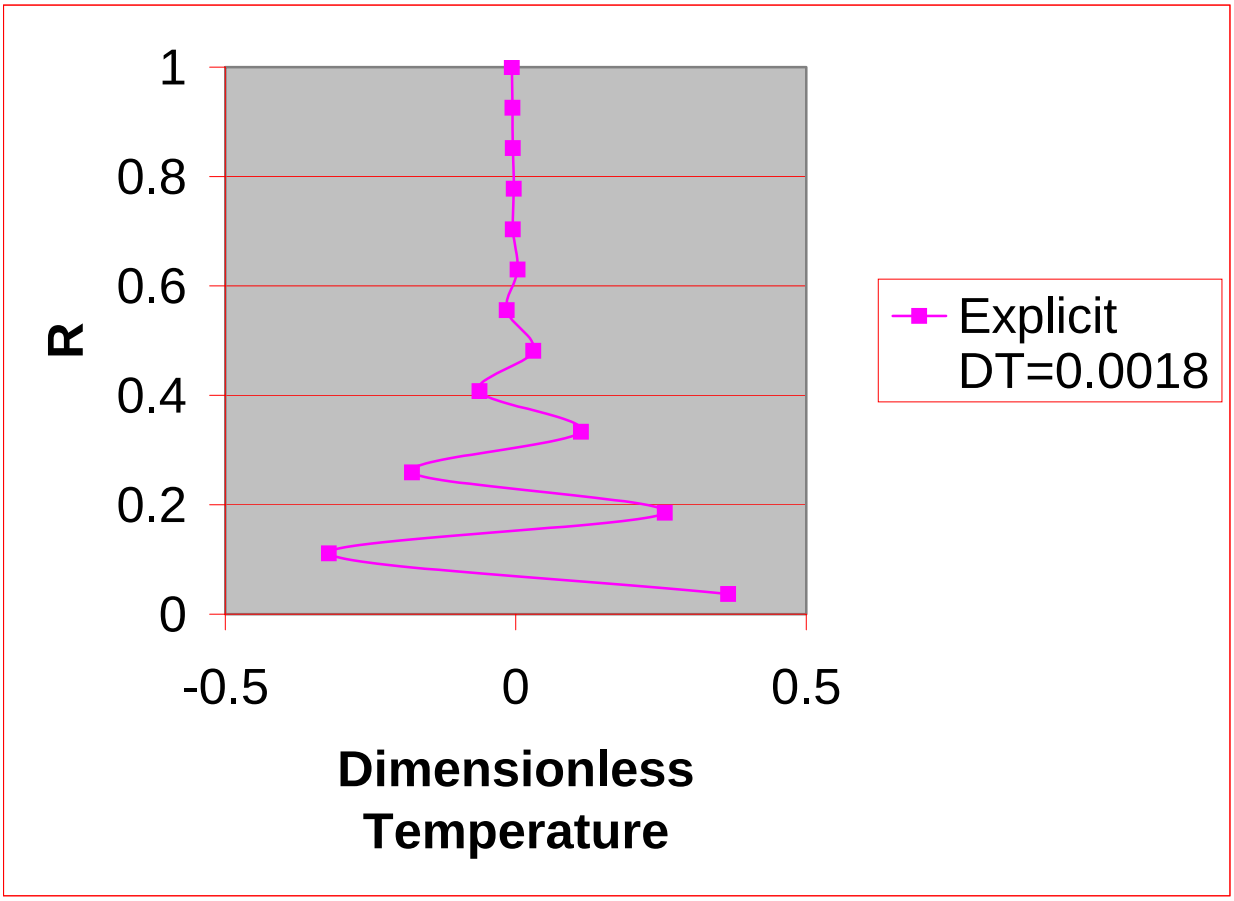

Figure 29 Explicit Scheme Solution with Nu_o =23.76425, Br =279E-09, a^* = 0.00378, Ω = 0.05459, Pe = 14.01245, T_{final} =0.15, ΔT = 0.0018, Θ_∞ = -0.5, n=1, Z*=3.

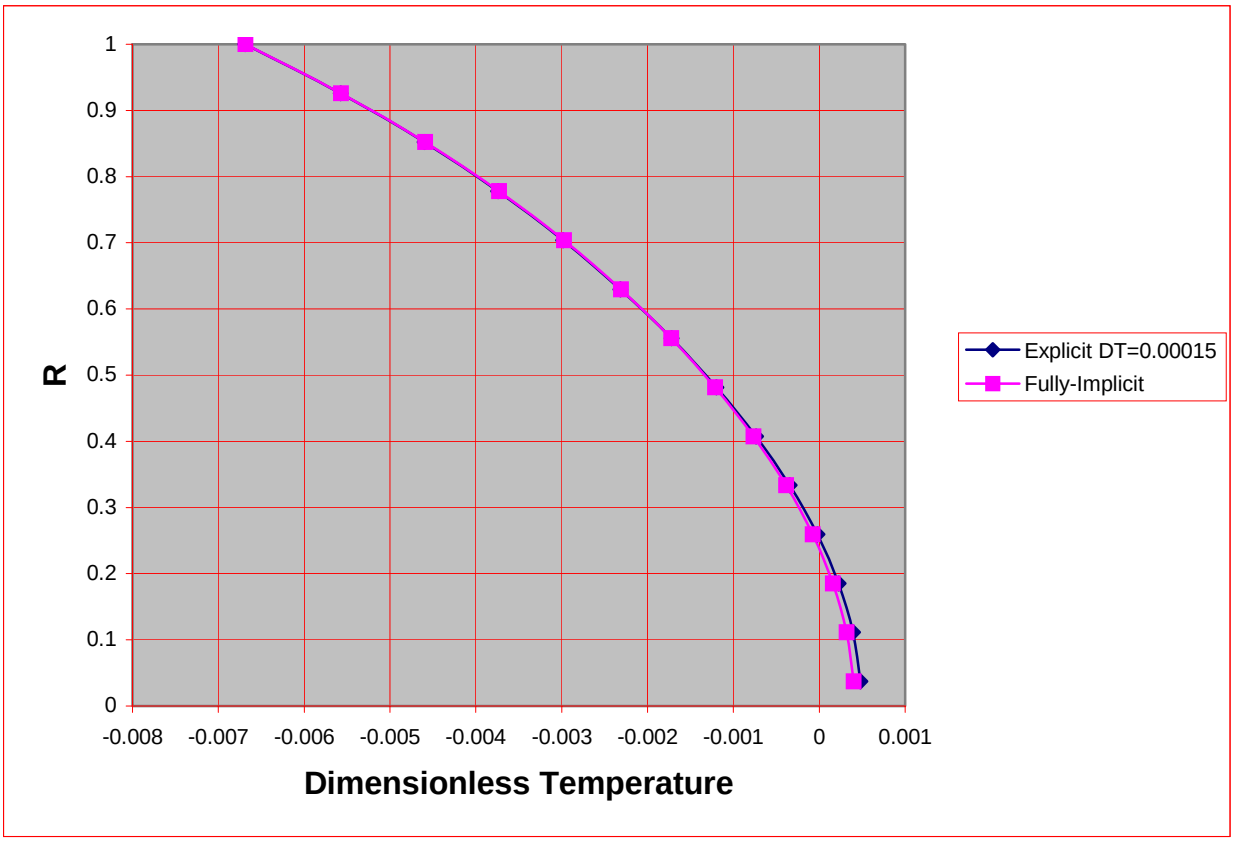

Figure 30 Comparison of Explicit and Fully-Implicit Scheme Solution with Nu_o =23.76425, Br =279E-09, a^* = 0.00378, Ω = 0.05459, Pe = 14.01245, T_{final} =0.15, ΔT = 0.00015, Θ_∞ = -0.5, n=1, Z*=3.

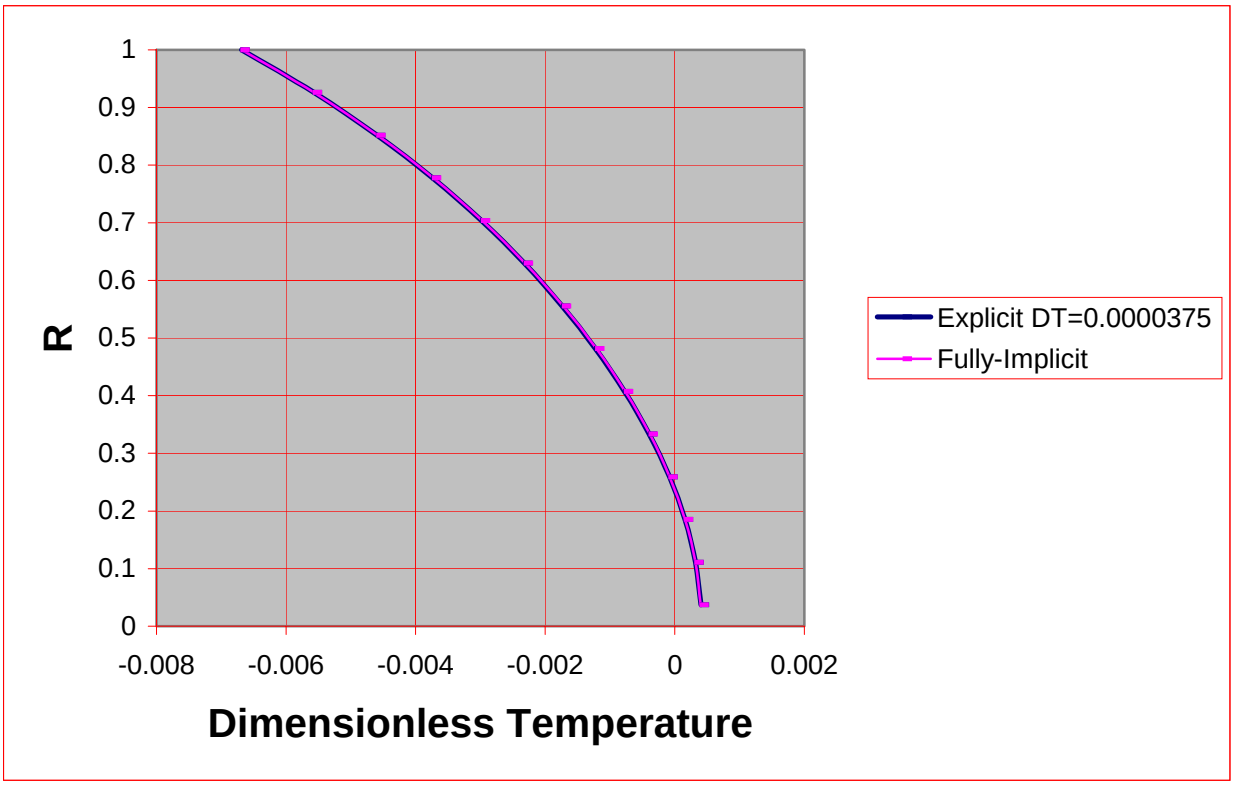

Figure 31 Comparison of Explicit and Fully-Implicit Scheme Solution with $Nu_o = 23.76425$, Br =279E-09, $a^* =$ 0.00378, Ω = 0.05459, Pe = 14.01245, T_{final} =0.15, ΔT = 0.0000375, Θ_∞ = -0.5, n=1, Z*=3.

Table 8 Comparison of Temperature with different time schemes with $Nu_o = 23.76425$, Br =279E-09, a^* = 0.00378, Ω = 0.05459, Pe = 14.01245, T_{final} =0.15, ΔT = 0.0000375, Θ_∞ = -0.5, n=1, Z*=3.

Explicit-Scheme

TEMPERATURE=	-0.00669	AT R=	1
TEMPERATURE=	-0.00557	AT R=	0.92593
TEMPERATURE=	-0.00459	AT R=	0.85185
TEMPERATURE=	-0.00374	AT R=	0.77778
TEMPERATURE=	-0.00299	AT R=	0.7037
TEMPERATURE=	-0.00232	AT R=	0.62963
TEMPERATURE=	-0.00174	AT R=	0.55556
TEMPERATURE=	-0.00122	AT R=	0.48148
TEMPERATURE=	-0.00077	AT R=	0.40741
TEMPERATURE=	-0.00039	AT R=	0.33333
TEMPERATURE=	-8.1E-05	AT R=	0.25926
TEMPERATURE=	0.000158	AT R=	0.18519
TEMPERATURE=	0.000321	AT R=	0.11111
TEMPERATURE=	0.000403	AT R=	0.03704

Fully-Implicit Scheme

TEMPERATURE=	-0.00669	AT R=	1
TEMPERATURE=	-0.00557	AT R=	0.92593
TEMPERATURE=	-0.00459	AT R=	0.85185
TEMPERATURE=	-0.00373	AT R=	0.77778
TEMPERATURE=	-0.00297	AT R=	0.7037
TEMPERATURE=	-0.00231	AT R=	0.62963
TEMPERATURE=	-0.00173	AT R=	0.55556
TEMPERATURE=	-0.00121	AT R=	0.48148
TEMPERATURE=	-0.00077	AT R=	0.40741
TEMPERATURE=	-0.00039	AT R=	0.33333
TEMPERATURE=	-7.8E-05	AT R=	0.25926
TEMPERATURE=	0.000159	AT R=	0.18519
TEMPERATURE=	0.00032	AT R=	0.11111
TEMPERATURE=	0.000401	AT R=	0.03704

4.2 GRID INDEPENDENT STUDY

In general, an accurate solution should be obtained when the grid is sufficiently fine. But there is no need to employ a fine grid in regions where the dependent variable (in this case Θ) changes rather slowly with the independent variable. On the other hand, a fine grid is required where the dependent variable~independent variable is steep [27]. The number of grid points needed for a given accuracy is a matter that depends on the nature of the problem to be solved.

In order to find the pattern of the dependent variable~independent variable variation, the grid sizes were varied. As seen from figure 32 and figure 35, the dependent variable Θ changes slowly with Z*. That is the reason we don't see much change in Θ with a different grid size in the Z* direction. On the other hand, the maximum solution difference with various grid sizes in R and Z* directions is found to be 10 percent (Figure 34). It is found that an appropriate grid size would be $R_{nodes} * Z^*_{nodes} \geq 50 * 30$, since there is not significant change in the solution. The independent variable became independent of grid size beyond $R_{nodes} * Z^*_{nodes} \geq 50 * 30$ as it can be seen from Figure 34. Hence, with the given parameters and boundary conditions, it is concluded that $R_{nodes} * Z^*_{nodes} \geq 50 * 30$ should be good enough to get a satisfactory solution for this problem. The maximum solution difference between grid sizes of $R_{nodes} * Z^*_{nodes} = 50 * 30$ and $R_{nodes} * Z^*_{nodes} = 10 * 10$ is found to be 1.3 percent. Keep in mind that using a very small grid size requires more CPU time and storage.

But if parameters and boundary conditions are changed, the preliminary grid solutions can be used to construct suitable grid. The grid spacing should be directly linked to the way the dependent variable changes in the calculation domain.

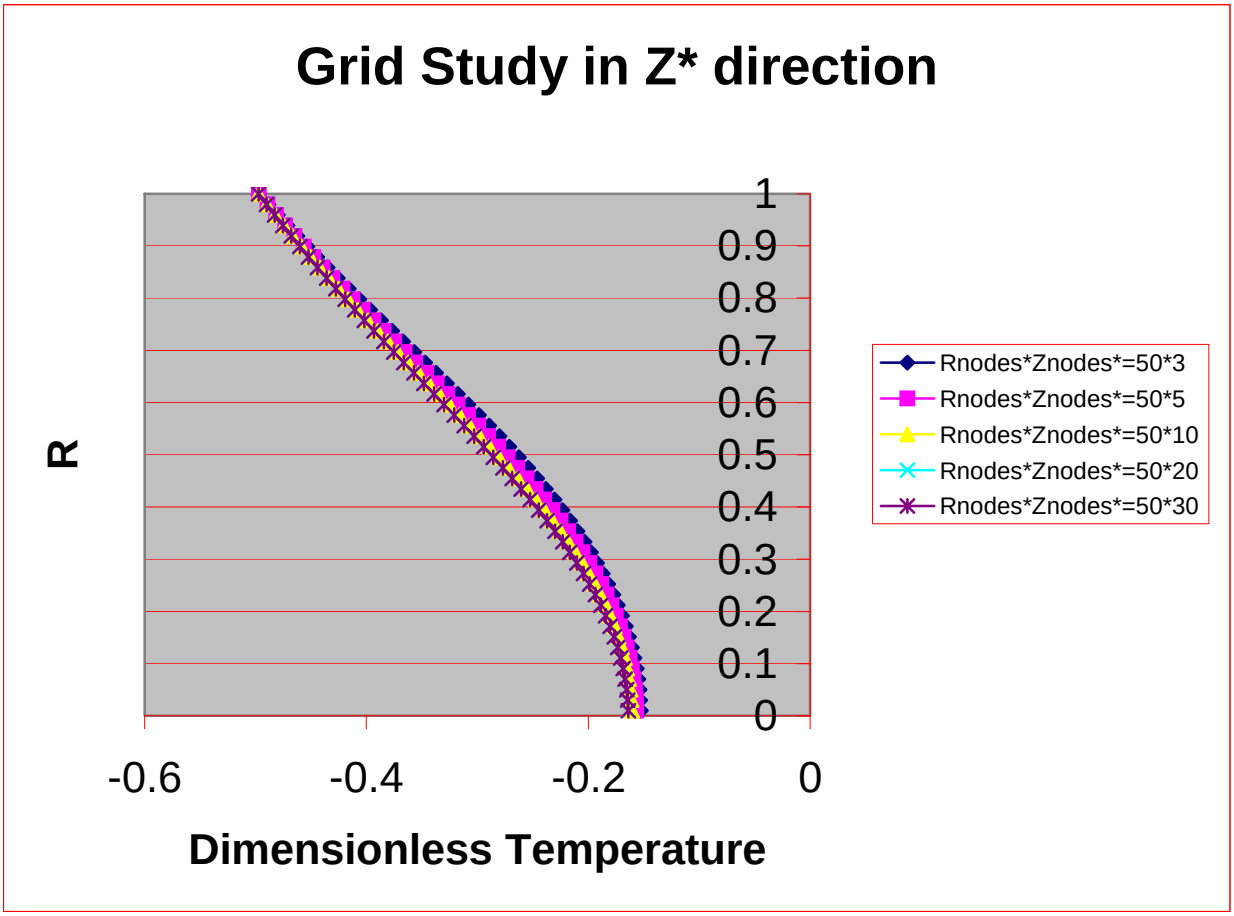

Figure 32 Grid Study with different grid size in Z* direction with Nu_o = 23.76425, Br =279E-09, a^* = 0.00378, Ω = 0.05459, Pe = 14.01245, T_{final} =115.13856, ΔT = 3.59808, Θ_∞ = -0.5, n=1, Z*=3.

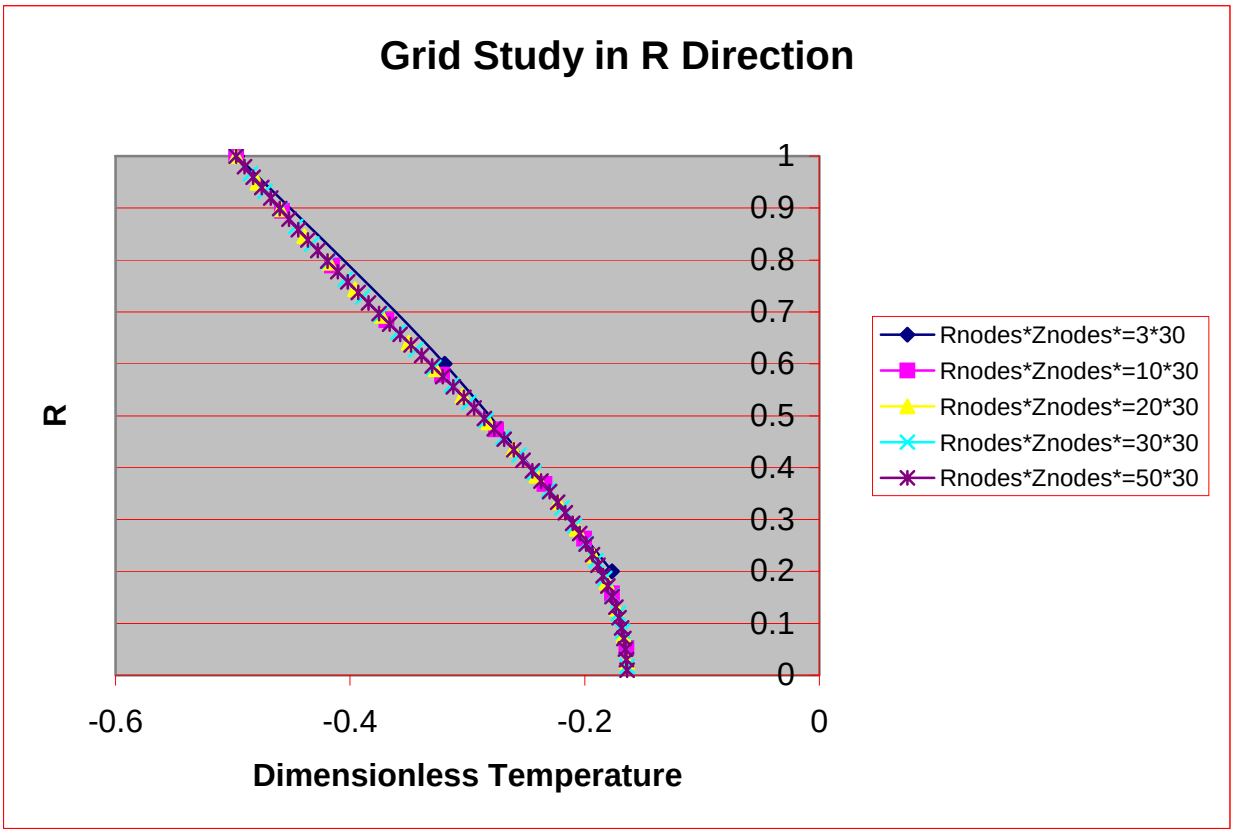

Figure 33 Grid Study with different grid size in R direction Nu_o =23.76425, Br =279E-09, a^* = 0.00378, Ω = 0.05459, Pe = 14.01245, T_{final} =115.13856, ΔT = 3.59808, Θ_∞ = -0.5, n=1, Z*=3.

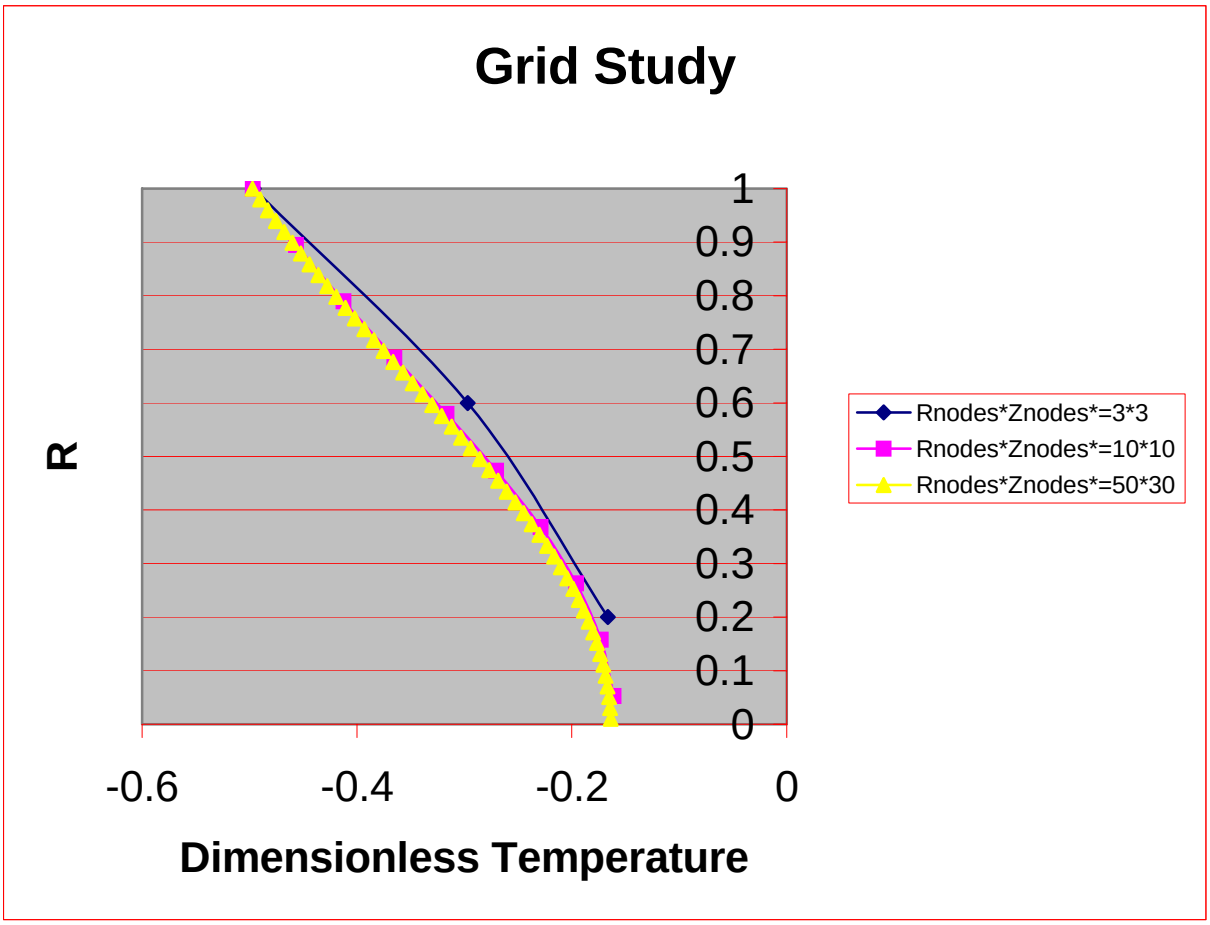

Figure 34 Grid Study with different grid size in R and Z* directions Nu_o = 23.76425, Br =279E-09, a^* = 0.00378, Ω = 0.05459, Pe = 14.01245, T_{final} =115.13856, ΔT = 3.59808, Θ_∞ = -0.5, n=1, Z*=3.

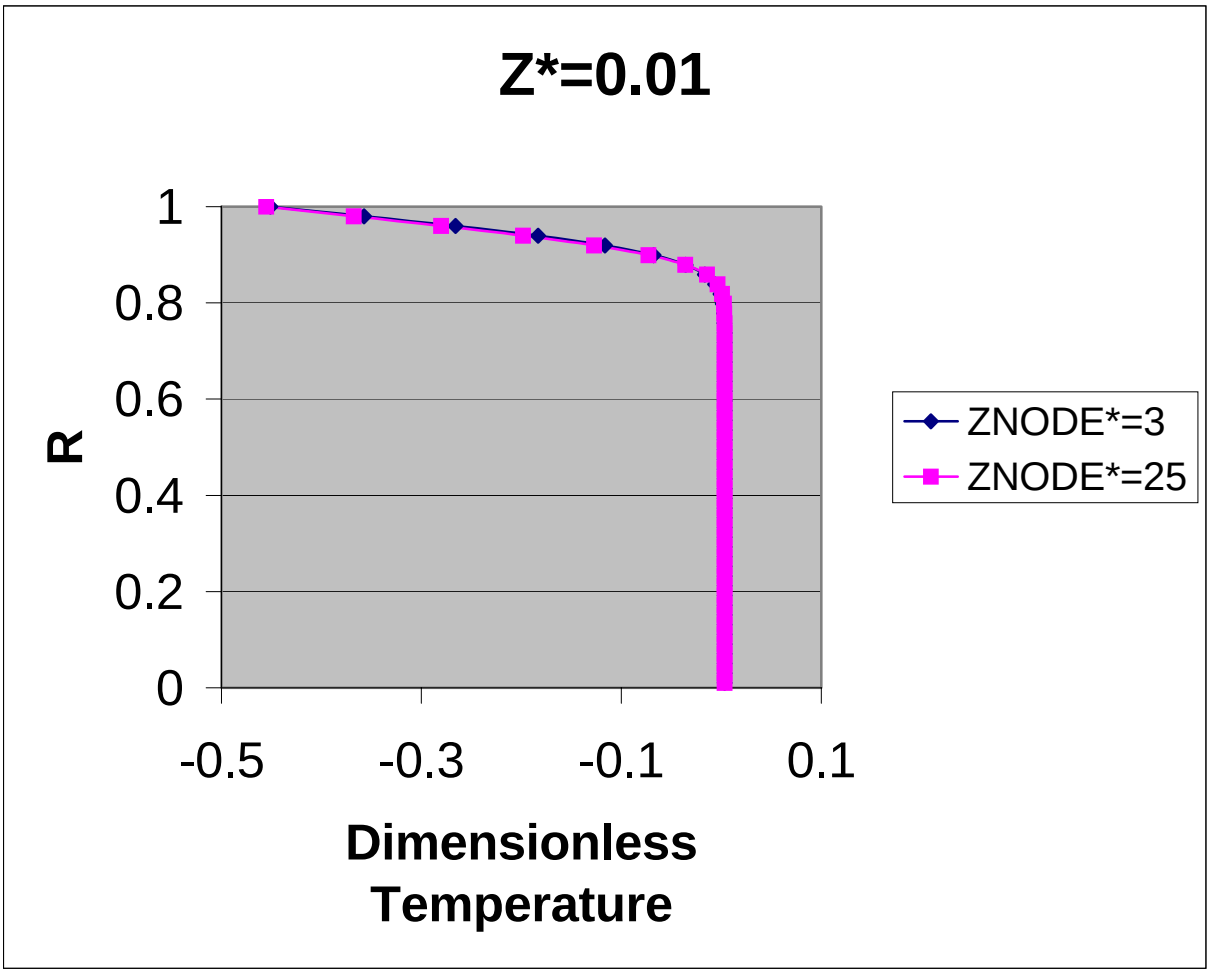

Figure 35 Grid Study with different grid size in Z* direction Nu_o =23.76425, Br =279E-09, a^* = 0.00378, Ω = 0.05459, Pe = 14.01245, T_{final} =115.13856, ΔT = 3.59808, Θ_∞ = -0.5, n=1, Z*=0.01, 50 nodes in R direction

4.3 HEAT TRANSFER WITH VISCOUS DISSIPATION

Since it has been established that results of our work are in good agreement with a commercial package and the benchmark solution, we would like to study the physical parameters. It will be interesting to see the effects of non-dimensional parameters especially on wall and fluid temperatures. The next step will be investigating these effects as a function of the parameters of the problem. In order to distinguish the effects of inlet temperature and ambient temperature, we use only a quarter cycle of the inlet temperature profile, which assures a positive inlet temperature (Figure 36), while using $\Theta_\infty = -0.5$ as ambient dimensionless temperature. At this point, we would like to introduce dimensionless bulk mean temperature, defined as

$$\Theta_b = \frac{\int_0^1 V_Z^* \Theta R dR}{\int_0^1 V_Z^* R dR} \tag{4.14}$$

This is usually applied in the case of forced convection inside a closed duct and is the mean fluid temperature at a cross section. Also, the local Nusselt number is given by,

$$Nu_{(Z^*,T)} = -2 \frac{\left.\frac{\partial \Theta}{\partial R}\right|_{R=1}}{\Theta_w - \Theta_b} \tag{4.15}$$

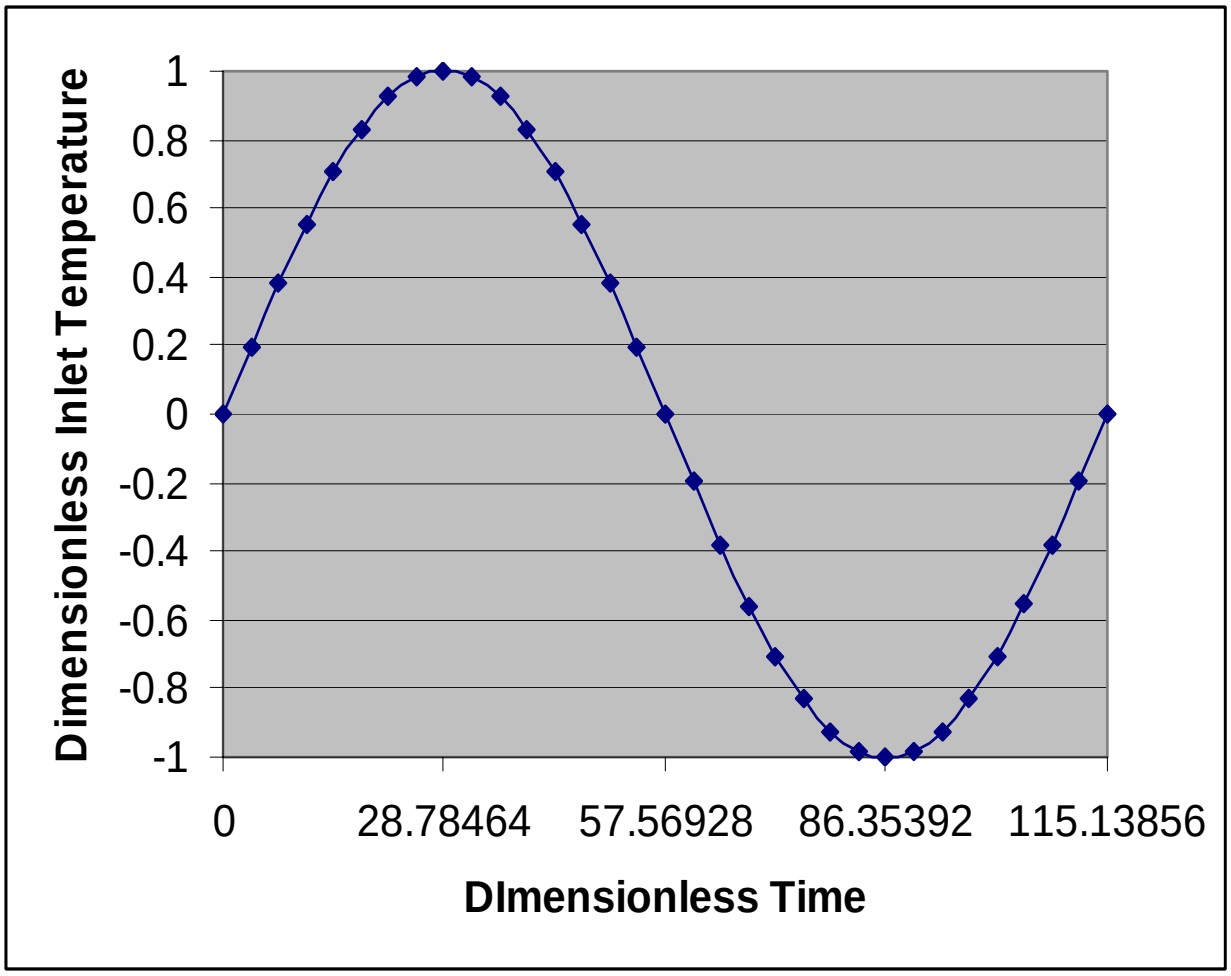

Figure 36 Dimensionless Inlet Temperature vs. Dimensionless Time Ω = 0.05459, T_{final} =115.13856, ΔT = 3.59808, $\Theta_{INLET} = Sin\Omega T$, Z*=0

4.3.1 Non-Newtonian Fluid

Figure 37 displays the dimensionless wall temperature profiles of non-Newtonian flows. The curve labeled as n=0.4 corresponds shear-thinning non-Newtonian flow, while the curve labeled n=1.8 represents shear-thickening non-Newtonian flow. Note in Figure 37, the increase in the dimensionless wall temperature as the power-law index decreases. Pseudo-plastic flows contribute to elevated viscous heating effects, thus forming higher temperatures near the liquid-solid interface. Figure 38 shows the dimensionless temperature profile at Z*=0.2. Due to viscous heating, the pseudo-plastic flow generates higher temperatures near the wall. As we move away from the wall, the effect of dilatant flow becomes more dominant. The dimensionless temperature increases as we move towards the center of the pipe for this kind of flow. The thermal wave of the inlet temperature has more penetration near the center than the wall.

Figures 39 and 40 show the dimensionless bulk temperature profile at different dimensionless axial distance. The bulk temperature profile flattens as distance from the inlet increases. The bulk temperature is higher for shear thickening fluids, since it has more effect of the positive inlet temperature on the overall fluid temperature than the shear thinning fluids.

Figure 41 shows the local Nusselt number for different power-law index. The steeper velocity gradient in the wall region for lower power-law index causes enhancement of the local Nusselt number. At locations very far from the inlet, local Nusselt number approaches to a certain value.

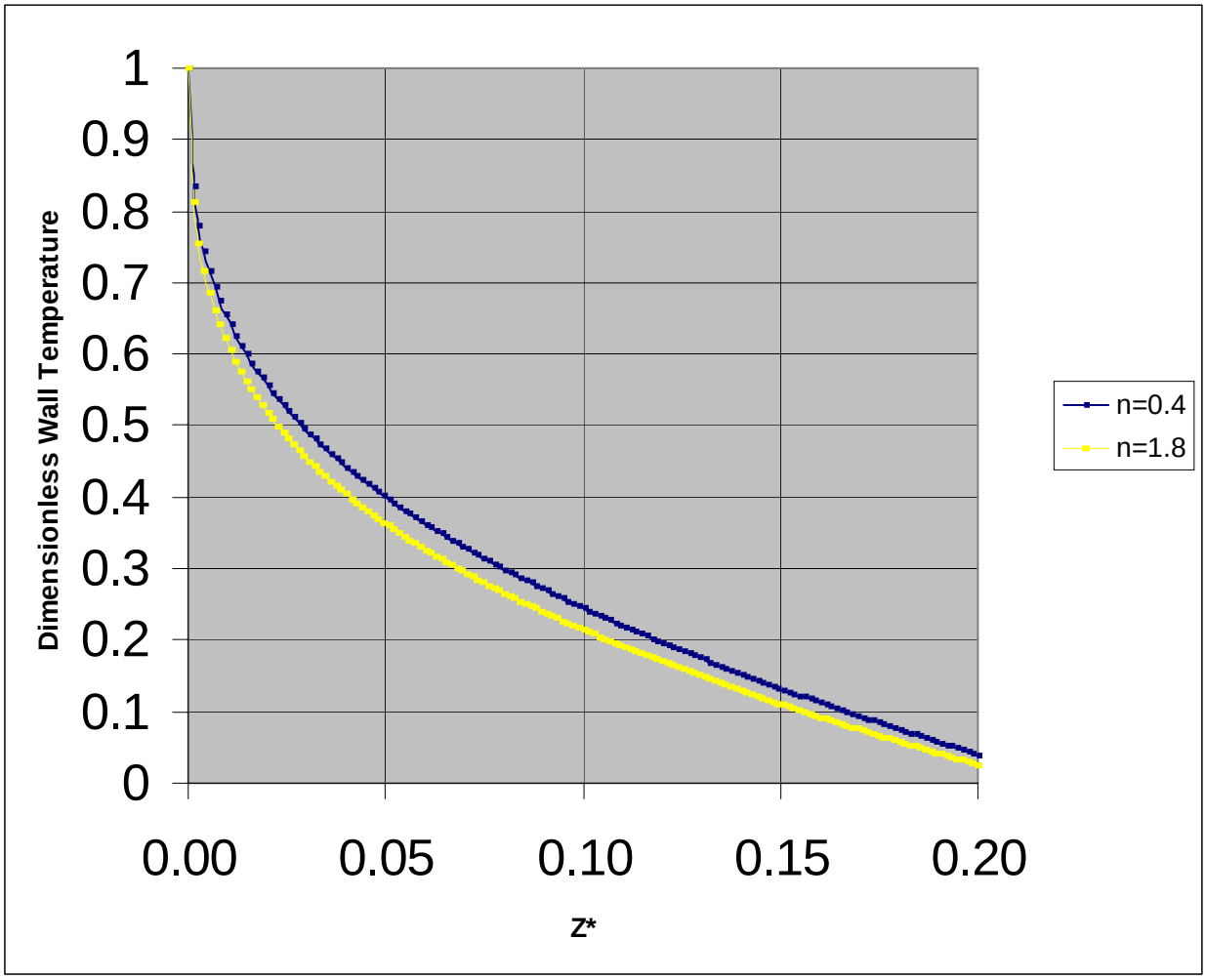

Figure 37 Comparison of Dimensionless Wall Temperature Profiles at different power-law index $Nu_o = 1.0$, Br =0.1, $a^* = 0.1, \Omega = 0.05459, Pe = 0.5, T_{final}$ =28.78464, $\Delta T = 3.59808$, Θ_∞ = -0.5, Z*=0.2

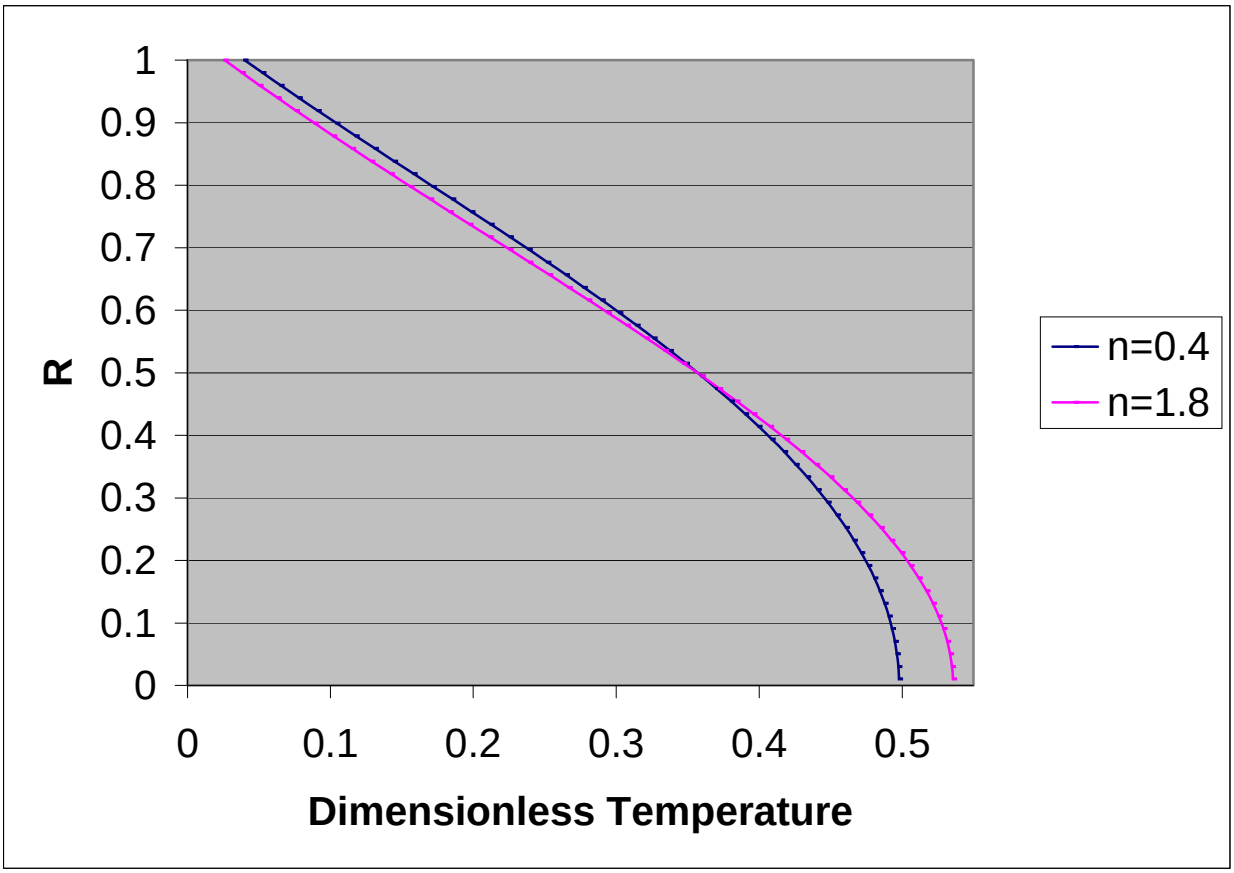

Figure 38 Comparison of Dimensionless Temperature Profiles at different power-law index, $Nu_o = 1.0$, Br =0.1, a^* = 0.1, Ω = 0.05459, Pe = 0.5, T_{final} =28.78464, ΔT = 3.59808, Θ_∞ = -0.5, Z*=0.2

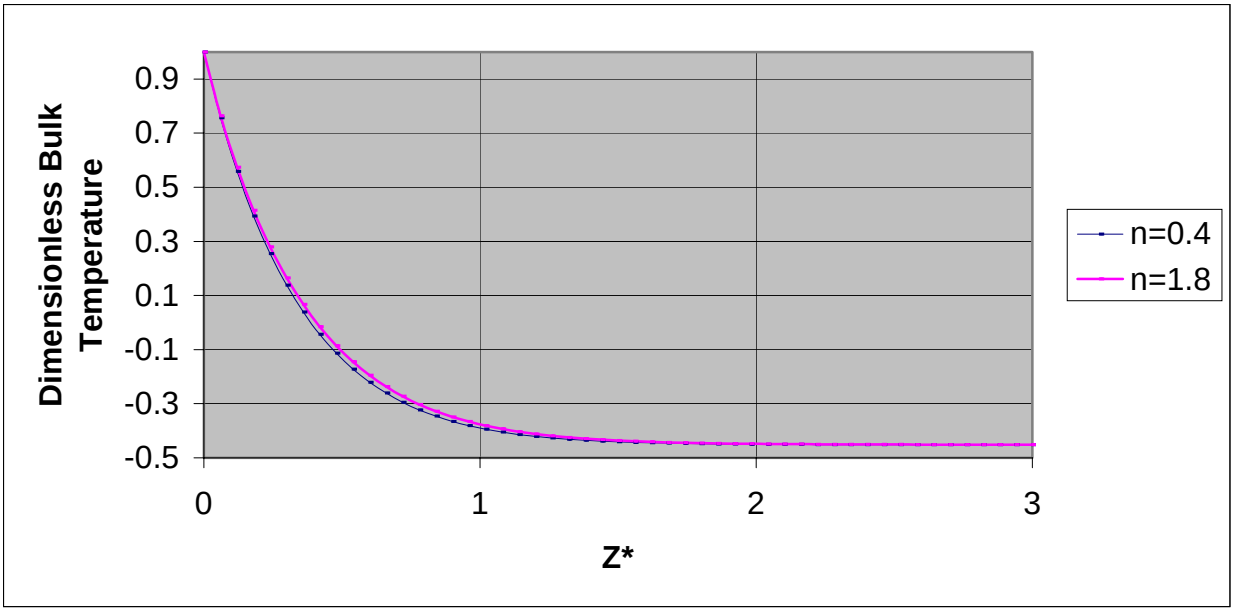

Figure 39 Comparison of Dimensionless Bulk Temperature Profiles at different Power-law index, $Nu_o = 1.0$, Br =0.1, a^* = 0.1, Ω = 0.05459, Pe = 0.5, T_{final} =28.78464, ΔT = 3.59808, Θ_∞ = -0.5, Z*=3

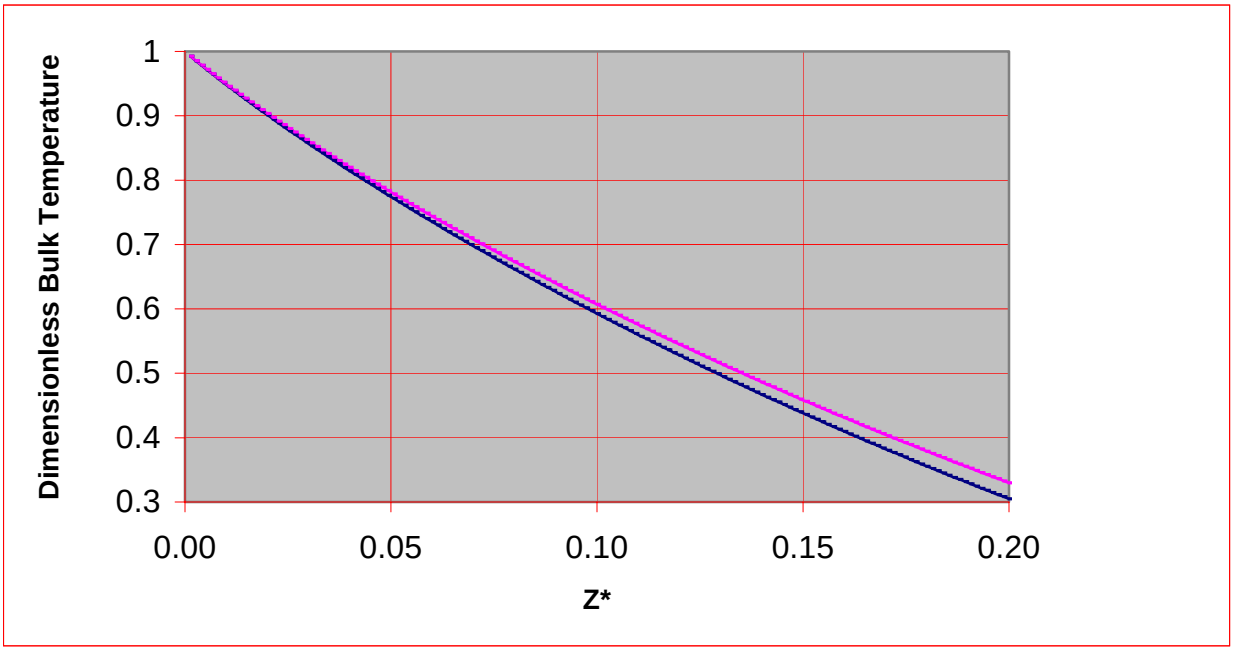

Figure 40 Comparison of Dimensionless Bulk Temperature Profiles at different Power-law index, $Nu_o = 1.0$, Br =0.1, a^* = 0.1, Ω = 0.05459, Pe = 0.5, T_{final} =28.78464, ΔT = 3.59808, Θ_∞ = -0.5, Z*=0.2

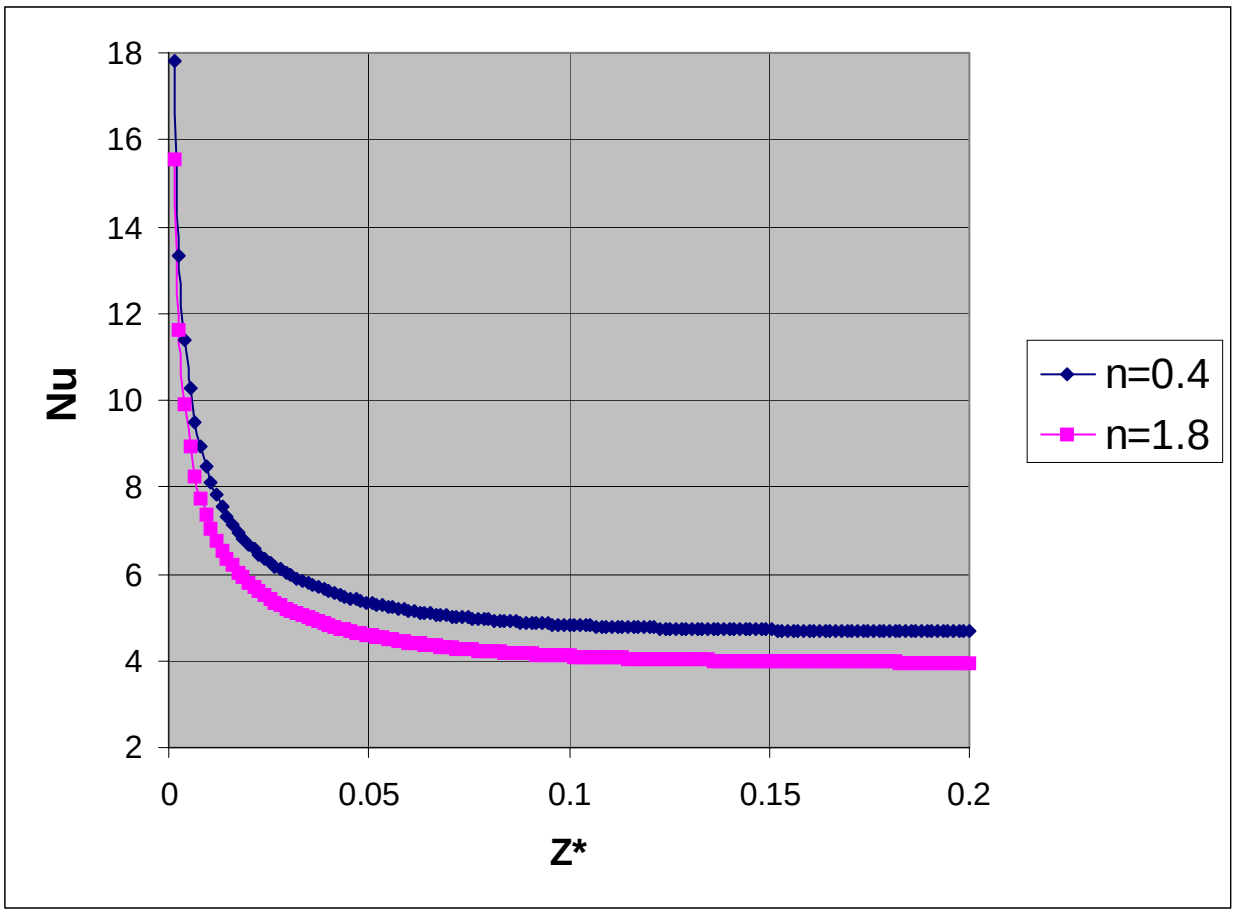

Figure 41 Comparison of Nusselt number at different Power-law index, $Nu_o = 1.0$, Br =0.1, a^* = 0.1, Ω = 0.05459, Pe =0.5, T_{final} =28.78464, ΔT =3.59808, Θ_∞ =-0.5,Z*=0.2

4.3.2 Brinkman Number

In this section, heat generation from viscous dissipation is taken into account, which is represented by the Brinkman number. Figure 42 and Figure 43 show the dimensionless wall temperature for different Brinkman numbers at different dimensionless axial distances. It is noticeable that dimensionless wall temperature increases as the Brinkman number increases. From the figure, this effect seems insignificant at the first glance. But Table 9 exhibits the effect of Brinkman number more clearly.

Table 9 Dimensionless Wall Temperature with different Brinkman numbers at various locations, $Nu_o = 1.0$, n=1.8, $a^* = 0.1$, $\Omega = 0.05459$, $Pe = 0.5$, $T_{final} = 28.78464$, $\Delta T = 3.59808$, $\Theta_\infty = -0.5$.

Dimensionless Wall Temperature at	Brinkman=3	Brinkman=0.1	Difference
Z*=0.10	0.21850	0.21434	1.9 %
Z*=0.15	0.11415	0.10908	4.4 %
Z*=0.18	0.06340	0.05788	8.7 %
Z*=0.20	0.03171	0.02590	18.3 %

Table 9 shows the dimensionless wall temperature at selected nodes for different Brinkman number. The effect from viscous dissipation is more noticeable downstream, where the inlet temperature has less effect on those regions.

The local Nusselt number also increases with increasing Brinkman number due to viscous heating. The variation of local Nusselt number with axial dimensionless distance is shown in Table 10.

Table 10 Local Nusselt number at different Brinkman numbers, $Nu_o = 1.0$, n=1.8, a^* = 0.1, Ω = 0.05459, Pe = 0.5, T_{final} =28.78464, ΔT = 3.59808, Θ_∞ = -0.5

Local Nusselt Number at	Br=0.1	Br=3
Z*=0.00267	11.59833	11.62345
Z*=0.04933	4.59676	4.62307
Z*=0.18	3.96616	4.00349

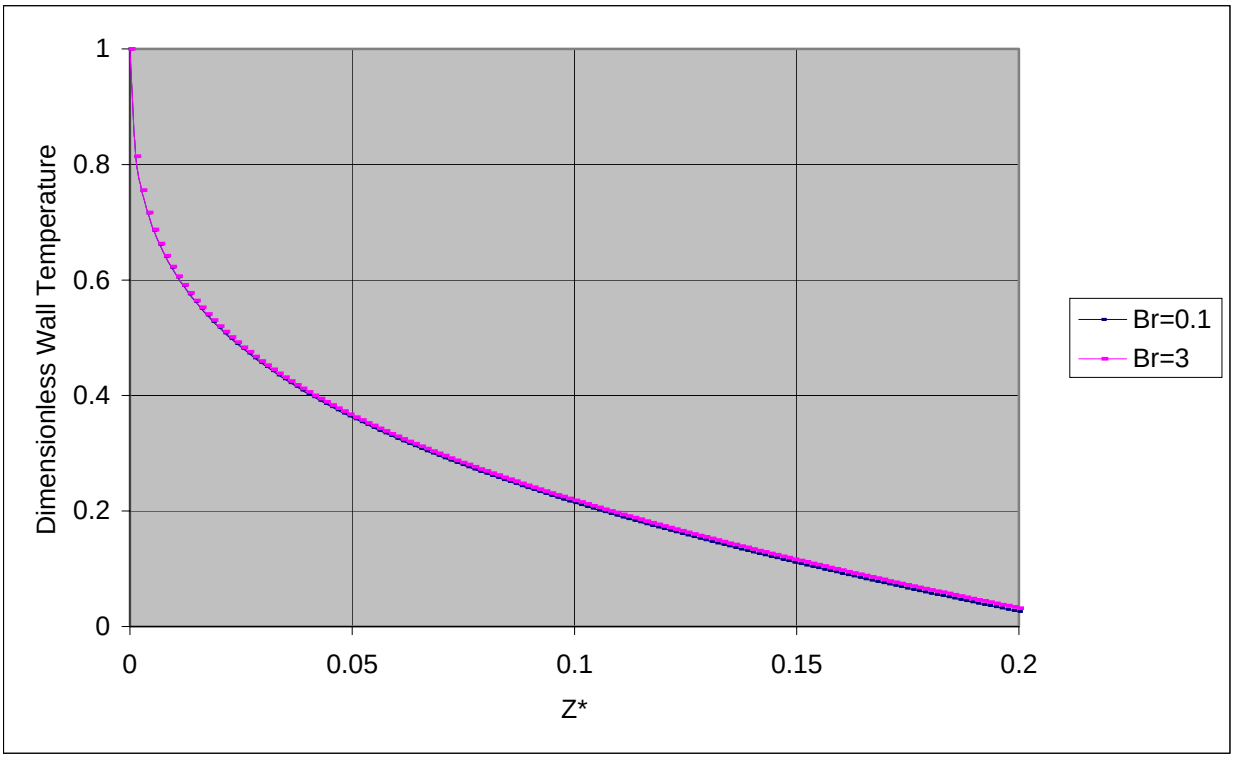

Figure 42 Comparison of Dimensionless Wall Temperature Profiles at different Brinkman numbers, $Nu_o = 1.0$, n=1.8, $a^* = 0.1$, $\Omega = 0.05459$, $Pe = 0.5$, $T_{final} = 28.78464$, $\Delta T = 3.59808$, $\Theta_\infty = -0.5$, Z*=0.2

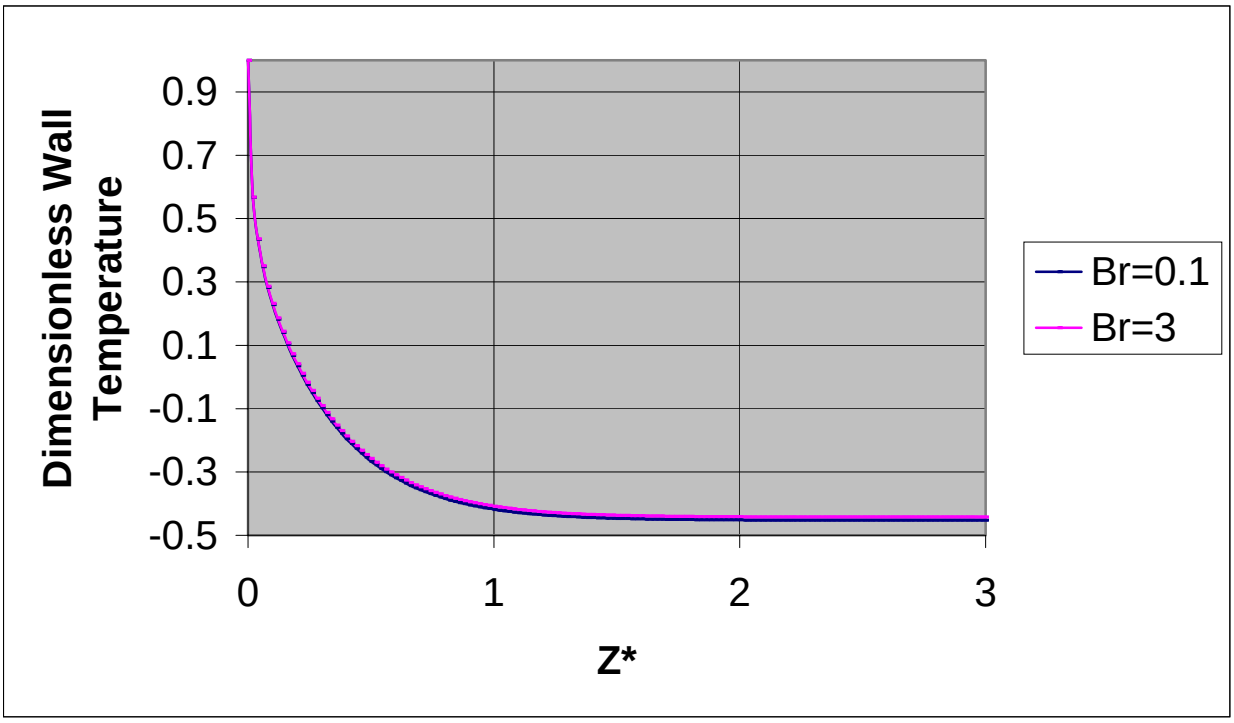

Figure 43 Comparison of Dimensionless Wall Temperature Profiles at different Brinkman numbers, $Nu_o = 1.0$, n=1.8, $a^* = 0.1$, $\Omega = 0.05459$, $Pe = 0.5$, $T_{final} = 28.78464$, $\Delta T = 3.59808$, $\Theta_\infty = -0.5$, Z*=3.

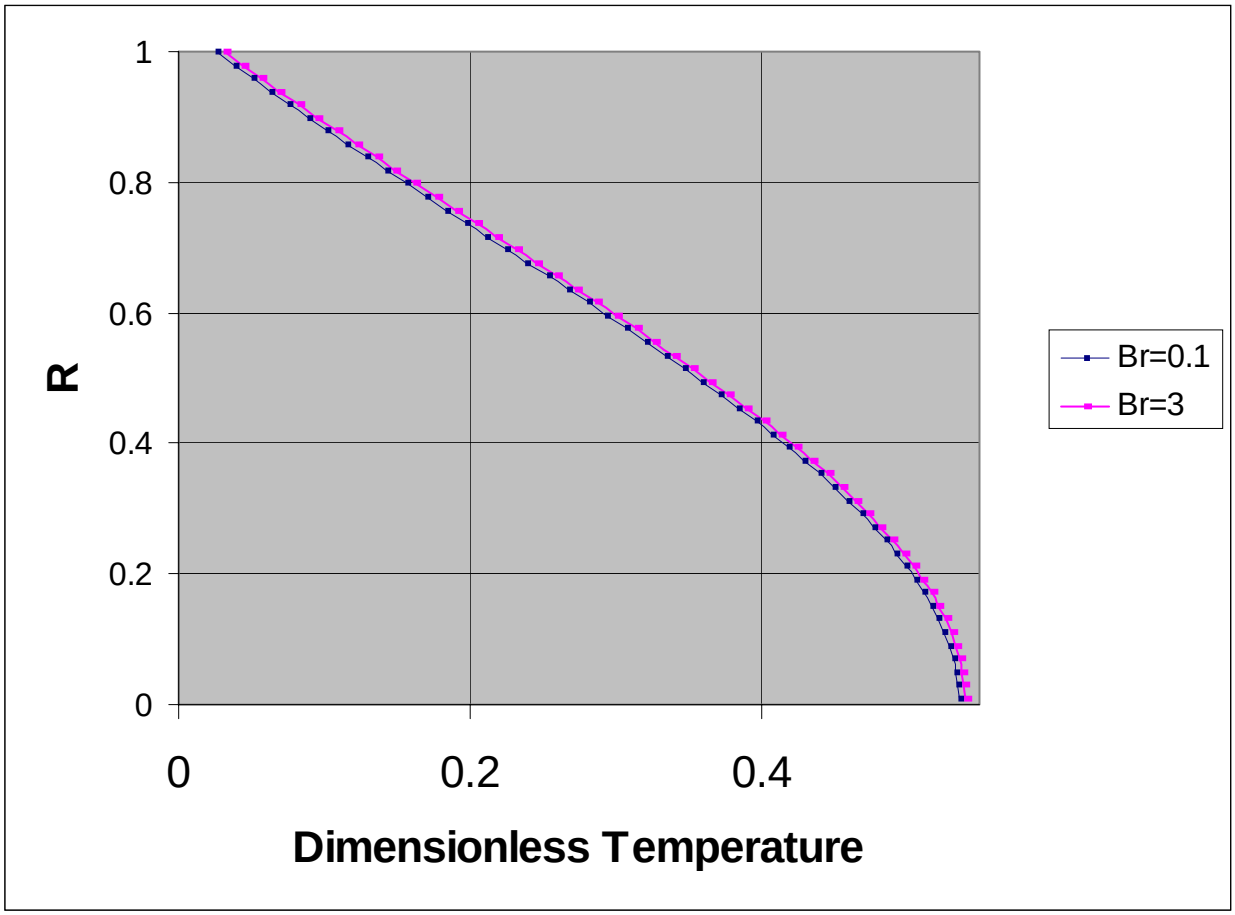

Figure 44 Dimensionless Temperature Profiles at different Brinkman numbers, Nu_o = 1.0, n=1.8, a^* = 0.1, Ω = 0.05459, Pe = 0.5, T_{final} =28.78464, ΔT = 3.59808, Θ_∞ = -0.5, Z*=0.2

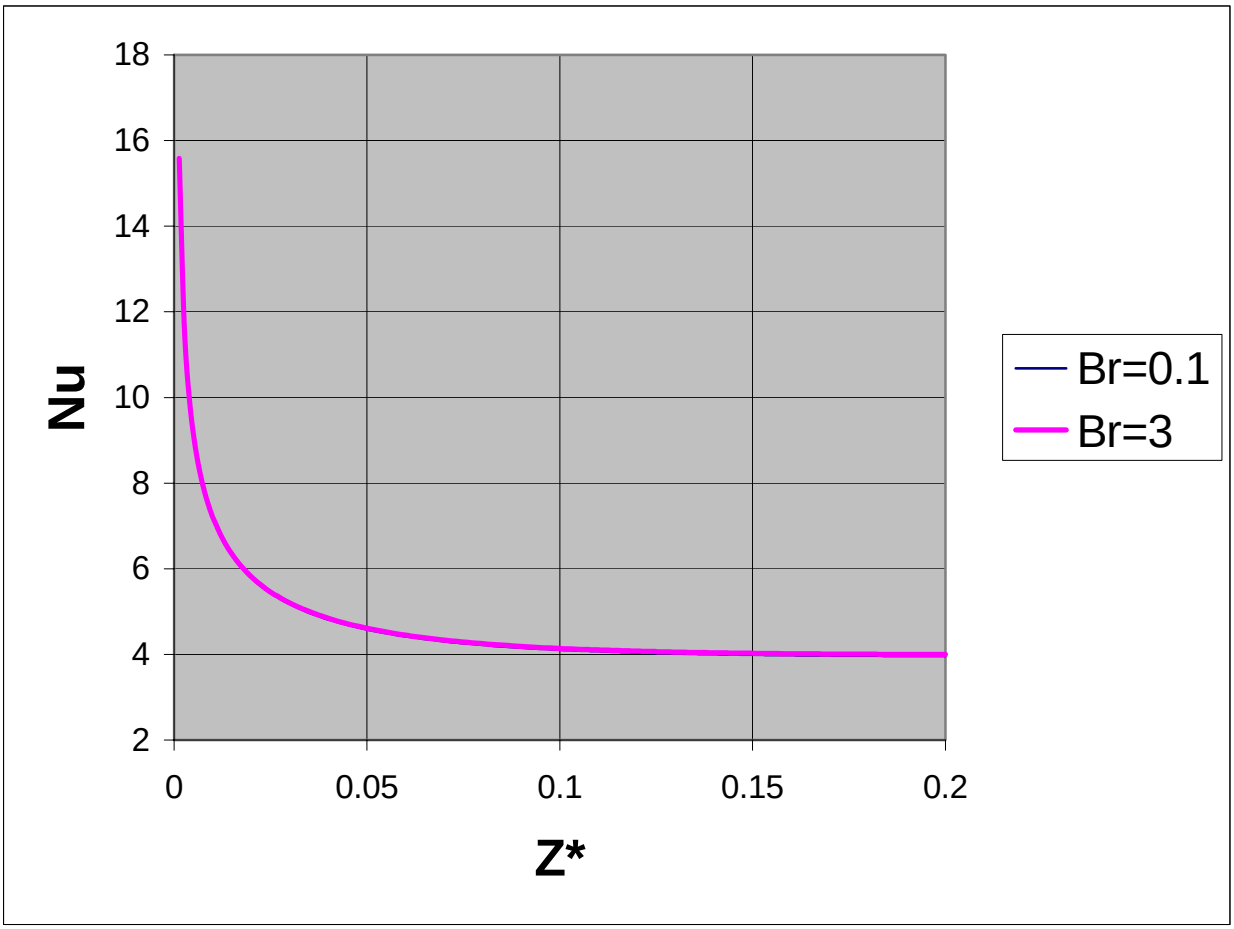

Figure 45 Nusselt number at different Brinkman numbers, $Nu_o = 1.0$, n=1.8, $a^* = 0.1$, $\Omega = 0.05459$, $Pe = 0.5$, $T_{final} = 28.78464$, $\Delta T = 3.59808$, $\Theta_\infty = -0.5$, Z*=0.2

4.3.3 Nusselt Number

The outside Nusselt number is one of the major parameters containing information on the wall heat flux. It represents the external thermal resistance. When the Nu_0 is small, when the thermal resistance is large, the thermal wave from the inlet has more penetration along the pipe as in Figures 46 and 47. Note that the dimensionless inlet temperature takes the value of one in this case.

For higher values of Nu_0, the influence of the ambient temperature on the wall temperature is very significant. When the external resistance is very small, with a high Nu_0 number, the dimensionless wall temperature approaches the dimensionless ambient temperature, as displayed in Figure 49 and Figure 50.

The local Nusselt number increases with the increase in external resistance as displayed in Figure 51. At locations very far from the inlet, the local Nusselt number approaches a certain value.

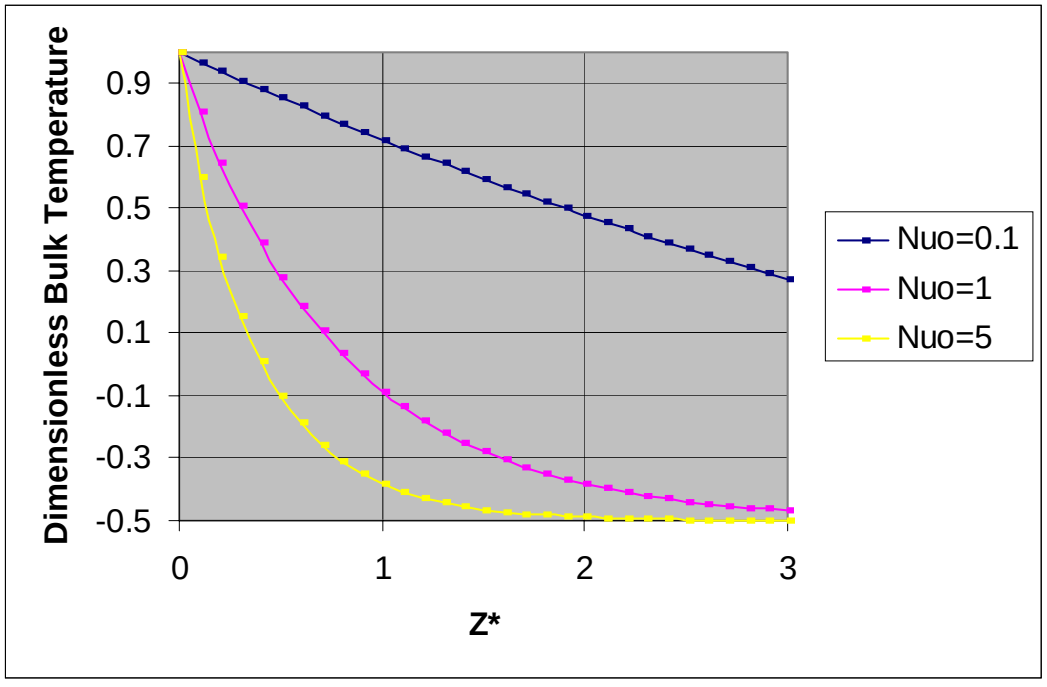

Figure 46 Dimensionless Bulk Temperature Profile at different Outside Nusselt numbers with n=1, a^* = 1.0, Ω = 0.05459, Pe = 1.0, Br =0.1, T_{final} =28.78464, ΔT = 3.59808, Θ_∞ = -0.5, Z*=3.

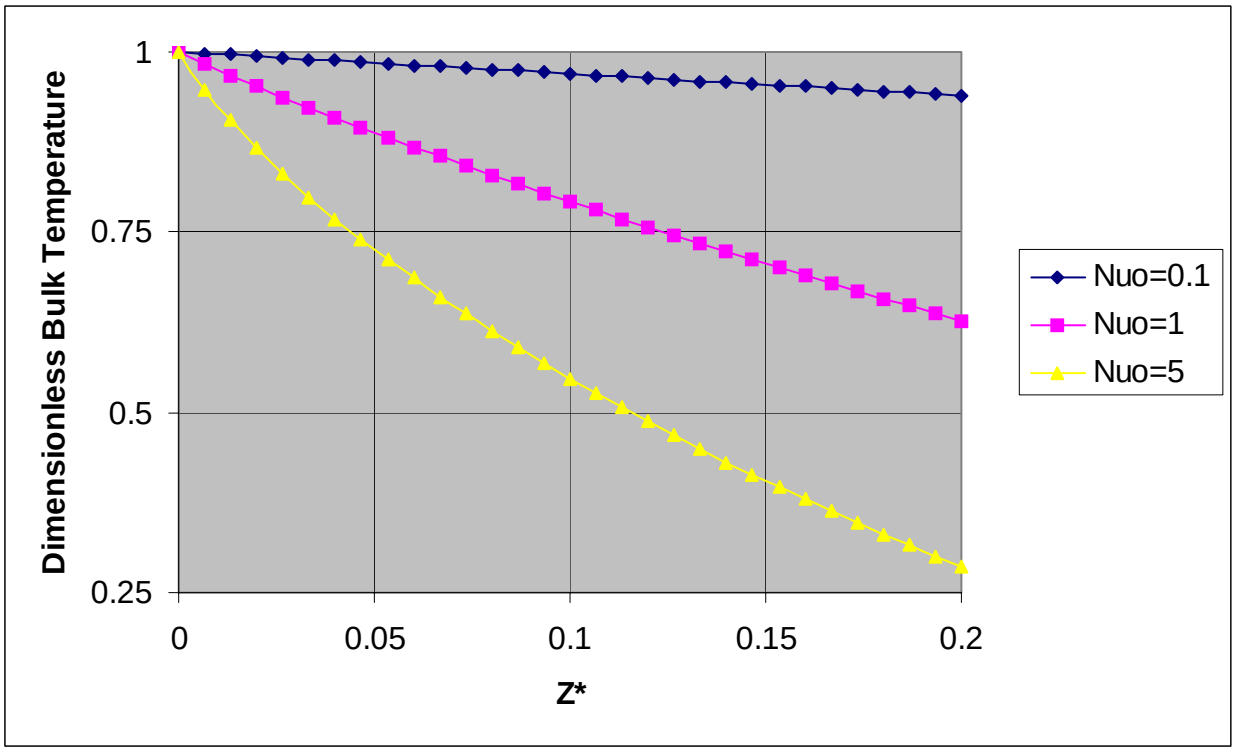

Figure 47 Dimensionless Bulk Temperature Profile at different Outside Nusselt numbers with n=1, a^* = 1.0, Ω = 0.05459, Pe = 1.0, Br =0.1, T_{final} =28.78464, ΔT = 3.59808, Θ_∞ = -0.5, Z*=0.2

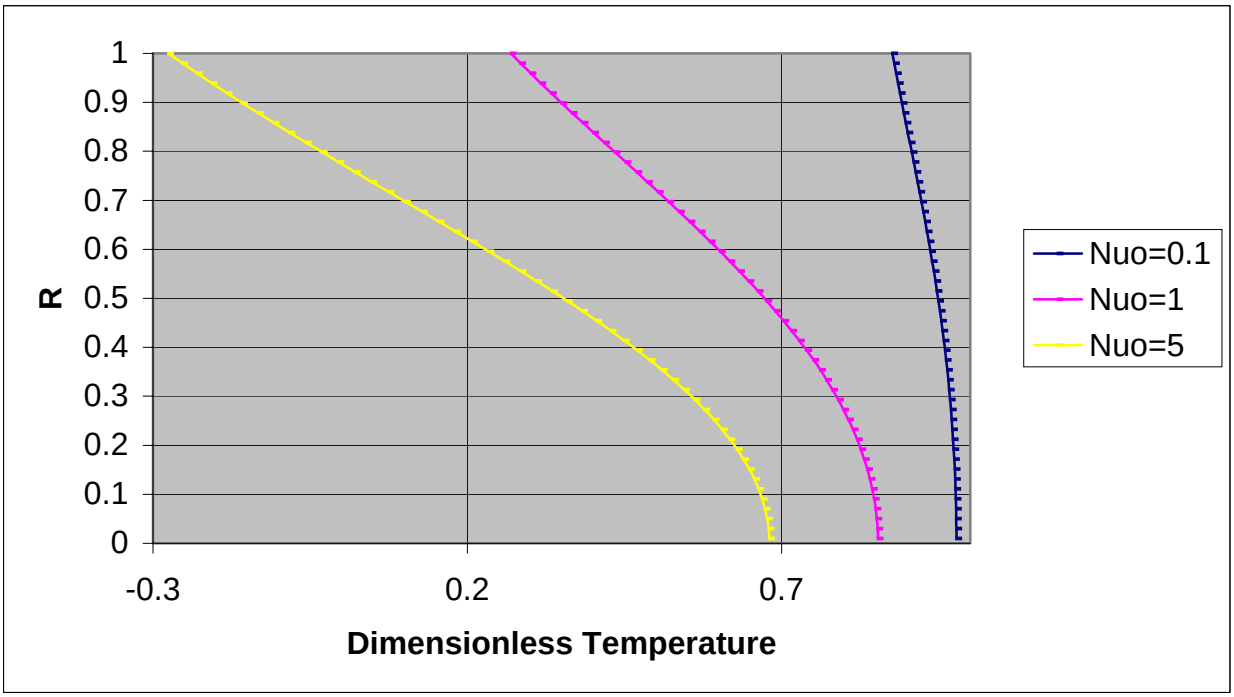

Figure 48 Dimensionless Temperature Profile at different Outside Nusselt numbers with n=1, a^* = 1.0, Ω = 0.05459, Pe = 1.0, Br =0.1, T_{final} =28.78464, ΔT = 3.59808, Θ_∞ = -0.5, Z*=0.2

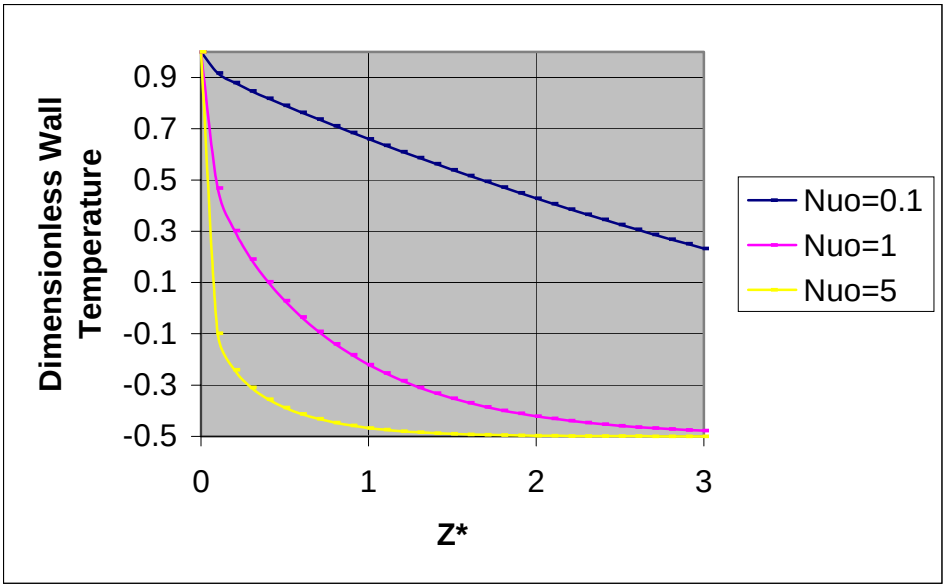

Figure 49 Dimensionless Wall Temperature Profile at different Outside Nusselt numbers with n=1, a^* = 1.0, Ω = 0.05459, Pe = 1.0, Br =0.1, T_{final} =28.78464, ΔT = 3.59808, Θ_∞ = -0.5, Z*=3.

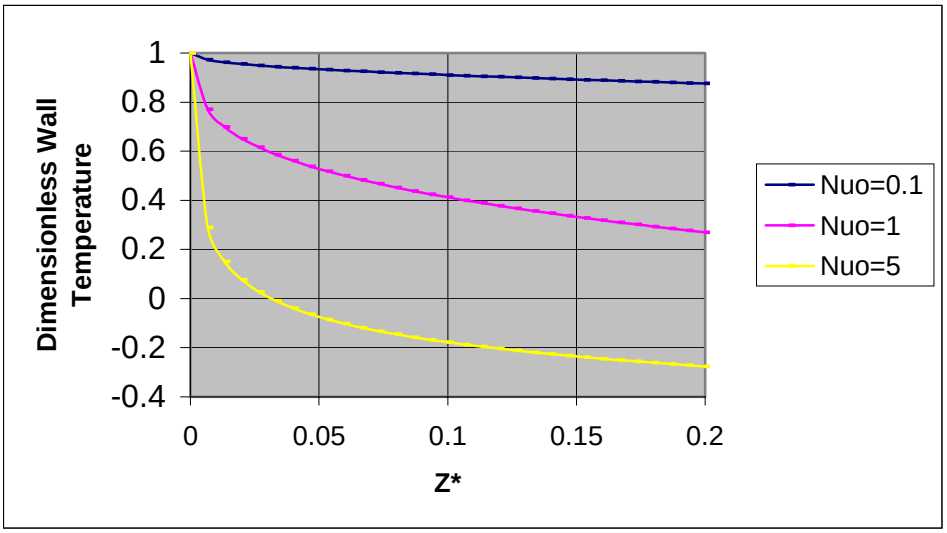

Figure 50 Dimensionless Wall Temperature Profile at different Outside Nusselt numbers with n=1, a^* = 1.0, Ω = 0.05459, Pe = 1.0, Br =0.1, T_{final} =28.78464, ΔT = 3.59808, Θ_∞ = -0.5, Z*=0.2

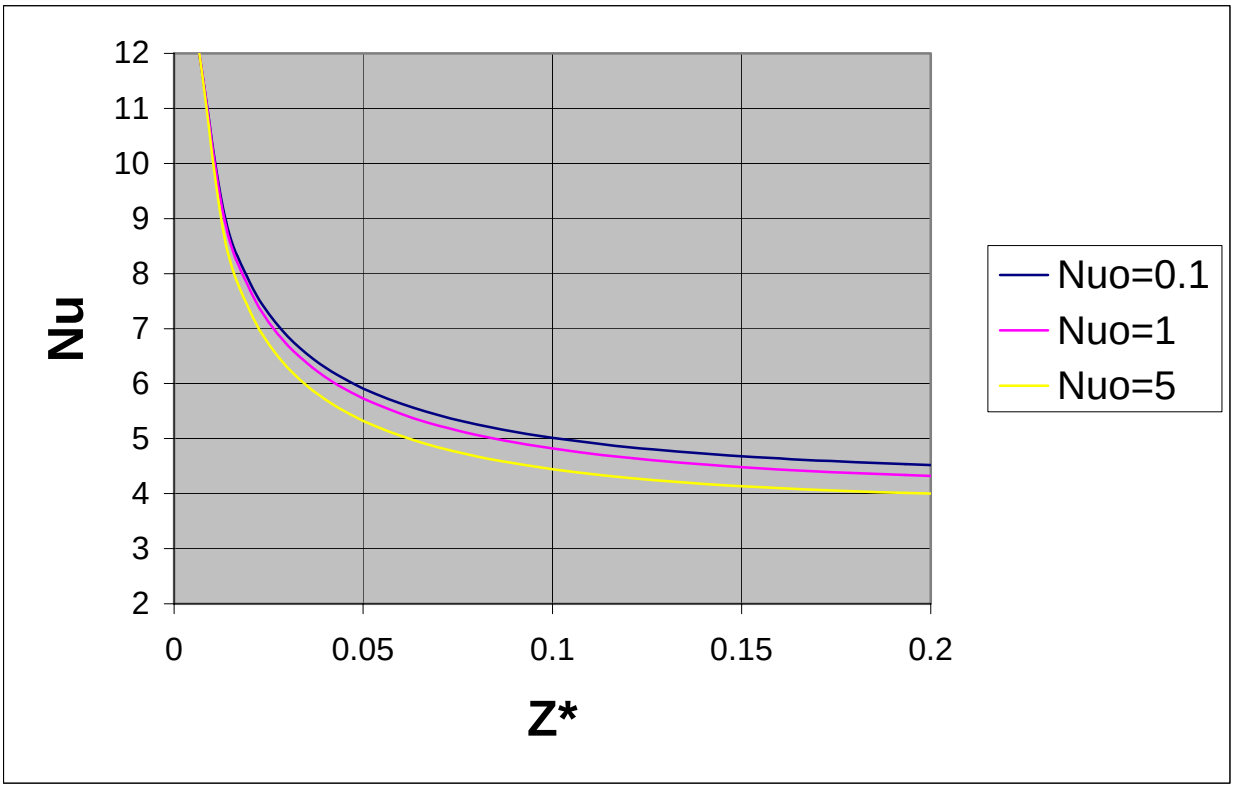

Figure 51 Local Nusselt number at different Outside Nusselt numbers with n=1, a^* = 1.0, Ω = 0.05459, Pe = 1.0, Br =0.1, T_{final} =28.78464, ΔT = 3.59808, Θ_∞ = -0.5, Z*=0.2

4.4 CONCLUSIONS AND FUTURE WORK

Transient forced convection heat transfer in ducts is of great importance to the design of heat exchanger systems. The variety of applications ranges from compact heat exchangers to cooling devices in electronics and aerospace, involving Newtonian as well as non-Newtonian fluids. Especially regenerative type heat exchangers, through which hot and cold fluids pass in succession, motivated the study of thermal response of duct flows to imposed cyclic variation in boundary conditions. The processes such as start-up, shut-down, power-surge, pump failure have also stimulated investigations to determine the transient thermal response of duct flows.

There are a large number of heat exchangers designed and manufactured for the food and chemical process industries to heat and cool non-Newtonian fluids. In the design of the control systems of heat transfer devices in organic-cooled nuclear reactors, it is important to have a detailed knowledge of the non-Newtonian fluid flow and heat transfer for circular ducts. The fluids, such as polymer solutions or melts, greases, starch suspensions, mayonnaise, paper pulp, soap and detergent slurries, are non-Newtonian.

In most polymer processing applications and in lubrication systems the changes of temperature with position and time are significant. In the manufacture of plastic objects, it starts by melting plastic pellets and then performing a sequence of processing operations on the molten material. The heat transfer plays significant role in the cooling process to obtain the finished product. In high speed processing operations, such as extrusion, and in lubrication problems, the temperature rise by viscous dissipation is considerable. The estimation of viscous heating effects and local temperatures is of particular interest in polymer flow problems because of the thermal instability of polymeric liquids; chemical degradation can occur if hot spots develop in the processing line.

In this dissertation, the transient conjugate heat transfer problem for fully-developed laminar flow of non-Newtonian fluids in a circular duct is studied by numerical analysis. A control volume based finite difference method is adopted in the numerical procedure for the integration of the governing equations. For the non-Newtonian fluid part, the power-law model is used. Heat generation from viscous dissipation is also taken into account and is represented by the Brinkman number. The steady-state results agree with the Graetz solution very well, and the transient solution is in good agreement with the results obtained from commercial engineering software as well. We

also investigated the effects of non-dimensional parameters especially on wall, fluid and bulk temperatures. In this study, a special focus is placed on the effects of the flow index, Brinkman and, Nusselt numbers. The increment of flow index leads to the increase of wall temperature. The steeper velocity gradient in the wall region for lower power-law index causes enhancement of the local Nusselt number. At locations very far from the inlet, local Nusselt number approaches to a certain value. The Brinkman number has the same effect on the wall temperature as well. The dimensionless wall temperature increases as the Brinkman number increases. The local Nusselt number also increases with increasing Brinkman number due to viscous heating. Another parameter, outside Nusselt number, represents the external resistance. Higher outside Nusselt numbers cause the wall temperature to approach to the ambient temperature. The local Nusselt number also increases with the increase in external resistance.

The viscosity of non-Newtonian fluids varies with both shear rate and temperature. Consequently, the heat transfer differs from those obtained with a constant property fluid. As part of the future work, temperature dependent model can be used to consider the temperature-dependent viscosity of a non-Newtonian fluid.

Relative to the complex geometries often found in industry. Therefore, different geometries should also be studied in the future. As an example, the physical mechanism of the heat transfer enhancement for the non-Newtonian fluids in the rectangular ducts has not been clearly understood, an interesting phenomenon that has never been observed in a circular pipe flow.

Even today, there is a lack of experimental data for heat transfer coefficients which are required for the design of heat exchangers. An experimental study is required to fully verify the correlation of the numerical investigation. The current study will help to set up such an experimental research, especially for rig design and planning.

APPENDIX A

APPENDIX A

ANSYS INPUT FILE

```
!ANSYS INPUT FILE by Alan L.Briggs
!This program calculates the velocity and the temperature distributions !for conjugate heat transfer problem.
/batch
/TITLE,CONJUGATE HEAT TRANSFER
/config,nproc,4                    ! 4 processors to be used
/PREP7
/unit,si
SMRT,OFF
ET,1,FLUID141,,,2                  ! 2D AXISYMMETRIC XR SYSTEM
MSHK,1                             ! MAPPED AREA MESH
MSHA,0,2D                          ! QUAD ELEMENTS
!DIMENSIONS AND PROPERTIES
PI   = ACOS(-1)
L    = 0.0125                      ! PIPE LENGTH (M)
R    = 0.0025                      ! PIPE RADIUS (M)
RF   = 0.0000926                   ! NEAR CENTER LOCATION (M)
PIN  = 0.0375                      ! INLET PRESSURE (PA)
TIN  = 300.0                       ! INLET TEMPERATURE (K)
TAMB = 300.0                       ! AMBIENT TEMPERATURE (K)
RHO  = 1.1614                      ! FLUID DENSITY (KG/M**3)
MU   = 184.6E-07                   ! FLUID VISCOSITY (KG/(M*SEC))
```

```
K    = 0.0263                    ! FLUID THERMAL CONDUCTIVITY (W/(M*K))
CP   = 1007                      ! FLUID SPECIFIC HEAT (J/(KG*K))
RSO  = 0.0002                    ! SOLID WIDTH
H    = 250                       ! HEAT TRANSFER COFFICIENT (W/M**2*K)
RECTNG,,L,,RF
RECTNG,,L,RF,R
RECT,,L,R,R+RSO
nummrg,all,0.0000001             !INCREASE RANGE OF TOLERANCE
numcmp,all
LSEL,S,,,2,4,2
!LESIZE,ALL,,,12,-2              ! GRADED RADIAL LINE DIVISIONS
LESIZE,ALL,,,1
LSEL,S,,,5,7,2
LESIZE,ALL,,,13
LSEL,S,,,1,3,2
LSEL,A,,,6
!LESIZE,ALL,,,50,1               ! GRADED AXIAL LINE DIVISIONS
LESIZE,ALL,,,50
ASEL,S,,,1
ASEL,A,,,2
ALLSEL,BELOW,AREA
MAT,1                            ! FLUID
AMESH,ALL
/PNUM,MAT,1
ALLSEL,ALL
ASEL,S,,,3
ALLSEL,BELOW,AREA
LSEL,S,,,8,10,2
```

```
LESIZE,ALL,,,5
LSEL,S,,,9
LESIZE,ALL,,,50
MAT,2                    !SOLID REGION
AMESH,3
ALLSEL,ALL
!LSEL,S,,,3              ! NO-SLIP WALL BOUNDARY
!NSLL,S,1
!D,ALL,VX
!D,ALL,VY
allsel,all
LSEL,S,,,1               ! SYMMETRY BOUNDARY
NSLL,S,1
D,ALL,VY
LSEL,S,,,4
LSEL,A,,,7               ! INLET BOUNDARY
NSLL,S,1
D,ALL,VY
D,ALL,PRES,PIN
LSEL,S,,,2
LSEL,A,,,5               ! OUTLET BOUNDARY
NSLL,S,1
D,ALL,VY
D,ALL,PRES
ALLSEL
MP,DENS,2,8055           ! SOLID PROPERTIES (AISI 302)
mp,kxx,2,15              ! SOLID THERMAL CONDUCTIVITY
MP,C,2,480               ! SOLID SPECIFIC HEAT
```

```
MP,DENS,1,RHO                    ! FLUID DENSITY
MP,VISC,1,MU                     ! FLUID VISCOSITY
MP,C,1,CP                        ! FLUID SPECIFIC HEAT
mp,kxx,1,K                       ! FLUID THERMAL CONDUCTIVITY
allsel,all
d,all,temp,320                   ! INITIAL TEMPERATURE
/SOLU
FLDATA,SOLU,FLOW,1               ! STEADY-STATE SOLUTION
FLDATA,SOLU,TEMP,1
FLDATA,ITER,EXEC,350             ! # OF GLOBAL ITERATIONS
FLDATA,ITER,CHEC,100             ! CHECKPOINT FREQUENCY
FLDATA,TEMP,NOMI,TIN             ! NOMINAL TEMPERATURE
FLDATA,OUTP,TAUW,T               ! OUTPUT WALL SHEAR STRESS
FLDA,NOMI,DENS,RHO       ! initial density for all fluid regions
FLDA,NOMI,VISC,MU        ! initial viscosity for all fluid regions
FLDA,NOMI,COND,K         ! initial conductivity for all fluid regions
FLDA,NOMI,SPHT,CP        ! initial specific heat for all fluid regions
FLDA,TERM,PRES,1.E-09    ! convergence criterion
solve
/prep7
ddele,all,temp
*DEL,_FNCNAME
*DEL,_FNCMTID
*SET,_FNCNAME,'time'
! /INPUT,time.func
*DIM,%_FNCNAME%,TABLE,6,12,1
!
! Begin of equation: 320+(40*sin((2*{PI}/32)*{TIME}))
```

```
%_FNCNAME%(0,0,1)= 0.0, -999
%_FNCNAME%(2,0,1)= 0.0
%_FNCNAME%(3,0,1)= 0.0
%_FNCNAME%(4,0,1)= 0.0
%_FNCNAME%(5,0,1)= 0.0
%_FNCNAME%(6,0,1)= 0.0
%_FNCNAME%(0,1,1)= 1.0, -1, 0, 2, 0, 0, 0
%_FNCNAME%(0,2,1)= 0.0, -2, 0, 3.14159265358979312, 0, 0, -1
%_FNCNAME%(0,3,1)=   0, -3, 0, 1, -1, 3, -2
%_FNCNAME%(0,4,1)= 0.0, -1, 0, 32, 0, 0, -3
%_FNCNAME%(0,5,1)= 0.0, -2, 0, 1, -3, 4, -1
%_FNCNAME%(0,6,1)= 0.0, -1, 0, 1, -2, 3, 1
%_FNCNAME%(0,7,1)= 0.0, -1, 9, 1, -1, 0, 0
%_FNCNAME%(0,8,1)= 0.0, -2, 0, 40, 0, 0, -1
%_FNCNAME%(0,9,1)= 0.0, -3, 0, 1, -2, 3, -1
%_FNCNAME%(0,10,1)= 0.0, -1, 0, 320, 0, 0, -3
%_FNCNAME%(0,11,1)= 0.0, -2, 0, 1, -1, 1, -3
%_FNCNAME%(0,12,1)= 0.0, 99, 0, 1, -2, 0, 0
! End of equation: 320+(40*sin((2*{PI}/32)*{TIME}))
!-->
LSEL,S,,,4,7,3                  ! INLET TEMPERATURE VARIATIONS
NSLL,S,1
D,ALL,TEMP,%time%
allsel,all
LSEL,S,,,9
NSLL,S,1
SF,ALL,CONV,H,TAMB                  ! APPLY CONVECTION H,TAMB
ALLSEL,all
```

```
/solu
FLDATA,SOLU,TRANS,1                ! TRANSIENT SOLUTION
FLDATA,TIME,GLOB,350               ! # OF GLOBAL ITERATIONS
FLDATA,SOLU,TEMP,T                 ! ACTIVATE ENERGY EQUATION
FLDATA,SOLU,FLOW,F                 ! DEACTIVATE FLOW EQUATIONS
!fldata,meth,enrg,3
FLDATA,RELX,TEMP,1.0               ! NO RELAXATION FOR TEMP
FLDATA,TIME,TEMP,1e-17,
FLDATA,TIME,STEP,1                 ! TIME STEP
FLDATA,TIME,TEND,32                ! FINAL TIME
FLDATA,TIME,NUMB,32
FLDATA,STEP,APPE,1
FLDATA,OUTP,HFLU,T                 ! OUTPUT HEAT FLUX
FLDATA,OUTP,HFLM,T
save
solve                      !solve for temperature only
FINISH
/post1                     ! POSTPROCESSING
SET,LAST
EPLOT
/CONTOUR,1,50
/TITLE,CONTOURS OF AXIAL VELOCITY
PLNSOL,VX
VXC=VX(2)
PATH,PIPE,2,,50
PPATH,1,,L,0,0
PPATH,2,,L,R,0
PDEF,VX,VX
```

```
PDEF,TEMP,TEMP
PCALC,MULT,PROD1,VX,S
PCALC,INTG,VXM,PROD1,S,2/R**2
*GET,VXM,PATH,,LAST,VXM              ! MEAN AXIAL VELOCITY
MDOT= RHO*VXM*PI*R**2                ! MASS FLOW RATE
/TITLE,CONTOURS OF WALL SHEAR STRESS
plnsol,tauw
*GET,TAU,PLNSOL,,MAX                 ! WALL SHEAR STRESS
PCALC,MULT,PROD2,VX,TEMP             ! MULTIPLY VX TIMES TEMP
PCALC,MULT,PROD3,PROD2,S             ! MULTIPLY ABOVE TIMES R COORDINATE
PCALC,INTG,TM,PROD3,S,2/VXM/R**2     ! INTEGRATE TEMPERATURE ALONG PATH
*GET,TM_O,PATH,,LAST,TM              ! GET OUTLET MEAN TEMPERATURE
/TITLE,CONTORS OF TEMPERATURE
PLNSOL,TEMP
*GET,TW_O,PLNSOL,,MAX                ! GET OUTLET WALL TEMPERATURE
TC_O = TEMP(2)                       ! GET OUTLET CENTERLINE TEMPERATURE
*STATUS                              ! LIST CURRENT PARAMETER VALUES
/TITLE,AXIAL VELOCITY PROFILE, VX(R)
/AXLAB,X,RADIAL COORDINATE, (M)
/AXLAB,Y,VELOCITY, (M/SEC)
PLPATH,VX
/TITLE,OUTLET TEMPERATURE PROFILE, T(R)
/AXLAB,Y,TEMPERATURE, (K)
PLPATH,TEMP                          ! PLOT TEMP ALONG PATH
/TITLE,WALL TEMPERATURE PROFILE
/AXLAB,Y,TEMPERATURE, (K)
/AXLAB,X,AXIAL COORDINATE, (M)
PATH,AXIAL,2,,50
```

```
PPATH,1,,0,R,0

PPATH,2,,L,R,0

PDEF,VX1,VX

PDEF,WALL TEMP,TEMP

plpath,WALL TEMP

NSEL,S,LOC,X,0.0075                !RESULTS ALONG PIPE-3L/5

PRNSOL,TEMP

FINISH
```

APPENDIX B

APPENDIX B

UNSTEADY CONJUGATE HEAT TRANSFER IN A CIRCULAR DUCT (FULLY-IMPLICIT)

```
**************************************************************************
*              UNSTEADY CONJUGATE HEAT TRANSFER                          *
*            IN A CIRCULAR DUCT (Fully-Implicit)                         *
*                 by Alan L. Briggs                                      *
**************************************************************************
 C    THE FOLLOWING ASSIGNS VARIABLES AS REAL OR INTEGER
      PARAMETER(NDIM=50,NDIMR=50,NDIMZ=1,ZNODES=30)
      REAL*8  A(NDIM,NDIM),B(NDIM),TEMP(NDIMR)
     .,OLDTEMP(NDIMR,ZNODES),INTEMP(NDIMR), FLUX(ZNODES),
     . OLDTIME,NEWTEMP(NDIMR,ZNODES),BULK(ZNODES)
     .,FTIME,DTIME,VEL, THETAINF,RN,RS,ROD,ROU,LOCR,DELRS,
     .DELRN,AW,AS,AN,DELZ,POWER,NUSSELT,ASTAR,OMEGA,PECKLET
     .,BRINKMAN,VISD,VELN,VELS,SOMET,CRN,CRS,NODECOUNT
     .,UPBULK,DOWNBULK,DIMNUSS(ZNODES)
      INTEGER IPVT(NDIM),N,I,J,IOUT,IFLAG,IIN,L
      N = NDIMR*NDIMZ
**************************************************************************
C     INPUT VALUES
**************************************************************************
*     OPEN(6,FILE='WALL.OUT',STATUS='NEW')
      NODECOUNT=NDIMR*ZNODES
```

```
      POWER=1.
      NUSSELT=23.764
      BRINKMAN=0.000000279
      ASTAR=0.00378
      OMEGA=0.0546
      PECKLET=14.01245
      IIN=5
      IOUT=6
      ROD=0
      ROU=1
      ZIN=0
      ZOUT=3
      OLDTIME=0
      DTIME=0.00015
      FTIME=DTIME*1000
      TOL=0.00000001
      THETAINF=-0.5
      GAPR=ROU-ROD
      GAPZ=ZOUT-ZIN
      DISR=GAPR/(NDIMR-0.5)
      write(6,*)'DISR=',DISR,'      ', 'NODECOUNT', NODECOUNT
      DISZ=GAPZ/(ZNODES)
*     OPEN(IOUT,FILE='INPUT3.DAT',STATUS='NEW')
      WRITE(IOUT,100)
100   FORMAT(/,'   Program to solve unsteady conjugate heat transfer
     . problem')
C     DISTANCES FROM POINT P TO N,S,E,W, RESPECTIVELY
      DELRN=DISR
```

```
      DELRS=DISR
      DELZ=DISZ
      DO I=1,NDIMR,1
      DO L=1,ZNODES,1
      OLDTEMP(I,L)=0
      ENDDO
      ENDDO
C     INLET TEMP DISTRIBUTION
 777  OLDTIME=OLDTIME+DTIME
      DO I=1,NDIMR,1
      INTEMP(I)=SIN(OMEGA*OLDTIME)
         SOMET=INTEMP(I)
      ENDDO
C      write(IOUT,*) somet,'Inlet temp'
          ZLOC=0
      DO L=1,ZNODES,1
      ZLOC=ZLOC+DISZ
      LOCR=1.0
C     WALL CONDITION
      AS=1/DELRS
      AO=1/(ASTAR*DTIME)
      A(1,1)=AS+AO+NUSSELT
      A(1,2)=-AS
      B(1)=NUSSELT*THETAINF+OLDTEMP(1,L)*AO
      DO J=2,NDIMR-1
      LOCR=LOCR-DISR
      CRN=LOCR+DISR
      CRS=LOCR-DISR
```

```
      RN=LOCR+DISR/2
      RS=LOCR-DISR/2
      VELN=((3*POWER+1)/(POWER+1))*(1-RN**((POWER+1)/POWER))
      VEL=((3*POWER+1)/(POWER+1))*(1-LOCR**((POWER+1)/POWER))
      VELS=((3*POWER+1)/(POWER+1))*(1-RS**((POWER+1)/POWER))
      AW=PECKLET*VEL*((RN**2)-(RS**2))/(2.*DELZ)
      AN=(RN)/(DELRN)
      AS=(RS)/(DELRS)
      AO=(((RN**2)-(RS**2))/2.)*(1./DTIME)
      A(J,J)=AW+AN+AS+AO
      A(J,J+1)=-AS
      A(J,J-1)=-AN
      VISD=BRINKMAN*LOCR*DISR*((ABS((VELN-VELS)/DISR))**(POWER-1))
     c*((VELN-VELS)**2)
      B(J)=AW*INTEMP(J)+OLDTEMP(J,L)*AO+VISD
      ENDDO
*     Next to Center
      LOCR=LOCR-DISR
      RN=LOCR+DISR/2
      RS=0
      VEL=((3*POWER+1)/(POWER+1))*(1-LOCR**((POWER+1)/POWER))
      VELN=((3*POWER+1)/(POWER+1))*(1-RN**((POWER+1)/POWER))
      VELS=((3*POWER+1)/(POWER+1))*(1-RS**((POWER+1)/POWER))
*     WRITE(6,*) 'CENTER VEL',VELS
      AW=PECKLET*VEL*((RN**2))/(2.*DISZ)
      AN=(RN)/(DELRN)
      AS=0
      AO=(((RN**2))/2)*(1.0/DTIME)
```

```
      VISD=BRINKMAN*LOCR*DISR*((ABS((VELN-VELS)/DISR))**(POWER-1))
     c*((VELN-VELS)**2)
      A(NDIMR,NDIMR)=AW+AN+AO
      A(NDIMR,NDIMR-1)=-AN
      B(NDIMR)=AW*INTEMP(NDIMR)+OLDTEMP(NDIMR,L)*AO+VISD
*       WRITE(IOUT,150)
*150   FORMAT('  The original A matrix is:')
*     DO I = 1,N
*            WRITE(IOUT,200) (A(I,J),J=1,N)
*200          FORMAT(400F8.4)
*     ENDDO
*       WRITE(IOUT,155)
*155   FORMAT('  The original B matrix is:')
*     DO I = 1,N
*            WRITE(IOUT,222) B(I)
*222         FORMAT(20F8.4)
*     ENDDO
C  DO THE LU DECOMPOSTION
      CALL LUD(A,N,IPVT,NDIM,IOUT,IFLAG)
      IF (IFLAG .LT. 0) STOP
*     WRITE(IOUT,300)
*300   FORMAT(/,'  The compact LU matrix is:')
*     DO I = 1,N
*            WRITE(IOUT,350) (A(I,J),J=1,N)
*350          FORMAT(20F8.4)
*     ENDDO
*     WRITE(IOUT,400)
*400   FORMAT(/,'  The pivoting order is:')
```

```
*     WRITE(IOUT,450) (IPVT(I), I=1,N)
*450   FORMAT(5I6)
      CALL SOLVE(A,N,IPVT,B,NDIM)
*     WRITE(IOUT,500)
*500   FORMAT(/,'  The solution to the set of equations is:')
*     DO I=1,N
*           WRITE(IOUT,550) I,B(I)
*550         FORMAT(' I = ',I3,' X(I) = ',E12.5)
*     ENDDO
      DO I=1,NDIMR,1
      TEMP(I)=B(I)
C     WRITE(6,*) 'TEMPERATURE=' ,I,TEMP(I)
      ENDDO
      LOCR=1.0
      BULK(L)=0
      DIMNUSS(L)=0
      UPBULK=0
      DOWNBULK=0
      DO I=2,NDIMR,1
      LOCR=LOCR-DISR
      VEL=((3*POWER+1)/(POWER+1))*(1-LOCR**((POWER+1)/POWER))
      UPBULK=(VEL*TEMP(I)*LOCR*DISR)+UPBULK
      DOWNBULK=(VEL*LOCR*DISR)+DOWNBULK
      ENDDO
C     BULK TEMPERATURE
      BULK(L)=UPBULK/DOWNBULK
C     LOCAL NUSSELT NUMBER
      DIMNUSS(L)=-2*(TEMP(1)-TEMP(2))/DISR/(BULK(L)-TEMP(1))
```

```
        IF((ABS(OLDTIME-FTIME)).LT.TOL) THEN
      WRITE(6,*) 'BULKTEMPERATURE AT Z=',ZLOC,'    ',BULK(L)
      ENDIF
      DO I=1,NDIMR,1
      NEWTEMP(I,L)=TEMP(I)
      INTEMP(I)=TEMP(I)
      ENDDO
      ENDDO
      IF((ABS(OLDTIME-FTIME)).LT.TOL) THEN
      WRITE(6,*) ' SOLUTION at=','         ','T=',FTIME,'    ','Z=',ZLOC
      write(6,*) '**********RESULTS**********'
      WRITE(IOUT,*) 'WALL TEMP=',TEMP(1),'  AT TIME=',OLDTIME
*     WRITE(IOUT,*) 'NEAR-CENTER TEMP=',TEMP(NDIMR)
      GO TO 333
      ELSE
      DO I=1,NDIMR,1
      DO L=1,ZNODES,1
      OLDTEMP(I,L)=NEWTEMP(I,L)
      ENDDO
      ENDDO
*     WRITE(IOUT,*) 'WALL TEMP=',TEMP(1),'  AT TIME=',OLDTIME
*      WRITE(IOUT,*) 'NEAR-CENTER TEMP=',TEMP(NDIMR)
*     .,'  AT TIME=',OLDTIME
      GO TO 777
      ENDIF
 ***************************************************************
C     THE END OF PROGRAM
 333  LOCR=1
```

```
      DO I=1,NDIMR,1
      WRITE(6,999)I,TEMP(I),LOCR
  999  FORMAT('NODE=',I3,'   ','TEMPERATURE=',F20.15,'     '
     .,'AT R=',F8.5)
      LOCR=LOCR-DISR
      ENDDO
        WHERE=0
      DO L=1,ZNODES,1
      WHERE=WHERE+DISZ
C     LOCAL NUSSELT NUMBER
      WRITE(6,998) DIMNUSS(L), WHERE
  998  FORMAT('NUSSELT=',F20.15,'   ','AT Z=',F8.5)
      ENDDO
      WHERE=0
      DO L=1,ZNODES,1
      WHERE=WHERE+DISZ
C     WALL TEMPERATURE
      WRITE(6,967)NEWTEMP(1,L),WHERE
  967  FORMAT('WALL TEMP=',F20.15,'   ','AT Z=',F8.5)
      ENDDO
      STOP
      END
      SUBROUTINE LUD(A,N,IPVT,NDIM,IOUT,IFLAG)
C  -----------------------------------------------------------------
C     THIS SUBROUTINE PRODUCES THE LU DECOMPOSITION OF A MATRIX A[I,J].
C     THE A-MATRIX IS DESTROYED DURING EXECUTION OF THIS PROCEDURE.
C     INPUT:  A  -  A SQUARE MATRIX OF SIZE NDIM BY NDIM
C             NDIM  -  THE MAXIMUM ROW DIMENSION OF A
```

```
C          IOUT  -  LOGICAL DEVICE NUMBER FOR OUTPUT
C          N  -  THE SIZE OF THE MATRIX A[I,J] BEING PROCESSED.
C    OUTPUT: A  -  THE LU DECOMPOSITION OF THE MATRIX A[I,J]
C          IPVT  -  AN ARRAY CONTAINING THE ORDER OF THE ROWS OF THE
C                REARRANGED MATRIX DUE TO PIVOTING
C          IFLAG -  SIGNAL OF STATUS ON RETURN
C           IFLAG = 1, NORMAL RETURN
C           IFLAG = -1, INDICATION OF SMALL PIVOT ELEMENT
C ---------------------------------------------------------------------
     REAL*8 A(NDIM,N),  SUM
     INTEGER IPVT(N),I,J,JM1,JP1,K,NM1,IOUT,IFLAG
     DO I = 1,N
       IPVT(I) = I
     ENDDO
     CALL PIVOT_A(A,IPVT,N,1,NDIM)
     IF (ABS(A(1,1)). LT. 1.0E-09) THEN
        WRITE(IOUT,10)
10      FORMAT(//,'   MATRIX IS SINGULAR OR NEAR SINGULAR  ',//)
        IFLAG = -1
        RETURN
     ENDIF
C  MODIFY THE REST OF THE FIRST ROW
     DO I = 2,N
       A(1,I) = A(1,I)/A(1,1)
     ENDDO
     NM1 = N - 1
C  LOOP THROUGH REST OF ROWS EXCEPT THE LAST
     DO J = 2,NM1
```

```
      JM1 = J - 1
C  FIND THE VALUES FOR THE L-MATRIX COLUMN
      DO I = J,N
        SUM = 0.0
        DO K = 1,JM1
          SUM = SUM + A(I,K)*A(K,J)
        ENDDO
        A(I,J) = A(I,J) - SUM
      ENDDO
      CALL PIVOT_A(A,IPVT,N,J,NDIM)
      IF (ABS(A(J,J)). LT. 1.0E-05) THEN
        WRITE(IOUT,10)
        IFLAG = -1
        RETURN
      ENDIF
C  FIND THE VALUES FOR THE U-MATRIX ROW
      JP1 = J + 1
      DO K = JP1,N
        SUM = 0.0
        DO I = 1,JM1
          SUM = SUM + A(J,I)*A(I,K)
        ENDDO
        A(J,K) = (A(J,K) - SUM)/A(J,J)
      ENDDO
    ENDDO
C  FIND THE LAST DIAGONAL ELEMENT OF THE LU MATRIX
    SUM = 0.0
    DO K = 1,NM1
```

```
        SUM = SUM + A(N,K)*A(K,N)
      ENDDO
      A(N,N) = A(N,N) - SUM
      IF (ABS(A(N,N)). LT. 1.0E-05) THEN
        WRITE(IOUT,10)
        IFLAG = -1
        RETURN
      ENDIF
C  NORMAL RETURN WITH GOOD LU MATRIX
      IFLAG = 1
      RETURN
      END
      SUBROUTINE PIVOT_A(A,IPVT,N,JCOL,NDIM)
C  ---------------------------------------------------------------------
C  THIS SUBROUTINE SEARCHES THE jTH COLUMN OF THE A[I,J] MATRIX FOR THE
C  LARGEST ELEMENT BELOW THE DIAGONAL.  IT THEN INTERHANGES ROWS TO
C  PLACE THIS ELEMENT ON THE DIAGONAL.  IT RECORDS THE CHAGES IN
C  THE ARRAY IPVT(I).
C  ---------------------------------------------------------------------
      REAL*8 A(NDIM,N),BIG,TEMP
      INTEGER IPVT(N),JCOL,I,INDEX,ITEMP,JCOL_P1
C  FIND IF ANY ELEMENTS IN THE COLUMN ARE BIGGER THAN DIAGONAL ELEMENT
      INDEX = JCOL
      BIG = ABS(A(JCOL,JCOL))
      JCOL_P1 = JCOL + 1
      DO I = JCOL_P1,N
        TEMP = ABS(A(I,JCOL))
        IF (TEMP .GT. BIG) THEN
```

```
          INDEX = I
          BIG = TEMP
        ENDIF
      ENDDO
C  INTERCHANGE ROWS IF NECESSARY
      IF (INDEX .NE. JCOL) THEN
        DO I = 1,N
          TEMP = A(JCOL,I)
          A(JCOL,I) = A(INDEX,I)
          A(INDEX,I) = TEMP
        ENDDO
        ITEMP = IPVT(JCOL)
        IPVT(JCOL) = IPVT(INDEX)
        IPVT(INDEX) = ITEMP
      ENDIF
      RETURN
      END
      SUBROUTINE SOLVE(A,N,IPVT,B,NDIM)
C  -----------------------------------------------------------------
C     THIS SUBROUTINE USES THE COMBINED LU MATRIX "A" TO SOLVE
C     A SYSTEM OF LINEAR EQUATIONS
C     INPUT:   A - LU MATRIX
C              N - NUMBER OF EQUATIONS TO BE SOLVED
C           IPVT - A RECORD OF THE REARRANGEMENT OF THE ROWS
C                  OF A[I,J] FROM THE LU DECOMPOSTION
C              B - RIGHT HAND SIDE OF THE SET OF EQUATIONS
C     OUTPUT:  B - THE SOLUTION VECTOR
C  -----------------------------------------------------------------
```

```
      REAL*8 A(NDIM,N), B(N), B_PRIM(80), SUM
      INTEGER IPVT(N),I,J,IM1
C  REARRANGE THE ELEMENTS OF THE B VECTOR & STORE THEM IN THE B_PRIM ARRAY.
      DO I = 1,N
        B_PRIM(I) = B(IPVT(I))
      ENDDO
C  OBTAIN B' BY DOING FORWARD SUBSTITUTION--LB' = B
      B_PRIM(1) = B_PRIM(1)/A(1,1)
      DO I = 2,N
        IM1 = I - 1
        SUM = 0.0
        DO J = 1,IM1
          SUM = SUM + A(I,J)*B_PRIM(J)
        ENDDO
        B_PRIM(I) = (B_PRIM(I) - SUM)/A(I,I)
      ENDDO
C  SOLVE FOR X BY BACK SUBSTITUTION--UX = B'
C  RESULTS STORED IN B ARRAY
      B(N) = B_PRIM(N)
      DO I = (N-1),1,-1
        B(I) = B_PRIM(I)
        DO J = (I+1),N
          B(I) = B(I) - A(I,J)*B(J)
        ENDDO
      ENDDO
      RETURN
      END
```

APPENDIX C

APPENDIX C

GRAETZ PROBLEM

```
**************************************************************************
*                  GRAETZ PROBLEM    BY ALAN L. BRIGGS                   *
**************************************************************************
C     THE FOLLOWING ASSIGNS VARIABLES AS REAL OR INTEGER
      PARAMETER(NDIM=50,NDIMR=50,NDIMZ=1,ZNODES=30)
      REAL*8  A(NDIM,NDIM),B(NDIM),TEMP(NDIMR)
     .,INTEMP(NDIMR), FLUX(ZNODES),
     . NEWTEMP(NDIMR,ZNODES)
     ., THETAINF,RN,RS,ROD,ROU,LOCR,DELRS,
     .DELRN,AW,AS,AN,DELZ,CRN,CRS,NODECOUNT
      INTEGER IPVT(NDIM),N,I,J,IOUT,IFLAG,IIN,L
      N = NDIMR*NDIMZ
**************************************************************************
C     INPUT VALUES
**************************************************************************
*     OPEN(6,FILE='WALL.OUT',STATUS='NEW')
      NODECOUNT=NDIMR*ZNODES
      IIN=5
      IOUT=6
      ROD=0
      ROU=1
```

```
      ZIN=0
      ZOUT=0.1
      THETAINF=0.0
      GAPR=ROU-ROD
      GAPZ=ZOUT-ZIN
      DISR=GAPR/(NDIMR+0.5)
*     WRITE(6,*)'DISR=',DISR,'      ', 'NODECOUNT', NODECOUNT
      DISZ=GAPZ/(ZNODES)
*     OPEN(IOUT,FILE='INPUT3.DAT',STATUS='NEW')
      WRITE(IOUT,100)
100   FORMAT(/,'   PROGRAM TO SOLVE GRAETZ PROBLEM')
C     DISTANCES FROM POINT P TO N,S,E,W, RESPECTIVELY
      DELRN=DISR
      DELRS=DISR
      DELZ=DISZ
*     INLET TEMPERATURE
      DO I=1,NDIMR,1
      INTEMP(I)=1.0
*     WRITE(IOUT,*) INTEMP(I),'INLET TEMP'
      ENDDO
      ZLOC=0
      DO L=1,ZNODES,1
      ZLOC=ZLOC+DISZ
      LOCR=1.0
*     FIRST NODE
      LOCR=LOCR-DISR
      CRN=LOCR+DISR
      CRS=LOCR-DISR
```

```
      RN=LOCR+DISR/2
      RS=LOCR-DISR/2
      AW=0.5*(((((RN**2)-(RS**2)))/(2.*DELZ))
     C-((((RN**4)-(RS**4)))/(4.*DELZ)))
      AN=(RN)/(DELRN)
      AS=(RS)/(DELRS)
      A(1,1)=AW+AN+AS
      A(1,2)=-AS
      B(1)=AW*INTEMP(1)+AN*THETAINF
      DO J=2,NDIMR-1
      LOCR=LOCR-DISR
*     WRITE(6,*) J,LOCR,' NODE LOC'
      CRN=LOCR+DISR
      CRS=LOCR-DISR
      RN=LOCR+DISR/2
      RS=LOCR-DISR/2
      AW=0.5*(((((RN**2)-(RS**2)))/(2.*DELZ))
     C-((((RN**4)-(RS**4)))/(4.*DELZ)))
      AN=(RN)/(DELRN)
      AS=(RS)/(DELRS)
      A(J,J)=AW+AN+AS
      A(J,J+1)=-AS
      A(J,J-1)=-AN
      B(J)=AW*INTEMP(J)
       ENDDO
*     NEXT TO CENTER
      LOCR=LOCR-DISR
      RN=LOCR+DISR/2
```

```
      RS=0
      AW=((((RN**2)-(RS**2)))/(2.*DELZ))-((((RN**4)-(RS**4)))/(4.*DELZ))
      AN=(RN)/(DELRN)
      AS=0
      A(NDIMR,NDIMR)=AW+AN
      A(NDIMR,NDIMR-1)=-AN
      B(NDIMR)=AW*INTEMP(NDIMR)
*       WRITE(IOUT,150)
*150   FORMAT('  THE ORIGINAL A MATRIX IS:')
*     DO I = 1,N
*           WRITE(IOUT,200) (A(I,J),J=1,N)
*200         FORMAT(400F8.4)
*     ENDDO
*       WRITE(IOUT,155)
*155   FORMAT('  THE ORIGINAL B MATRIX IS:')
*     DO I = 1,N
*           WRITE(IOUT,222) B(I)
*222         FORMAT(20F8.4)
*     ENDDO
C  DO THE LU DECOMPOSTION
      CALL LUD(A,N,IPVT,NDIM,IOUT,IFLAG)
      IF (IFLAG .LT. 0) STOP
*     WRITE(IOUT,300)
*300   FORMAT(/,'  THE COMPACT LU MATRIX IS:')
*     DO I = 1,N
*           WRITE(IOUT,350) (A(I,J),J=1,N)
*350         FORMAT(20F8.4)
*     ENDDO
```

```
*     WRITE(IOUT,400)
*400   FORMAT(/,'  THE PIVOTING ORDER IS:')
*     WRITE(IOUT,450) (IPVT(I), I=1,N)
*450   FORMAT(5I6)
      CALL SOLVE(A,N,IPVT,B,NDIM)
*     WRITE(IOUT,500)
*500   FORMAT(/,'  THE SOLUTION TO THE SET OF EQUATIONS IS:')
*     DO I=1,N
*           WRITE(IOUT,550) I,B(I)
*550         FORMAT(' I = ',I3,' X(I) = ',E12.5)
*     ENDDO
*     DO I=1,NDIMR,1
*     TEMP(I)=B(I)
*      WRITE(6,*) 'TEMPERATURE=' ,I,TEMP(I)
*     ENDDO
*    WRITE(6,*) 'AXIAL LOCATION=' ,ZLOC
      LOCR=1
      DO I=1,NDIMR,1
      LOCR=LOCR-DISR
      TEMP(I)=B(I)
*     WRITE(6,999)I,TEMP(I),LOCR
* 999  FORMAT('NODE=',I3,'   ','TEMPERATURE=',F20.15,'   '
*    .,'AT R=',F8.5)
      ENDDO
      DO I=1,NDIMR,1
      INTEMP(I)=TEMP(I)
*      WRITE(6,*) 'TEMPERATURE=' ,I,TEMP(I)
      ENDDO
```

```
      ENDDO
**********************************************************************
C     THE END OF PROGRAM
      WRITE(6,*) 'AXIAL LOCATION=' ,ZLOC
      LOCR=1
      DO I=1,NDIMR,1
      LOCR=LOCR-DISR
      TEMP(I)=B(I)
      WRITE(6,999)I,TEMP(I),LOCR
 999  FORMAT('NODE=',I3,'   ','TEMPERATURE=',F20.15,'   '
     .,'AT R=',F8.5)
      ENDDO
       WHERE=0
      DO L=1,ZNODES,1
      WHERE=WHERE+DISZ
*     WRITE(6,*) NEWTEMP(1,L),'WALL TEMP'
      FLUX(LXS)=-(NEWTEMP(1,L)-NEWTEMP(2,L))/DISR/2
*     WRITE(6,*) 'WALL HEAT FLUX=',FLUX(L),'       ','AT Z=',WHERE
      ENDDO
      STOP
      END
      SUBROUTINE LUD(A,N,IPVT,NDIM,IOUT,IFLAG)
C  ------------------------------------------------------------
C     THIS SUBROUTINE PRODUCES THE LU DECOMPOSITION OF A MATRIX A[I,J].
C     THE A-MATRIX IS DESTROYED DURING EXECUTION OF THIS PROCEDURE.
C     INPUT:  A  -  A SQUARE MATRIX OF SIZE NDIM BY NDIM
C             NDIM  -  THE MAXIMUM ROW DIMENSION OF A
C             IOUT  -  LOGICAL DEVICE NUMBER FOR OUTPUT
```

```
C           N  -  THE SIZE OF THE MATRIX A[I,J] BEING PROCESSED.
C     OUTPUT: A  -  THE LU DECOMPOSITION OF THE MATRIX A[I,J]
C           IPVT  -  AN ARRAY CONTAINING THE ORDER OF THE ROWS OF THE
C                    REARRANGED MATRIX DUE TO PIVOTING
C           IFLAG -  SIGNAL OF STATUS ON RETURN
C             IFLAG = 1, NORMAL RETURN
C             IFLAG = -1, INDICATION OF SMALL PIVOT ELEMENT
C  ------------------------------------------------------------------
      REAL*8 A(NDIM,N),  SUM
      INTEGER IPVT(N),I,J,JM1,JP1,K,NM1,IOUT,IFLAG
      DO I = 1,N
        IPVT(I) = I
      ENDDO
      CALL PIVOT_A(A,IPVT,N,1,NDIM)
      IF (ABS(A(1,1)). LT. 1.0E-09) THEN
         WRITE(IOUT,10)
10        FORMAT(//,'   MATRIX IS SINGULAR OR NEAR SINGULAR  ',//)
         IFLAG = -1
         RETURN
      ENDIF
C  MODIFY THE REST OF THE FIRST ROW
      DO I = 2,N
        A(1,I) = A(1,I)/A(1,1)
      ENDDO
      NM1 = N - 1
C  LOOP THROUGH REST OF ROWS EXCEPT THE LAST
      DO J = 2,NM1
        JM1 = J - 1
```

```
C  FIND THE VALUES FOR THE L-MATRIX COLUMN
      DO I = J,N
        SUM = 0.0
        DO K = 1,JM1
          SUM = SUM + A(I,K)*A(K,J)
        ENDDO
        A(I,J) = A(I,J) - SUM
      ENDDO
      CALL PIVOT_A(A,IPVT,N,J,NDIM)
      IF (ABS(A(J,J)). LT. 1.0E-05) THEN
        WRITE(IOUT,10)
        IFLAG = -1
        RETURN
      ENDIF
C  FIND THE VALUES FOR THE U-MATRIX ROW
      JP1 = J + 1
      DO K = JP1,N
        SUM = 0.0
        DO I = 1,JM1
          SUM = SUM + A(J,I)*A(I,K)
        ENDDO
        A(J,K) = (A(J,K) - SUM)/A(J,J)
      ENDDO
    ENDDO
C  FIND THE LAST DIAGONAL ELEMENT OF THE LU MATRIX
    SUM = 0.0
    DO K = 1,NM1
      SUM = SUM + A(N,K)*A(K,N)
```

```
      ENDDO
      A(N,N) = A(N,N) - SUM
      IF (ABS(A(N,N)). LT. 1.0E-05) THEN
        WRITE(IOUT,10)
        IFLAG = -1
        RETURN
      ENDIF
C  NORMAL RETURN WITH GOOD LU MATRIX
      IFLAG = 1
      RETURN
      END
      SUBROUTINE PIVOT_A(A,IPVT,N,JCOL,NDIM)
C  -----------------------------------------------------------------
C  THIS SUBROUTINE SEARCHES THE JTH COLUMN OF THE A[I,J] MATRIX FOR THE
C  LARGEST ELEMENT BELOW THE DIAGONAL.  IT THEN INTERHANGES ROWS TO
C  PLACE THIS ELEMENT ON THE DIAGONAL.  IT RECORDS THE CHAGES IN
C  THE ARRAY IPVT(I).
C  -----------------------------------------------------------------
      REAL*8 A(NDIM,N),BIG,TEMP
      INTEGER IPVT(N),JCOL,I,INDEX,ITEMP,JCOL_P1
C  FIND IF ANY ELEMENTS IN THE COLUMN ARE BIGGER THAN DIAGONAL ELEMENT
      INDEX = JCOL
      BIG = ABS(A(JCOL,JCOL))
      JCOL_P1 = JCOL + 1
      DO I = JCOL_P1,N
        TEMP = ABS(A(I,JCOL))
        IF (TEMP .GT. BIG) THEN
          INDEX = I
```

```
          BIG = TEMP
        ENDIF
      ENDDO
C  INTERCHANGE ROWS IF NECESSARY
      IF (INDEX .NE. JCOL) THEN
        DO I = 1,N
          TEMP = A(JCOL,I)
          A(JCOL,I) = A(INDEX,I)
          A(INDEX,I) = TEMP
        ENDDO
        ITEMP = IPVT(JCOL)
        IPVT(JCOL) = IPVT(INDEX)
        IPVT(INDEX) = ITEMP
      ENDIF
      RETURN
      END
      SUBROUTINE SOLVE(A,N,IPVT,B,NDIM)
C  -----------------------------------------------------------------
C     THIS SUBROUTINE USES THE COMBINED LU MATRIX "A" TO SOLVE
C     A SYSTEM OF LINEAR EQUATIONS
C     INPUT:   A - LU MATRIX
C              N - NUMBER OF EQUATIONS TO BE SOLVED
C           IPVT - A RECORD OF THE REARRANGEMENT OF THE ROWS
C                  OF A[I,J] FROM THE LU DECOMPOSTION
C              B - RIGHT HAND SIDE OF THE SET OF EQUATIONS
C     OUTPUT:  B - THE SOLUTION VECTOR
C  -----------------------------------------------------------------
      REAL*8 A(NDIM,N), B(N), B_PRIM(80), SUM
```

```
      INTEGER IPVT(N),I,J,IM1
C  REARRANGE THE ELEMENTS OF THE B VECTOR & STORE THEM IN THE B_PRIM ARRAY.
      DO I = 1,N
        B_PRIM(I) = B(IPVT(I))
      ENDDO
C  OBTAIN B' BY DOING FORWARD SUBSTITUTION--LB' = B
      B_PRIM(1) = B_PRIM(1)/A(1,1)
      DO I = 2,N
        IM1 = I - 1
        SUM = 0.0
        DO J = 1,IM1
          SUM = SUM + A(I,J)*B_PRIM(J)
        ENDDO
        B_PRIM(I) = (B_PRIM(I) - SUM)/A(I,I)
      ENDDO
C  SOLVE FOR X BY BACK SUBSTITUTION--UX = B'
C  RESULTS STORED IN B ARRAY
      B(N) = B_PRIM(N)
      DO I = (N-1),1,-1
        B(I) = B_PRIM(I)
        DO J = (I+1),N
          B(I) = B(I) - A(I,J)*B(J)
        ENDDO
      ENDDO
      RETURN
      END
```

APPENDIX D

APPENDIX D

UNSTEADY CONJUGATE HEAT TRANSFER IN A CIRCULAR DUCT (EXPLICIT-SCHEME)

```
**************************************************************************
*       UNSTEADY CONJUGATE HEAT TRANSFER IN A CIRCULAR DUCT              *
*                          (EXPLICIT SCHEME)                             *
**************************************************************************
C     THE FOLLOWING ASSIGNS VARIABLES AS REAL OR INTEGER
      PARAMETER(NDIM=50,NDIMR=50,NDIMZ=1,ZNODES=30)
      REAL*8 TEMP(NDIMR)
     .,OLDTEMP(NDIMR,ZNODES),INTEMP(NDIMR), FLUX(ZNODES),
     . OLDTIME,NEWTEMP(NDIMR,ZNODES)
     .,FTIME,DTIME,VEL, THETAINF,RN,RS,ROD,ROU,LOCR,DELRS,
     .DELRN,AW,AS,AN,DELZ,POWER,NUSSELT,ASTAR,OMEGA,PECKLET
     .,BRINKMAN,VISD,VELN,VELS,SOMET,CRN,CRS,NODECOUNT
      INTEGER N,I,J,IOUT,IIN,L
      N = NDIMR*NDIMZ
C     INPUT VALUES
*     OPEN(6,FILE='WALL.OUT',STATUS='NEW')
      NODECOUNT=NDIMR*ZNODES
      POWER=1
      NUSSELT=23.764
      BRINKMAN=0.000000279
      ASTAR=0.00378
```

```
      OMEGA=0.0546
      PECKLET=14.01245
      IIN=5
      IOUT=6
      ROD=0
      ROU=1
      ZIN=0
      ZOUT=3
      OLDTIME=0
      DTIME=0.00015
      FTIME=DTIME*1000
      TOL=0.00000001
      THETAINF=-0.5
      GAPR=ROU-ROD
      GAPZ=ZOUT-ZIN
      DISR=GAPR/(NDIMR-0.5)
      WRITE(6,*)'DISR=',DISR,'      ', 'NODECOUNT', NODECOUNT
      DISZ=GAPZ/(ZNODES)
*     OPEN(IOUT,FILE='INPUT3.DAT',STATUS='NEW')
      WRITE(IOUT,100)
100   FORMAT(/,'   PROGRAM TO SOLVE UNSTEADY CONJUGATE HEAT TRANSFER
     . PROBLEM-EXPLICIT SCHEME')
C     DISTANCES FROM POINT P TO N,S,E,W, RESPECTIVELY
      DELRN=DISR
      DELRS=DISR
      DELZ=DISZ
      DO I=1,NDIMR,1
      DO L=1,ZNODES,1
```

```
      OLDTEMP(I,L)=0
      ENDDO
      ENDDO
C     INLET TEMP DISTRIBUTION
 777  OLDTIME=OLDTIME+DTIME
      DO I=1,NDIMR,1
      INTEMP(I)=SIN(OMEGA*OLDTIME)
       SOMET=INTEMP(I)
      ENDDO
*     WRITE(IOUT,*) SOMET,'INLET TEMP'
      ZLOC=0
      DO L=1,ZNODES,1
      ZLOC=ZLOC+DISZ
      LOCR=1.0
*     WALL CONDITION
      AS=1/DELRS
      AO=1/(ASTAR*DTIME)-AS-NUSSELT
*     WRITE(6,*) AO,'AOWALL'
      AP=AS+AO+NUSSELT
      TEMP(1)=(NUSSELT*THETAINF+OLDTEMP(1,L)*AO+AS*OLDTEMP(2,L))/AP
      DO J=2,NDIMR-1
      LOCR=LOCR-DISR
      CRN=LOCR+DISR
      CRS=LOCR-DISR
      RN=LOCR+DISR/2
      RS=LOCR-DISR/2
      VELN=((3*POWER+1)/(POWER+1))*(1-RN**((POWER+1)/POWER))
      VEL=((3*POWER+1)/(POWER+1))*(1-LOCR**((POWER+1)/POWER))
```

```
      VELS=((3*POWER+1)/(POWER+1))*(1-RS**((POWER+1)/POWER))
      AW=PECKLET*VEL*((RN**2)-(RS**2))/(2.*DELZ)
      AN=(RN)/(DELRN)
      AS=(RS)/(DELRS)
      AO=((((RN**2)-(RS**2))/2.)*(1./DTIME))-AW-AN-AS
*     WRITE(6,*) AO,'AO',J
      AP=AW+AN+AS+AO
      VISD=BRINKMAN*LOCR*DISR*((ABS((VELN-VELS)/DISR))**(POWER-1))
     C*((VELN-VELS)**2)
      TEMP(J)=(AW*INTEMP(J)+OLDTEMP(J,L)*AO+VISD
     C+AN*OLDTEMP(J-1,L)+AS*OLDTEMP(J+1,L))/AP
      ENDDO
*     NEXT TO CENTER
      LOCR=LOCR-DISR
      RN=LOCR+DISR/2
      RS=0
      VEL=((3*POWER+1)/(POWER+1))*(1-LOCR**((POWER+1)/POWER))
      VELN=((3*POWER+1)/(POWER+1))*(1-RN**((POWER+1)/POWER))
       VELS=((3*POWER+1)/(POWER+1))*(1-RS**((POWER+1)/POWER))
*     WRITE(6,*) 'CENTER VEL',VELS
      AW=PECKLET*VEL*((RN**2))/(2.*DISZ)
      AN=(RN)/(DELRN)
      AS=0
      AO=((((RN**2))/2)*(1.0/DTIME))-AW-AN-AS
*     WRITE(6,*) AO,'NEAR CENTER AO'
      VISD=BRINKMAN*LOCR*DISR*((ABS((VELN-VELS)/DISR))**(POWER-1))
     C*((VELN-VELS)**2)
      AP=AW+AN+AO
```

```
      TEMP(NDIMR)=(AW*INTEMP(NDIMR)+OLDTEMP(NDIMR,L)*AO+VISD
     C+AN*OLDTEMP(NDIMR-1,L))/AP
      DO I=1,NDIMR,1
*       WRITE(6,*) 'TEMPERATURE=' ,I,TEMP(I)
      ENDDO
       DO I=1,NDIMR,1
      NEWTEMP(I,L)=TEMP(I)
      INTEMP(I)=TEMP(I)
      ENDDO
      ENDDO
*     WRITE(6,*) OLDTIME,FTIME,'OLDTIME,FTIME'
      IF((ABS(OLDTIME-FTIME)).LT.TOL) THEN
      WRITE(6,*) ' SOLUTION AT=',         ','T=',FTIME,'    ','Z=',ZLOC
      WRITE(6,*) '**********RESULTS**********'
*     WRITE(IOUT,*) 'WALL TEMP=',TEMP(1),'  AT TIME=',OLDTIME
*     WRITE(IOUT,*) 'NEAR-CENTER TEMP=',TEMP(NDIMR)
      GO TO 333
      ELSE
      DO I=1,NDIMR,1
      DO L=1,ZNODES,1
      OLDTEMP(I,L)=NEWTEMP(I,L)
      ENDDO
      ENDDO
*     WRITE(IOUT,*) 'WALL TEMP=',TEMP(1),'  AT TIME=',OLDTIME
*      WRITE(IOUT,*) 'NEAR-CENTER TEMP=',TEMP(NDIMR)
*     .,'  AT TIME=',OLDTIME
      GO TO 777
      ENDIF
```

```
*****************************************************************
C     THE END OF PROGRAM
 333  LOCR=1
      DO I=1,NDIMR,1
      WRITE(6,999)I,TEMP(I),LOCR
 999  FORMAT('NODE=',I3,'   ','TEMPERATURE=',F20.15,'   '
     .,'AT R=',F8.5)
      LOCR=LOCR-DISR
      ENDDO
      WHERE=0
      DO L=1,ZNODES,1
      WHERE=WHERE+DISZ
*     WRITE(6,*) NEWTEMP(1,L),'WALL TEMP'
      FLUX(LXS)=-(NEWTEMP(1,L)-NEWTEMP(2,L))/DISR/2
*     WRITE(6,*) 'WALL HEAT FLUX=',FLUX(L),'        ','AT Z=',WHERE
      ENDDO
      STOP
      END
```

BIBLIOGRAPHY

BIBLIOGRAPHY

[1] Aleksashenko V. A., "Conjugate Stationary Problem of Heat Transfer with a Moving Fluid in a Semi-Infinite Tube Allowing for Viscous Dissipation," Journal of Engineering Physics, Vol. 14, No. 1, 1968, pp. 55-58.

[2] Alkam M. K., and Al-Nimr M. A., " Transient non-Darcian forced convection flow in a pipe partially filled with a porous material," International Journal of Heat and Mass Transfer, Vol. 41, No 2, 1998, pp347- 356.

[3] Al-Nimr M.A., Aldoss T., and Naji M.I., " Transient Convection in the Entrance Region of a Porous Tube," The Canadian Journal of Chemical Engineering, Vol. 72, April, 1994, pp. 249-255.

[4] Al-Nimr M. A, and Alkam M.K., "Unsteady Non-Darcian Forced Convection Analysis in an Annulus Partially filled with a Porous Material," Journal of Heat Transfer, Vol. 119, November, 1997, pp. 799-804.

[5] Barletta A., " On Forced Convection in a Circular Duct with Slug Flow and Viscous Dissipation," International Communications in Heat and Mass Transfer, Vol. 23, No 1, 1996, pp. 69-78.

[6] Barletta A., and Zanchini E., " Thermal entrance region for laminar forced convection in a circular tube with a power-law wall heat flux," International Journal of Heat and Mass Transfer, Vol. 39, No 6, 1996, pp. 1265-1272.

[7] Barletta A., and Zanchini E., "Forced Convection in the thermal entrance region of a circular duct with slug flow and viscous dissipation," International Journal of Heat and Mass Transfer, Vol. 40, No 5, 1997, pp.1181-1190.

[8] Barletta A., "Fully Developed Laminar Forced Convection in circular ducts for power-law fluids with viscous dissipation," International Journal of Heat and Mass Transfer, Vol. 40, No 1, 1997, pp. 15-26.

[9] Barletta A., "Slug Flow Heat Transfer in Circular Ducts with Viscous Dissipation and Convective Boundary Conditions," International Journal of Heat and Mass Transfer, Vol. 40, No 17, 1997, pp. 4219-4228.

[10] Barletta A., "Combined Forced and Free Convection with Viscous Dissipation in a Vertical Circular Duct," International Journal of Heat and Mass Transfer, Vol. 42, No 12, 1999, pp. 2243-2253.

[11] Barletta A., "Laminar Convection in a Vertical Channel with Viscous Dissipation and Buoyancy Effects," International Communications in Heat and Mass Transfer, Vol. 26, No 2, 1999, pp. 153-164.

[12] Barozzi G. S. and Pagliarini G., " A Method to Solve Conjugate Heat Transfer Problems: The Case of Fully Developed Laminar Flow in a Pipe," Journal of Heat Transfer, Vol. 107, 1985, pp. 77-83.

[13] Basu T., and Roy D.N., "Laminar Heat Transfer in a Tube with Viscous Dissipation," International Journal of Heat and Mass Transfer, Vol. 28, No 3, 1985, pp. 699-701.

[14] Bejan A., "Convection Heat Transfer," John Wiley & Sons, 1995

[15] Buyruk E., Barrow H, and Owen I., " Heat Transfer in Laminar Flow in a Concentric annulus with peripherally varying heat transfer," International Journal of Heat and Mass Transfer, Vol. 42, No 3, 1999, pp. 487-496.

[16] Cho Y.I., and Hartnett J.P., "Non-Newtonian Fluids in Circular Pipe Flow," Advances in Heat Transfer, Academic Press, Vol.15, 1982.

[17] Cotta R.M., and Ozisik M.N., "Laminar Forced Convection to Non-Newtonian Fluids in Ducts with Prescribed Wall Heat Flux," International Communications in Heat and Mass Transfer, Vol. 13, 1986, pp. 325-334.

[18] Cotta R. M., Mikhailov M.D., and Ozisik M.N., " Transient Conjugated Forced Convection in Ducts with Periodically Varying Inlet Temperature," International Journal of Heat and Mass Transfer, Vol. 30, No.10, 1987, pp. 2073-2082.

[19] Cotta R.M., and Ozisik M.N., "Transient Forced Convection in Laminar Channel Flow with Stepwise Variations of Wall Temperature," The Canadian Journal of Chemical Engineering, Vol. 64, October 1986, pp. 734-742.

[20] El-Shaarawi M.A.I., and Alkam M.K., " Transient Forced Convection in the Entrance Region of Concentric Annuli," International Journal of Heat and Mass Transfer, Vol. 35, No 12, 1992, pp. 3335-3344.

[21] Etemad S.Gh., and Mujumdar A.S., " Effects of Variable Viscosity and Viscous Dissipation on Laminar Convection Heat Transfer of a Power Law Fluid in the entrance region of a semi-circular duct," International Journal of Heat and Mass Transfer, Vol. 38, No 12, 1995, pp. 2225-2238.

[22] Hammad K.J., and Vradis G. C., "Viscous Dissipation and Heat Transfer In Pulsatile Flows of A Yield-Stress Fluid," International Communications in Heat and Mass Transfer, Vol. 23, No 5, 1996, pp. 599-612.

[23] Harms T. M., Jog M.A., and Manglik R.M., " Effects of Temperature-Dependent Viscosity Variations and Boundary Conditions on Fully-Developed Laminar Forced Convection in a Semicircular Duct," Journal of Heat Transfer, Vol.120, August 1998, pp. 600-605.

[24] Joshi S. D., and Bergles A. E., "Experimental Study of Laminar Heat Transfer to In-Tube Flow of Non-Newtonian Fluids," Journal of Heat Transfer, Vol.102, no. 102, 980, pp. 397-401.

[25] Kakac S., "Effects of Boundary Conditions on Forced Convection Heat Transfer ", M.E.T.U. Publication, No.19, 1968.

[26] Kakac S., Shah R.K., and Aung W., "Handbook of Single-Phase Convective Heat Transfer," John Wiley & Sons, 1987.

[27] Lin H., Shih Y., "Unsteady thermal Entrance Heat Transfer of Power Fluids in Pipes and Plate Slits," International Journal of Heat and Mass Transfer, Vol. 24, 1981, pp. 1531-1539.

[28] Patankar S.V., "Numerical Heat Transfer and Fluid Flow", Hemisphere Publishing Corporation, 1980

[29] Piva S., " An Analytical Approach to Fully Developed Heating of Laminar Flows in Circular Pipes," International Communications in Heat and Mass Transfer, Vol. 22, No 6, 1995, pp. 815-824.

[30] Prusa J., and Manglik R.M., " Asymptotic and Numerical solutions for Thermally Developing Flows of Newtonian and Non-Newtonian fluids in Circular Tubes with Uniform Wall Temperature," Numerical Heat Transfer, Vol. 26, 1994, pp.199-217.

[31] Shin S., Ahn H., Young I.C., and Sohn C., " Heat Transfer Behavior of a Temperature-Dependent Of Non-Newtonian Fluid with Reiner-Rivlin Model in a 2:1 Rectangular Duct," International Journal of Heat and Mass Transfer, Vol. 42, August, 1999, pp. 2935-2942.

[32] Shome B. " Effect of Uncertainties in Fluid Properties on Mixed Convection Laminar Flow and Heat Transfer in a Uniformly Heated Smooth Tube," Numerical Heat Transfer, Vol. 35, 1999, pp.875-889.

[33] Sparrow E. M., and De Farias F.N., " Unsteady Heat Transfer in Ducts with Time-Varying InletTemperature and Participating Walls,"" International Journal of Heat and Mass Transfer, Vol. 11, 1968, pp. 837-853.

[34] Sparrow E.M., and Patankar S.V., " Relationship Among Boundary Conditions and Nusselt Numbers for Thermally Developed Duct Flows," Journal of Heat Transfer, Vol.99, August 1977, pp.483-485.

[35] Travelho J. S., and Santos W. F. N. "Solution for Transient Conjugated Forced Convection in the Thermal Entrance Region of A Duct With Periodically Varying Inlet Temperature," Journal of Heat Transfer, Vol. 113, August 1991, pp. 558-562.

[36] Travelho J. S., and Santos W. F. N. "Unsteady Conjugate Heat Transfer in a Circular Duct with Convection from the Ambient and Periodically Varying Inlet Temperature," Journal of Heat Transfer, Vol. 120, August 1998, pp. 506-510.

[37] Unsal M., " Solution of the Complex Eigenvalue Problem for a Transient Laminar Forced Convection Inside Tubes, "International Communications in Heat and Mass Transfer," Vol. 26, No 1, 1999, pp. 125-134.

[38] Van Doormall J. P. And Raithby G.D., "Enhancements of the Simple Method for Predicting Incompressible Flows, " Numerical Heat Transfer, Vol. 7, 1984, pp.147-163.

[39] Wheatley P. O., Curtis G. F. Applied Numerical Analysis, Edition 6, 1999.

[40] Zanchini E., "Effect of Viscous Dissipation on the Asymptotic Behavior of Laminar Forced Convection in Circular Tubes," International Journal of Heat and Mass Transfer, Vol. 40, No 1, 1997, pp. 169-178.